CENTRO INTERNACIONAL DE ESTUDOS
DE DOUTORAMENTO E AVANZADOS
DA USC (CIEDUS)

TESE DE DOUTORAMENTO

THE OBESTATIN/GPR39 SYSTEM: FROM SATELLITE CELL REGULATION TO ITS APPLICABILITY IN DUCHENNE MUSCULAR DYSTROPHY

Jessica González Sánchez

ESCOLA DE DOUTORAMENTO INTERNACIONAL

PROGRAMA DE DOUTORAMENTO EN ENDOCRINOLOXÍA

SANTIAGO DE COMPOSTELA

2018

USC
UNIVERSIDADE
DE SANTIAGO
DE COMPOSTELA

DECLARACIÓN DA AUTORA DA TESE

The obestatin/GPR39 system: from satellite cell regulation to its applicability in Duchenne muscular dystrophy

Dna. Jessica González Sánchez

Presento a miña tese, seguindo o procedemento axeitado ao Regulamento, e declaro que:

1) A tese abarca os resultados da elaboración do meu traballo.
2) De selo caso, na tese faise referencia ás colaboracións que tivo este traballo.
3) A tese é a versión definitiva presentada para a súa defensa e coincide coa versión enviada en formato electrónico.
4) Confirmo que a tese non incorre en ningún tipo de plaxio doutros autores nin de traballos presentados por min para a obtención doutros títulos.

En Santiago de Compostela, 17 de outubro de 2018.

Asdo.: Jessica González Sánchez

USC
UNIVERSIDADE
DE SANTIAGO
DE COMPOSTELA

AUTORIZACIÓN DO DIRECTOR / TITOR DA TESE

The obestatin/GPR39 system: from satellite cell regulation to its applicability in Duchenne muscular dystrophy

D. Jesús Pérez Camiña
D. Felipe Casanueva Freijo
D. José Luis Relova Quinteiro

INFORMAN:

Que a presente tese, correspóndese co traballo realizado por Dna. Jessica González Sánchez, baixo a nosa dirección, e autorizamos a súa presentación, considerando que reúne os requisitos esixidos no Regulamento de Estudos de Doutoramento da USC, e que como directores desta non incorre nas causas de abstención establecidas na Lei 40/2015.

En Santiago de Compostela, 17 de outubro de 2018.

Asdo.:	Asdo.:	Asdo.:
Jesús Pérez Camiña	Felipe Casanueva Freijo	José Luis Relova Quinteiro

USC
UNIVERSIDADE
DE SANTIAGO
DE COMPOSTELA

Dna. Jessica González Sánchez

DECLARA:

Non ter ningún conflito de interese en relación coa Tese de doutoramento.

En Santiago de Compostela, 17 de outubro de 2018.

Asdo.: Jessica González Sánchez

USC
UNIVERSIDADE
DE SANTIAGO
DE COMPOSTELA



INDEX

USC
UNIVERSIDADE
DE SANTIAGO
DE COMPOSTELA

ABSTRACT/RESUMO/RESUMEN **15**

ABBREVIATIONS **19**

INTRODUCTION **25**

SKELETAL MUSCLE **27**

-Heterogeneity and plasticity of skeletal muscle 28

-Skeletal muscle regeneration 30

-Satellite cells 32

-Role of secreted factors in the regulation of MuSCs and muscle regeneration 38

DUCHENNE MUSCULAR DYSTROPHY **41**

-Molecular basis of DMD 41

-Clinical features of DMD 44

-Diagnosis 45

-Current management of DMD 45

-Emerging therapies for DMD 46

-Combined therapies for DMD 48

THE OBESTATIN/GPR39 SYSTEM **49**

-Obestatin 49

-Obestatin receptor: GPR39 51

-Obestatin bioactivity 53

-Role of the obestatin/GPR39 system in myogenesis 55

-Obestatin signalling 56

OBJECTIVES **59**

MATERIALS AND METHODS **63**

MATERIALS **65**

-Antibodies 65

-Primers 71

METHODS **71**

-Animals 71

-Single myofibre isolation and culture 72

-Small interfering RNA (siRNA) silencing of gene expression assays in single myofibres 72
-Cell cycle analysis in single myofibres 72
-Obestatin dosing in *mdx* mice 73
-Measurements of muscle force *in vivo* in *mdx* mice 73
-Blood measurements in *mdx* mice 74
-RNA extraction, cDNA synthesis and real-time PCR 74
-Cell culture and differentiation of human immortalized DMD myoblast 74
-Immunoblot analysis 75
-Histological analysis of skeletal muscle 75
-Immunofluorescence analysis of single myofibres 76
-Immunofluorescence analysis of skeletal muscle 76
-Immunofluorescence analysis in DMD cells 76
-Statistical analysis 77

RESULTS 79

CHAPTER 1: ROLE OF THE OBESTATIN/GPR39 SYSTEM IN THE REGULATION OF SATELLITE CELLS 81

-The obestatin/GPR39 system is differentially expressed during MuSC activation 83
-GPR39 signalling drives MuSCs expansion 85
-The balance between proliferation and differentiation of MuSCs is regulated by the obestatin/GPR39 system 87
-Obestatin/GPR39 signalling in MuSCs fate 92
-Obestatin activity controls Notch and β-catenin signalling pathways in MuSCs 94
-EGFR regulates the obestatin activity in MuSCs 97

CHAPTER 2: EFFECT OF OBESTATIN TREATMENT ON *mdx* MICE 99

-Obestatin treatment improves muscle strength on *mdx* mice 101
-Obestatin regulates oxidative fibre expression 105
-Obestatin modulates molecular markers of protein synthesis and degradation 110
-Obestatin-treated *mdx* mice have increased sarcolemma adhesion protein components 113
-Obestatin enhances AchRα gene 116

-Obestatin alleviates the phenotype of muscular dystrophy 116
-Toxicological analysis 118
-Obestatin signalling regulates differentiation of human DMD cells 120

CHAPTER 3: REGULATION OF UTROPHIN EXPRESSION AND AUTOPHAGY BY THE OBESTATIN/GPR39 SYSTEM IN DMD **125**

-Obestatin-dependent modulation of utrophin expression by class II HDAC/MEF2 and calcineurin/NFATc1 axis 127
-Obestatin enhances autophagy but does not stimulate the ubiquitin E3-ligases 134
-Obestatin signalling regulates autophagy in *mdx* mice 146

DISCUSSION **149**

CONCLUSIONS **163**

RESUMO **167**

AGRADECEMENTOS **179**

BIBLIOGRAPHY **183**

USC UNIVERSIDADE DE SANTIAGO DE COMPOSTELA

USC
UNIVERSIDADE
DE SANTIAGO
DE COMPOSTELA

ABSTRACT/ RESUMO/ RESUMEN

USC
UNIVERSIDADE
DE SANTIAGO
DE COMPOSTELA

ABSTRACT

The obestatin/GPR39 system functions as a mediator of skeletal muscle determination, maintenance and plasticity in physiological and pathological conditions. In satellite cells, the obestatin/GPR39 system acts as an autocrine factor regulating cell cycle progression and fate determination. In Duchenne muscular dystrophy, obestatin signalling addresses multiple pathways needed for phenotypic amelioration, including regulation of myofibre regeneration, activation of the slow oxidative myofibre program, regulation of proteasomal signalling, stabilization of the sarcolemma and induction of corrective autophagy. The results point to the obestatin/GPR39 system as a practical and effective target for future Duchenne muscular dystrophy therapies.

Keywords: obestatin signalling; skeletal muscle; muscle satellite cell; Duchenne muscular dystrophy.

RESUMO

O sistema obestatina/GPR39 funciona como un mediador de determinación, mantemento e plasticidade do músculo esquelético en condicións fisiolóxicas e patolóxicas. Nas células satélite, o sistema obestatina/GPR39 actúa como un factor autocrino que regula a progresión do ciclo celular e a determinación do destino celular. Na distrofia muscular de Duchenne, a sinalización da obestatina dirixe múltiples vías necesarias para a mellora fenotípica, incluíndo a regulación da rexeneración da miofibra, a activación do programa de miofibras de tipo lento oxidativo, a regulación da sinalización proteosomal, a estabilización do sarcolema e a indución de autofaxia correctiva. Os resultados apuntan ao sistema obestatina/GPR39 como unha diana práctica e efectiva para futuras terapias en distrofia muscular de Duchenne.

Palabras clave: sinalización da obestatina; músculo esquelético, célula satélite do músculo; distrofia muscular de Duchenne.

RESUMEN

El sistema obestatina/GPR39 funciona como un mediador de determinación, mantenimiento y plasticidad del músculo esquelético en condiciones fisiológicas y patológicas. En las células satélite, el sistema obestatina/GPR39 actúa como un factor autocrino que regula la progresión del ciclo celular y la determinación del destino celular. En la distrofia muscular de Duchenne, la señalización de la obestatina dirige múltiples vías necesarias para la mejora fenotípica, incluyendo la regulación de la regeneración de la miofibra, la activación del programa de miofibras de tipo lento oxidativo, la regulación de la señalización proteosomal, la estabilización del sarcolema y la inducción de autofagia correctiva. Los resultados apuntan al sistema obestatina/GPR39 como una diana práctica y efectiva para futuras terapias en distrofia muscular de Duchenne.

Palabras clave: señalización de la obestatina; músculo esquelético, célula satélite del músculo; distrofia muscular de Duchenne.

USC UNIVERSIDADE DE SANTIAGO DE COMPOSTELA

ABBREVIATIONS

USC
UNIVERSIDADE
DE SANTIAGO
DE COMPOSTELA

AAV: Adeno-associated virus

AchR: Acetylcholine receptor

ALT: Alanine aminotransferase

AMPK: 5' adenosine monophosphate-activated protein kinase

AONs: Antisense oligonucleotides

AST: Aspartate aminotransferase

bFGF: Basic fibroblast growth factor

BSA: Bovine serum albumin

CaMKII: Ca^{2+}/calmodulin-dependent protein kinase II

CDK: Cyclin-dependent kinase

CK: Creatine kinase

CLN: Centrally located nuclei

Coll I: Collagen type I

CPT1: Carnitine palmitoyltransferase I

CRISPR-Cas9: Clustered regularly interspaced short palindromic repeats-CRISPR associated 9

CSA: Cross-sectional area

CTGF: Connective tissue growth factor

DAPC: Dystrophin-associated protein complex

DAPI: 4',6-diamidino-2-phenylindole

dKO: double knockout

DMD: Duchenne muscular dystrophy

DM: differentiation medium

DMEM: Dulbecco's modified Eagle's medium

ECL: Enhanced chemiluminescence

EDTA: Ethylenediamine tetra-acetic acid

EdU: 5-ethynyl-2'-deoxyuridine

EGFR: Epidermal growth factor receptor

ERK1/2: Extracellular signal-regulated kinase-1/2

EERγ: Estrogen-related receptor gamma

FAPs: Fibro-adipogenic progenitors

FBS: Foetal bovine serum

FGF: Fibroblast growth factor

FoxO: Forkhead box protein O

GAPDH: Glyceraldehyde 3-phosphate dehydrogenase

GLP-1: Glucagon-like peptide-1

GLP-1R: Glucagon-like peptide-1 receptor

GLUT4: Glucose transporter type 4

GM: Growth medium

GPCR: G-protein-coupled receptor

GPR39: G-protein 39-coupled receptor

GSK3: Glycogen synthase kinase 3

HDAC: Histone deacetylase

hEGF: Human hepatocyte growth factor

HE: Haematoxylin and eosin

HEK: Human embryonic kidney

HGFA: Hepatocyte growth factor activator

HGF: Hepatocyte growth factor

hpd: hours post-differentiation

IF: Immunofluorescence

IGF-1: Insulin-like growth factor 1

IgG: Immunoglobulin G

IL-1: Interleukin 1

iPS: Induced pluripotent stem

LC3: Microtubule-associated protein light chain 3

MAFbx: Muscle atrophy F-box

MAPK: Mitogen-activated protein kinase

MEF2: Myocyte enhancer factor-2

MFI: Mean fluorescence intensity

MHC: Myosin heavy chain

MLPA: Multiplex-ligation-dependent probe amplification

MMPs: Matrix metalloproteinases

MRF4: Myogenic regulatory factor 4

MRFs: Myogenic regulatory factors

mTORC1: Mammalian target of rapamycin complex 1

mTOR: Mammalian target of rapamycin

mtTFA: Mitochondrial transcription factor A

MuRF-1: Muscle RING-finger protein-1

MuSCs: Muscle satellite cells

Musk: Muscle-specific kinase

Myf5: Myogenic factor 5

MyoD: Myogenic differentiation

NFAT: Nuclear factor of activated T-cells

NF-κB: Nuclear factor kappa-light-chain-enhancer of activated B cells

NICD: Notch intracellular domain

NMJ: Neuromuscular junction

nNOS/NOS1: Neuronal nitric oxide synthase

PAR: Partitioning-defective protein

Pax3: Paired box protein 3

Pax7: Paired box protein 7

PBS: Phosphate-buffered saline

PCP: Planar cell polarity

PFA: Paraformaldehyde

PGC-1α: Peroxisome proliferator-activated receptor gamma coactivator 1-alpha

PKCλ: Protein kinase C lambda

p62/SQSTM1: Sequestosome-1

RPS20: Ribosomal protein S20

SDH: Succinate dehydrogenase

SDS-PAGE: Sodium dodecyl sulfate-polyacrylamide gel electrophoresis

SEM: Standard error of the mean

SER: Serum response element

siRNA: Small interfering RNA

TA: *Tibialis anterior*

TGF-β: Transforming growth factor beta

TNF-α: Tumour necrosis factor alpha

UCP3: Uncoupling protein 3

ULK1: Unc-51 like autophagy activating kinase 1

Vangl2: Vang-like protein 2

VEGFR2: Vascular endothelial growth factor receptor 2

VEGF: Vascular endothelial growth factor

WB: Western blot

WT: wild-type

ZnR: Zn+2-sensing receptor

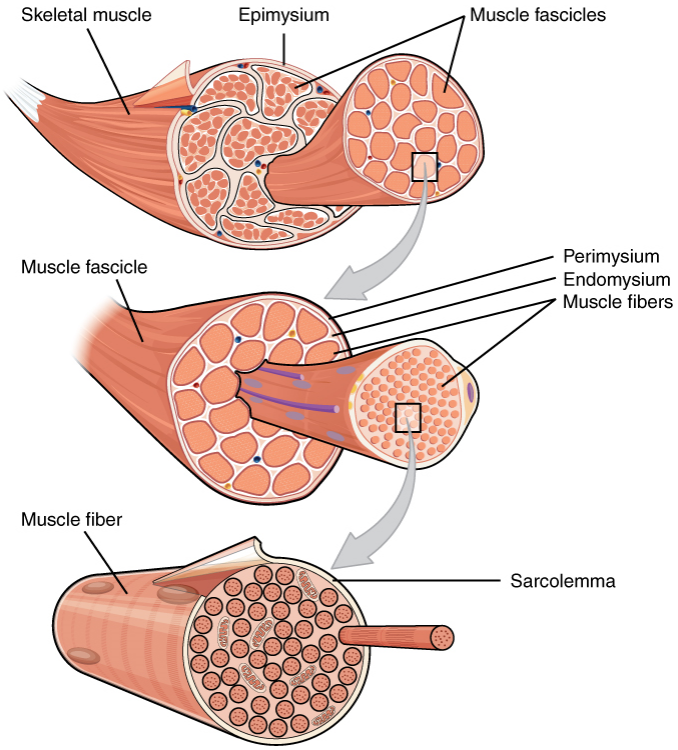
α-SMA: Alpha-smooth muscle actin

INTRODUCTION

USC
UNIVERSIDADE
DE SANTIAGO
DE COMPOSTELA

SKELETAL MUSCLE

Skeletal muscle is one of the largest tissues in the body, accounting for 30-50% of adult human body weight, and is responsible for maintaining posture as well as locomotion. In addition, skeletal muscle plays a central role in the control of whole-body metabolism, acting as an endocrine organ[1].



Scheme 1. Structure of skeletal muscle tissue. Skeletal muscle is composed of myofibres wrapped by endomysium. Bundles of myofibres are surrounded by perimysium, and these bundles are grouped to form muscle, lined by epimysium. From OpenStax College, Anatomy and Physiology. OpenStax CNX. 17 oct. 2018 http://cnx.org/contents/14fb4ad7-39a1-4eee-ab6e-3ef2482e3e22@12.6. Licensed under Creative Commons.

Skeletal muscle is an organ that consists of various integrated tissues, including the skeletal muscle fibres, blood vessels, nerve fibres and connective tissue. It is composed of bundles of contractile muscle fibres-

called myofibres- that are large, differentiated, multinucleated cells formed by the fusion of committed myogenic progenitors. Each myofibre is surrounded by a layer of connective tissue called endomysium. Bundles of myofibres are surrounded by the perimysium, while the entire muscle is contained within the epimysium (Scheme 1). Myofibres are composed of functional units called sarcomeres, which are responsible for the striated appearance of skeletal muscle. Within each sarcomere are the myofibrillar proteins myosin (the thick filament) and actin (the thin filament). The interaction of these two myofibrillar proteins allows the muscle to contract, as a response to the calcium released from the sarcoplasmic reticulum due to signals from motor neurons[2,3].

HETEROGENEITY AND PLASTICITY OF SKELETAL MUSCLE

Muscle heterogeneity: classification of myofibre types

Skeletal muscle is comprised of heterogeneous muscle fibres that differ in their physiological, biochemical and metabolic parameters. This diversity of myofibres enables different muscle groups to provide a variety of functional properties[4]. The classification of myofibre types have employed many different criteria, including: colour of muscle fibres (red *vs.* white) that correlates with myoglobin content; contractile properties of the motor units in response to electrical stimulation; speed of shortening during a single twitch (fast *vs.* slow); degree of fatigability during sustained activation (fatigable *vs.* fatigue-resistant); predominance of certain metabolic or enzymatic pathways (oxidative *vs.* glycolytic); enzyme-histochemical stain reaction (based on ATPase or SDH staining techniques); calcium handling by the sarcoplasmic reticulum (slow *vs.* fast); and protein isoform expression, among others[5].

Of the multitude of classification schemes, one of the most informative method to determine muscle fibre types is the based on specific myosin heavy chain (MHC) isoform expression[6]. On this basis, myofibres are classified into type I (also termed slow-twitch), and type II (or fast-twitch) fibres. Type II myofibres can be classified, as well, as type IIa, type IIx and type IIb fibres. According to metabolic parameters, type I and type IIa fibres exhibit and oxidative metabolism, whereas types IIx and IIb are mainly

glycolytic. Thereby, type I fibres are rich in mitochondria, are more vascularized, exert a slow contraction, and have a high resistance to fatigue, thus they are required for maintenance of posture and task involving endurance. On the contrary, type II fibres exert quick contractions and fatigue rapidly, so they are used for movements involving strength and speed (Table 1). On the other hand, myofibres can contain a single MHC isoform ("pure fibres") or multiple MHC isoforms ("hybrid fibres")[4].

Table 1. Properties of MHC type I, IIa, IIx and IIb myofibres

	MHC I	MHC IIa	MHC IIx	MHC IIb
Contraction speed	Slow	Moderately fast	Fast	Very fast
Resistance to fatigue	High	Moderately high	Intermediate	Low
Mitochondrial density	High	High	Medium	Low
Capillary density	High	Intermediate	Low	Low
Myoglobin content	High	High	Low	Low
Colour	Red	Red	White	White
Oxidative capacity	High	High	Intermediate	Low
Glycolytic capacity	Low	High	High	High
Fibre diameter	Small	Intermediate	Large	Large
Activity used for	Aerobic	Long-term anaerobic	Short-term anaerobic	Short-term anaerobic

Myofibre adaptability: the plasticity of skeletal muscle

The structural and functional properties of the myofibres, which are generally referred to as fibre phenotype, can change in response to a variety of physiological and pathological signals. This ability of remodelling to adapt to the environmental demands is defined as muscle plasticity[7]. This remarkable capacity of the skeletal muscle was firstly observed by Buller et al. in 1960 by a cross-innervation experiment in which the innervation of a fast-twitch muscle with nerve fibres that normally supply slow-twitch muscle resulted in a slower contraction, that is, the myofibres acquired the

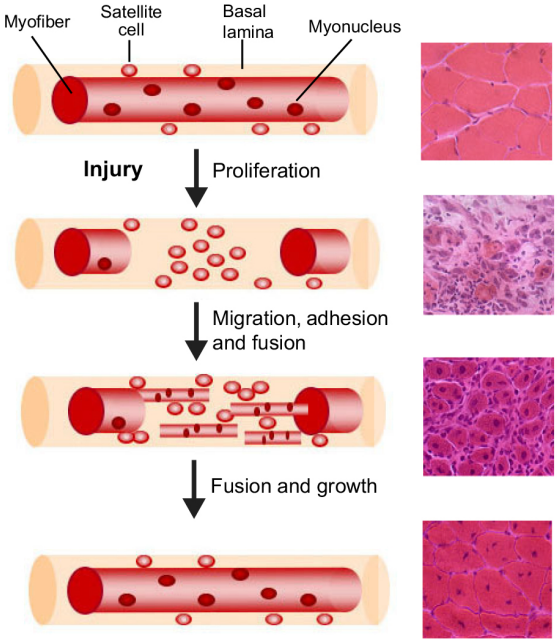
characteristics of slow-twitch fibres[8]. This study showed the importance of the neuromuscular activity in fibre phenotype transitions, but many different conditions such mechanical loading or unloading, altered hormonal profiles (especially of the thyroid hormones), or ageing can induce myofibre remodeling[6].

The diversity in fibre types along with fibre type plasticity not only provide for a wide range of functions but also provide differential susceptibility to certain muscle diseases. Actually, there are many myopathies and acquired muscle wasting and metabolic disorders that preferentially affect specific skeletal muscle fibre types, like Duchenne muscular dystrophy (DMD), sarcopenia, diabetes or obesity, among others[9]. In particular, it was observed that DMD affects preferentially fast myofibres[10], so the transition to a slow myofibre phenotype has emerged as a strategy to ameliorate this disease[11]. Thus, understanding the mechanisms that regulate skeletal muscle plasticity may provide important insights into muscle disease pathologies and potential treatments. In this sense, several signalling pathways have been identified as powerful regulators in the specification and remodelling of skeletal muscle phenotype, including calcineurin/ nuclear factor of activated T-cells (NFAT), myocyte enhancer factor-2 (MEF2), histone deacetylases (HDACs), peroxisome proliferator-activated receptor gamma coactivator 1-alpha (PGC-1α) and AMP-activated protein kinase (AMPK)[4,7].

SKELETAL MUSCLE REGENERATION

Adult skeletal muscle is a stable postmitotic tissue with little turnover of nuclei, with only ~1-2% of myofibre nuclei replaced each week under normal physiological conditions[12]. However, skeletal muscle has the remarkable ability to complete a rapid and extensive repair process in response to severe damage caused by intense trauma (i.e. extensive physical activity, resistance training) or muscle degenerative diseases. Upon injury, skeletal muscle undergoes a highly orchestrated process that takes place at the tissue, cellular and molecular levels, leading to the formation of functional contractile apparatus[13,14].

Muscle tissue repair consists of two phases: degeneration and regeneration[2,13,14]. The muscle degenerative phase begins with a rapid necrosis of the damaged myofibres. This event is initiated by the disruption of the sarcolemma integrity, which leads to increased myofibre permeability. As a consequence, there is an increase in the serum levels of muscle proteins, such as creatine kinase (CK), along with an increment of calcium influx that activates calcium-dependent proteolysis and drives tissue degeneration. Myofibre necrosis also activates the complement cascade and induces inflammatory responses that play an important role in the activation of repair processes necessary for successful recovery from injury. As a result, there is a chemotactic recruitment of inflammatory cells at local sites of damage. The first inflammatory cells to invade the injured muscle are the neutrophils[15]. Following neutrophil infiltration, two distinct subpopulations of macrophages sequentially invade the injured muscle and become the predominant inflammatory cells[16]. The early invading macrophages, characterized by the surface markers $CD38^{+}/CD163^{-}$, secrete proinflammatory cytokines, such as tumour necrosis factor alpha (TNF-α) and interleukin-1 (IL-1), and are responsible for the phagocytosis of cellular debris. The second population of macrophages, characterized by the surface markers $CD38^{-}/CD163^{+}$, secrete anti-inflammatory cytokines and facilitate the proliferation and differentiation of satellite cells[17]. After the degenerative phase, it takes place the activation of the regeneration process. The impressive ability of skeletal muscle to repair itself greatly relies on satellite cells (MuSCs)[18]. Under physiological conditions, MuSCs remain in a quiescent state, but after injury, quiescent MuSCs are activated to enter the cell cycle and proliferate. This proliferation step is considered a crucial event in muscle regeneration. Then, MuSCs differentiate and fuse to form new myofibres or to repair the damaged fibres in a process that resembles embryonic myogenesis. Finally, the regenerated muscle is morphologically and functionally indistinguishable from undamaged muscle (Scheme 2)[19].

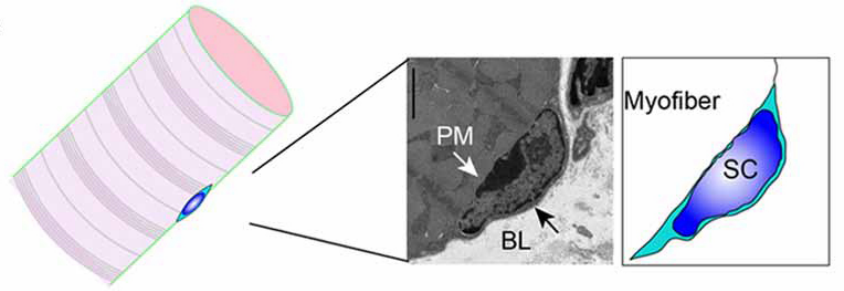


Scheme 2. Skeletal muscle regeneration. *Left panel.* Schematic representation of the skeletal muscle regeneration process after injury. *Right panel.* Mouse muscle sections stained with haematoxylin-eosin (HE) representative of the morphological characteristics of the different stages of the regeneration process. From Abbmayr SM et al. Myoblast fusion: lessons from flies and mice. *Development*. 2012; 139(4):641-56. Permitted by The Company of Biologists Ltd.

SATELLITE CELLS

In 1961, Alexander Mauro et al. described a population of mononuclear cells located at the periphery of myofibres in electron micrographs of skeletal muscle. These cells were named satellite cells (MuSCs) due to their relative anatomical position, between the muscle sarcolemma and the basal lamina of individual myofibres (Scheme 3)[20]. MuSCs are skeletal muscle stem cells that play a crucial role in maintaining muscle homeostasis and regeneration after injury[21]. They represent ~2-10% of total myonuclei of adult muscle, and can be characterized by the expression of the canonical MuSC regulator, paired box protein 7 (Pax7)[22,23]. Most MuSCs in postnatal muscle originate from a population of embryonic

precursors of mesodermal origin that express Pax7 and/or Pax3 and which arise from a dorsal structure of the developing somite, known as the dermomyotome[24,25].



Scheme 3. The satellite cell. MuSCs reside adjacent to the plasma membrane under the basal lamina on the surface of the myofibre. Electron microscopy of the MuSC and schematic representation of MuSC position on the myofibre. PM, plasma membrane; BL, basal lamina; SC, satellite cell. From Fukada S et al. Isolation, characterization, and molecular regulation of muscle stem cells*. Front Physiol.* 2013;12(4):317. Licensed under Creative Commons.

MuSCs comprise a heterogeneous population of cells that differ in their expression profile, proliferation/differentiation potential and stemness[2,26]. The heterogeneity in the expression profile of MuSCs is evidenced by the differences observed in the expression of different factors, such as Pax3[27], or cell surface markers, like CD34 and M-cadherin[28]. In relation to the mitotic rate, it was demonstrated that MuSCs are a mixture of 80% fast-cycling cells that rapidly enter the cell cycle and 20% slow-cycling "reserve cells" that only proliferate in response to the need for extensive muscle growth/regeneration[29]. Most important, MuSCs are heterogeneous in terms of stemness, indicating that only a small percentage of MuSCs are "true stem cells". In this sense, a study revealed the existence of two subpopulations of MuSCs based on the expression of the myogenic factor 5 (Myf5): $Myf5^-$ cells, which are stem cells, and $Myf5^+$ cells, that represent committed myogenic progenitors. These two subpopulations also differ in their regenerative potential: after transplantation, $Myf5^+$ cells undergo myogenic differentiation whereas $Myf5^-$ cells repair muscle and extensively contribute to replenishment of the MuSC compartment[30]. This correlates with previous studies that proved

that only a portion of MuSCs exhibit repopulating activity[31]. Various degenerative or disease states, such as DMD and sarcopenia, affect the functional capacity of MuSCs and, consequently, impairs muscle regeneration. Thereby, understanding MuSCs behaviour is indispensable for the development of new therapeutic approaches[32].

Quiescence, activation and differentiation of MuSCs

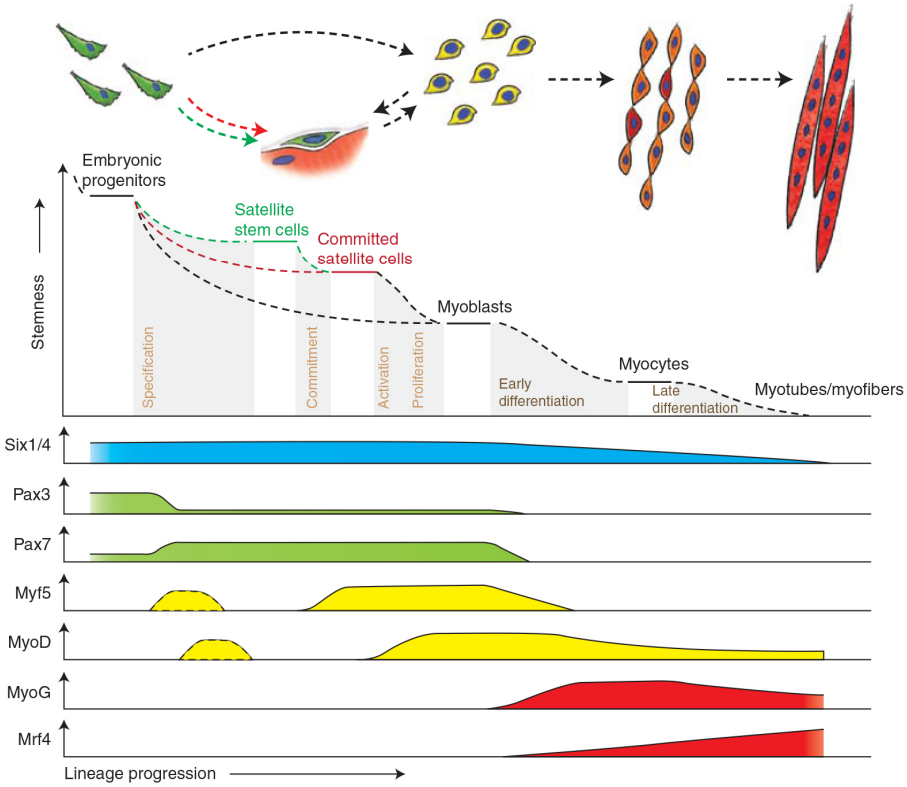
Quiescence and the MuSC niche

In resting adult muscles, MuSCs exist in a dormant, non-mitotic state known as quiescent. Quiescent MuSCs are characterized by the expression of Pax7 and the absence of the myoblast determination factor (MyoD). They reside in a specialized location between the muscle sarcolemma and the basal lamina of myofibres, termed the MuSC niche. The concept of MuSC niche refers to a microenvironment composed of cellular and acellular components, including extracellular matrix proteins, growth factors, myofibres and muscle-resident non-myogenic cells [such as fibro-adipogenic progenitors (FAPs), macrophages, etc.] that play a crucial role in maintaining quiescence and regulating fate determination of MuSCs[33]. The ability of MuSCs to maintain quiescence in the resting state is essential for the long-term conservation of the MuSC pool. In this sense, Notch pathway acts as a master regulator of MuSC quiescence[34].

Activation and differentiation

Upon muscle injury, quiescent MuSCs become activated and proliferate to give rise to a population of myogenic precursor cells known as myoblast. Following several rounds of proliferation, myoblast exit the cell cycle and start to differentiate and fuse to form multinuclear myotubes or repair the existing damaged myofibres. The process of MuSC activation and differentiation is regulated by a family of muscle-specific, basic helix-loop-helix transcription factors called myogenic regulatory factors (MRFs), consisting of Myf5, MyoD, myogenin and myogenic regulatory factor 4 (MRF4). Myf5 and MyoD are critical for myogenic cell determination. During muscle regeneration, MuSCs can be distinguished based on Pax7 and MyoD expression. Activated MuSCs co-express Pax7 and MyoD. After some rounds

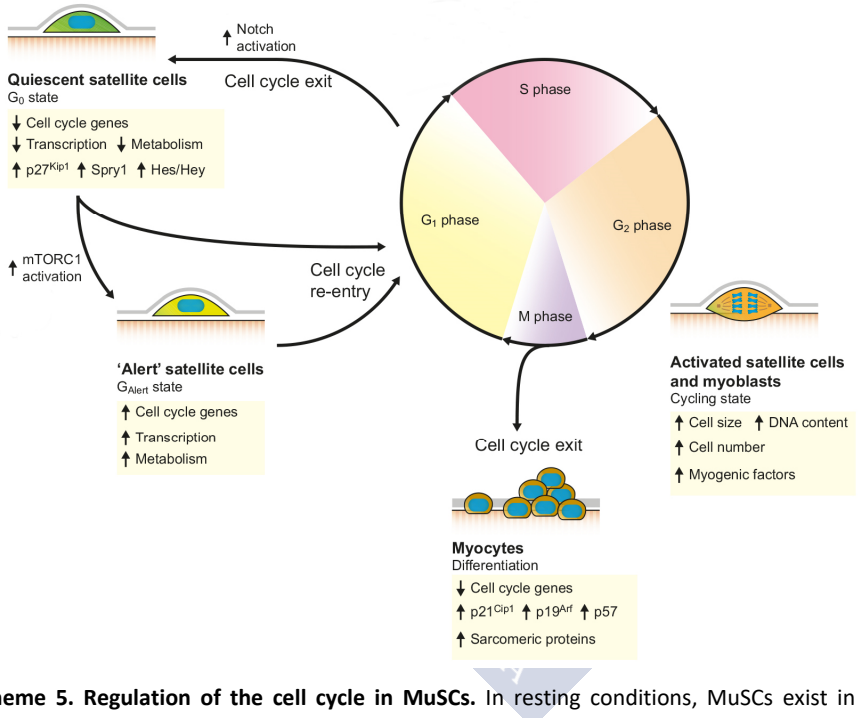
of proliferation, activated MuSCs give rise to Pax7^{-}/MyoD^{+} cells, which are committed to proliferation[35]. A subset of activated MuSCs originates Pax7^{+}/MyoD^{-} cells, which revert to a quiescent state to replenish the MuSC pool, thus ensuring the capacity to respond to future injuries[31]. Finally, the terminal differentiation of myogenic progenitors is marked by the early expression of myogenin and MRF4, and the subsequent expression of myofibrillar proteins, such as MHC, just prior to fusion into myotubes (Scheme 4)[19,33,36].



Scheme 4. Hierarchy of transcription factors regulating progression through the myogenic lineage. Pax3 and Pax7 are master regulators of early lineage specification. Myf5 and MyoD determine commitment of MuSCs. Myogenin (MyoG) and MRF4 are required for terminal differentiation of myogenic precursors. From Bentzinger CF et al. Building muscle: molecular regulation of myogenesis. *Cold Spring Harb Perspect Biol*. 2012;4(2):a008342. With permission from Cold Spring Harbor Laboratory Press.

G_{Alert} state: between quiescence and activation

Recently, it was described a new MuSC functional phase termed "alert" phase or G_{Alert}[37]. This intermediate phase or state between the G_o quiescent and activated cell states can be reversibly adopted by MuSCs, allowing a rapid transition from quiescence to activation to enable efficient muscle repair (Scheme 5).



Scheme 5. Regulation of the cell cycle in MuSCs. In resting conditions, MuSCs exist in a reversible and quiescent G_0 state. Upon activation, MuSCs re-enter the cell cycle either directly or via the intermediate G_{Alert} state. Then, MuSCs can exit the cell cycle and return to quiescence or progress into the myogenic lineage. Adapted from Dumont NA et al. Intrinsic and extrinsic mechanisms regulating satellite cell function. *Development*. 2015;142(9):1572-1581. Licensed under Creative Commons.

MuSCs in "alert" state are phenotypically different from classical quiescent cells, as they are larger in size and have more functional mitochondria. In addition, these "alert" MuSCs exhibit a greater regenerative potential as a consequence of a shortened time until their first division and a higher propensity to differentiate and fuse with damaged

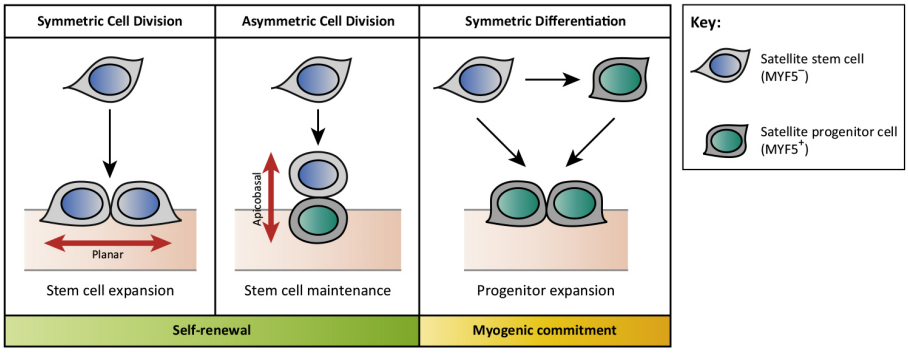
myofibres compared to quiescent cells. Thus, G_{Alert} represents a discrete stage of the cell cycle that prime MuSCs for activation, enabling them to respond more rapidly to muscle damage. It was demonstrated that the transition of MuSCs from quiescence to G_{Alert} requires mTORC1 activation[37]. A recent study also proved that hepatocyte growth factor activator (HGFA) acts as a systemic factor that induces the entry of MuSCs into the G_{Alert} sate, suggesting the existence of a system-wide response mechanism after injury[38].

Self-renewal of MuSCs: symmetric and asymmetric divisions

The self-renewal ability of MuSCs is essential for the maintenance of muscle homeostasis since provides the myogenic progenitors necessary for muscle regeneration but also maintains the stem cell population[30]. Thus, a defect in self-renewal ability leads to a decrease in MuSC number, resulting in depletion of the MuSC pool as well as in reduced muscle regeneration capacity. MuSCs can regulate self-renewal by performing two different types of cell division: symmetric or asymmetric (Scheme 6). Trough asymmetric division, one parental stem cell gives rise to two functionally different daughter cells: one stem cell that replenishes the stem cell pool, and one committed progenitor that participates in muscle regeneration. On the contrary, in the symmetric division, one parental stem cell divides into two identical daughter stem cells[19,33,34,39].

Fate decisions in MuSCs involve two major interacting events: the mitotic spindle orientation and the distribution of polarity proteins and cell fate determinants. Regarding division orientation, symmetric division occurs parallel to the myofibre axis so both cells are in contact with the myofibre plasma membrane and the basal lamina. By contrast, asymmetric division takes place in an apicobasal orientation, such that the satellite stem cell ($Myf5^-$) remains attached to the basal membrane while the committed progenitor ($Myf5^+$) is in contact with the myofibre (Scheme 6). It seems that the apical cell becomes committed due to loss of contact with the basal lamina and the extracellular matrix, which suggest that the MuSC niche plays an important role in division orientation and hence in cell fate determination[30]. Concerning polarity distribution, it was demonstrated that

symmetric division is promoted by the activation of the planar cell polarity (PCP) pathway, which leads to the symmetric distribution of polarity effectors such as Vang-like protein 2 (Vangl2) in daughter cells[40]. Conversely, asymmetric division is characterized by the segregation of different cell fate determinants into de daughter cells. In this sense, recent findings highlight the role of the partitioning-defective protein (PAR) complex, a known master regulator of cell polarity establishment in many different stem cell types. During asymmetric division, the complex partitioning defective 3-protein kinase C lambda (PAR-3-PKCλ) is asymmetrically distributed in the committed daughter cell and activates phospho-p38α/β MAPK. Activation of phospho-p38α/β MAPK leads to induction of MyoD and consequently, the commitment of the daughter cell into a myogenic progenitor[41]. Nonetheless, the exact mechanisms that govern MuSC fate decisions remain to be characterized.

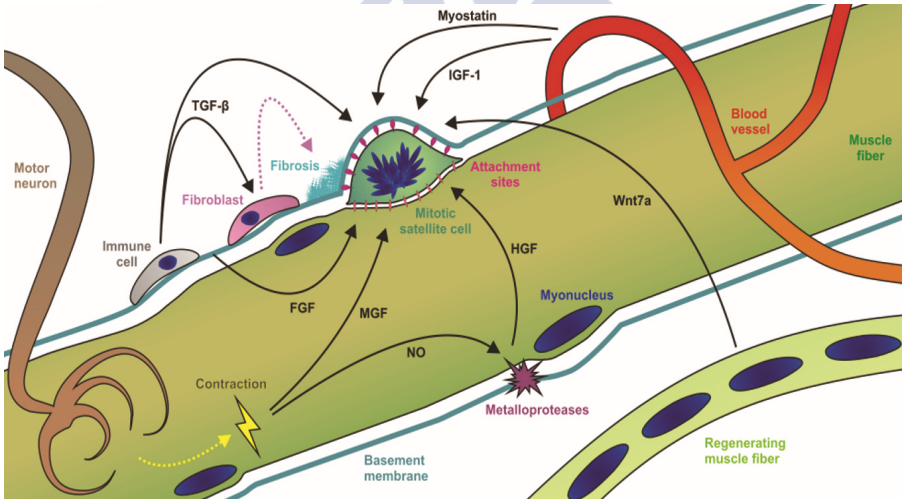


Scheme 6. Asymmetric and symmetric division of MuSCs. Asymmetric divisions occur perpendicular to the fibre axis generating one self-renewing cell (Myf5$^-$; *blue*) and one committed cell (Myf5$^+$; *green*). Symmetric divisions occur parallel to the muscle fibre axis and generate two identical (either stem or committed progenitor) daughter cells. From Chang NC et al. Satellite cells in muscular dystrophy-Lost in polarity. *Trends Mol Med*. 2016;22(6):479-496. With permission from Elsevier.

ROLE OF SECRETED FACTORS IN THE REGULATION OF MuSCs AND MUSCLE REGENERATION

MuSCs emerged as a promising cell-based therapy to restore or enhance the regenerative capacity of diseased muscle. However, this

approach has several limitations that need to be overcome, such as the incompatibility with systemic delivery, the difficulty of obtaining large number of MuSCs from a donor as well as their reduced myogenic potential after culture, the poor migration and survival of MuSCs after transplantation, and the development of an immune response. Moreover, to successfully apply MuSCs to cell-based regenerative medicine, it is crucial to have a comprehensive understanding of the extrinsic factors that regulate MuSC function (Scheme 7)[42,43]. Muscle injuries cause the release of biologically active molecules into the extracellular space that may be endogenous to the injured tissue itself or may be synthesized and secreted by other cell types at the wound site, including neutrophils and macrophages[13]. All these factors are thought to play a role in the different stages of muscle regeneration. The identification of these factors provides the opportunity to develop new therapies that mimic or interfere with these molecules[42,43].



Scheme 7. Secreted factors regulating MuSCs. Schematic representation of the different environmental cues influencing a MuSC in its niche. FGF, fibroblast growth factor; HGF, hepatocyte growth factor; IGF, insulin-like growth factor; MGF, mechano growth factor; NO, nitric oxide; TGF, transforming growth factor. From Bentzinger CF et al. Extrinsic regulation of satellite cell specification. *Stem Cell Res Ther*. 2010;1(3):27. Licensed under Creative Commons.

TGF-β family: myostatin. Transforming growth factor beta (TGF-β) family members are known modulators of myoblast activity, inhibiting both proliferation and differentiation[13]. Myostatin, a member of the TGF-β family, has been demonstrated to be a powerful antagonist of muscle growth, and its inhibition leads to increased muscle mass[44]. Several circulating factors that modulate the activity of myostatin have been discovered such as follistatin, a potent myostatin antagonist that causes muscle gain[45].

HGF. Hepatocyte growth factor (HGF) is bound to the extracellular matrix in muscle tissue and is released in response to injury. HGF is believed to play a fundamental role during muscle regeneration, especially during the initial phase of muscle repair[46]. HGF exerts a mitogenic activity and promotes the quiescent MuSCs to enter the cell cycle[38] while inhibiting differentiation of myogenic precursor cells[46].

FGF. Several fibroblast growth factors (FGFs), particularly the isoforms FGF-6 and FGF-2, have been demonstrated to induce the proliferation of cultured myoblasts while inhibiting their differentiation, indicating a role for these factors in the expansion of MuSCs[43,47].

IGF-1. Insulin-like growth factor 1 (IGF-1) operates in a paracrine/autocrine manner, causing increased muscle mass and enhanced regeneration. IGF-1 acts by promoting both the proliferation and the differentiation/fusion of myoblasts. Moreover, the hypertrophic effect of IGF-I is attributed to both the activation of MuSC to proliferate providing more myonuclei and to the increased protein synthesis within existing myofibre[48].

Wnt-7. Wnt proteins are secreted lipid-modified glycoproteins that act through Frizzled receptors. There is a wide variety of Wnts that perform different functions, both promoting and inhibiting myogenesis. Among them, Wnt-7a improves remarkably muscle regeneration by promoting hypertrophy and symmetric expansion of MuSCs[40,49].

DUCHENNE MUSCULAR DYSTROPHY

Duchenne muscular dystrophy (DMD) is a lethal X-linked recessive neuromuscular disorder caused by mutations in the *DMD* gene that result in absence of dystrophin, a cytoskeletal protein that enables the strength, stability, and functionality of myofibres[50,51]. The absence of dystrophin leads to progressive muscle weakness, degeneration, and wasting, with premature death due to respiratory and/or cardiac failure[50]. DMD is the most common form of muscular dystrophy in childhood, affecting one in 5000 newborn males[52]. Female carriers are usually asymptomatic, but some show mild symptoms of muscle disease, and about 10% may develop isolated cardiomyopathy[53,54]. Currently, there is no cure for DMD, and the treatments available are destined to alleviate the symptoms[55].

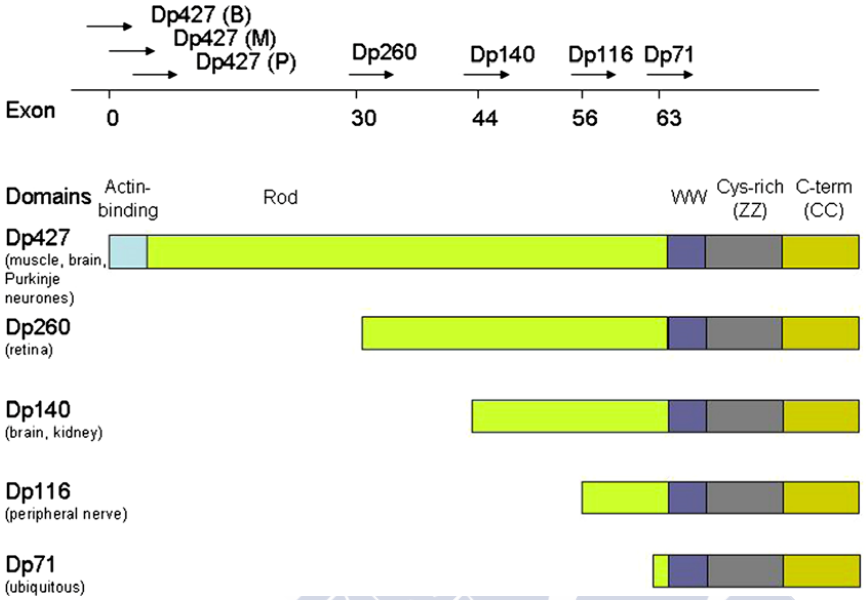
MOLECULAR BASIS OF DMD

The *DMD* gene

The *DMD* gene is located to Xp21 and is composed of 79 exons. It is the largest gene described in humans, spanning 2,5 Mb of genomic sequence[56]. Its transcription is regulated in a tissue-specific manner by several promoters. The full-length dystrophin isoform, Dp427, is expressed in cardiac and skeletal muscle, brain and cerebellar Purkinje neurons. Four shorter non-muscle isoforms are also expressed from the dystrophin gene and they are named in accordance with their molecular weights: Dp260 is found in the outer plexiform layer of the retina; Dp140 is detected in the kidney, retina, and brain; Dp116 is mainly expressed in Schwann cells in spinal cord; and Dp71 is broadly expressed in cardiac muscle, retina, kidney, liver, lung and brain (Scheme 8). Mutations in these shorter isoforms contribute to the non-muscle symptoms of DMD[51].

The *DMD* gene has one of the highest spontaneous mutation rates. About 68% of DMD patients present large “out of frame” deletions, mainly involving two “hot spots” located around exons 45-53 and exons 2-30, that disrupt the translational reading frame resulting in loss of dystrophin. Conversely, “in frame” mutations result in truncated but semi-functional dystrophin protein, leading to a clinically milder disease defined as Becker

muscular dystrophy. Duplications represent 11% of DMD cases, and small deletions or point mutations that introduce a stop codon are responsible for about 20% of DMD cases[57].

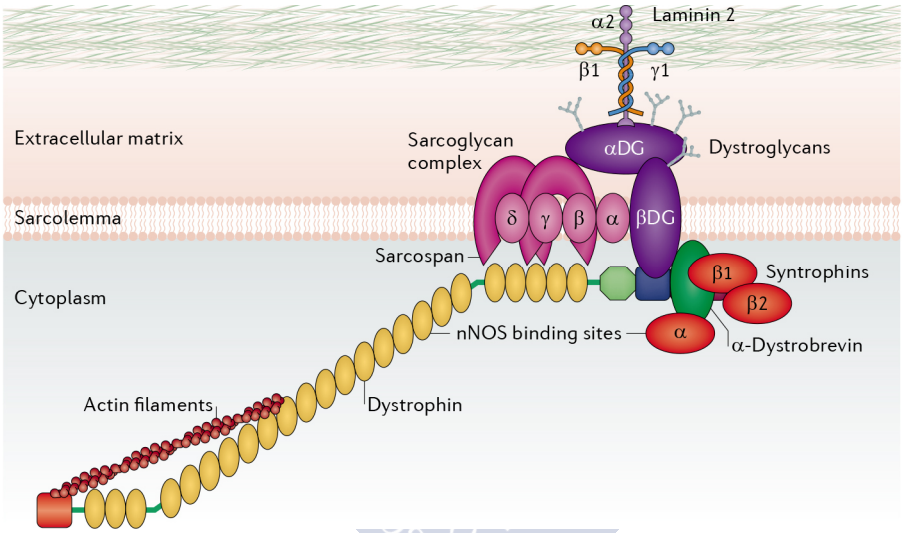


Scheme 8. The dystrophin gene and its protein products. Schematic representation of the location of the promoters within the dystrophin gene and the composition of the different dystrophin isoforms. Dp, dystrophin protein; (B), brain; (M), muscle; (P), Purkinje neurons. From Willmann R et al. Mammalian animal models for Duchenne muscular dystrophy. *Neuromuscul Disord*. 2009;19(4):241-9. With permission from Elsevier.

Dystrophin and the dystrophin-associated protein complex

Dystrophin is a large, 427 kDa, rod-shaped intracellular protein localized to the cytoplasmic face of the sarcolemma[58,59]. It is a critical component of the dystrophin-associated protein complex (DAPC), anchoring the F-actin filaments of the intracellular cytoskeleton within the myofibre to the basal lamina and extracellular matrix. Dystrophin belongs to the spectrin protein superfamily and is composed of four domains: the N-terminal domain, which binds to F-actin filaments; a long central rod domain, consisting of 24 spectrin-like repeats and containing an additional actin-binding region as well as an nNOS binding site; a cysteine-rich domain;

and a C-terminal domain, which binds to the DAPC. DAPC is a structural complex that provides a linkage between the cytoskeleton and the extracellular matrix. It is comprised of sarcoplasmic proteins (α-dystrobrevin, syntrophins and nNOS), transmembrane proteins (β-dystroglycan, sarcoglycans, caveolin-3 and sarcospan), and extracellular proteins (α-dystroglycan and laminin). Mutations on different members of the DAPC cause distinct muscular dystrophies that vary in terms of severity, age of onset and involvement of muscle groups (Scheme 9)[51,60].



Scheme 9. The dystrophin-associated protein complex (DAPC). DAPC connects the internal cytoskeleton and the extracellular matrix through a large multiprotein complex that includes dystrophin, laminin, sarcoglycans, dystroglycans, sarcospan, dystrobrevin, syntrophins, and associated proteins such as nNOS. αDG, α-dystroglycan; βDG, β-dystroglycan. From Fairclough RJ et al. Therapy for Duchenne muscular dystrophy: renewed optimism from genetic approaches. *Nat Rev Genet*. 2013;14(6):373-8. With permission from Springer Nature.

Dystrophin provides structural stability to the skeletal muscle, maintains strength and flexibility and protects the sarcolemma from contraction-induced injury[61]. In absence of dystrophin, the DAPC becomes destabilized and the levels of the other DAPC proteins diminish. As a consequence, the sarcolemma is more susceptible to contraction-injury,

provoking membrane damage that increases the permeability to calcium, which causes cell dysfunction and death. The continued cell death provokes an inflammatory response and an imbalance between muscle degeneration and regeneration of skeletal muscle. These chronic cycles of degeneration and regeneration progressively incapacitate MuSCs to compensate the dystrophic damage. This leads to the disease pathology, resulting in a progressive decline of muscle function from the loss of muscle myofibres and their replacement by connective and fatty tissue[62–64].

CLINICAL FEATURES OF DMD

DMD usually manifests at the age of 3-5 years, when patients start to display symptoms of skeletal muscle decline including fatigue, difficulty standing (resulting in the Gower maneuverer), walking, running, climbing stairs and jumping, as well as frequent falls and a characteristic waddling or Trendelenburg gait[65]. Skeletal muscles of DMD patients, particularly the calves, develop muscle pseudohypertrophy due to fibrosis and increased fat deposition[66]. Most boys gain strength and motor skills until about 6-8 years of age, but after this stage, strength progressively deteriorates. Around the age of 12, patients lose the ability to walk and are confined to wheelchair use[67]. Although skeletal muscle symptoms are considered the defining characteristic of DMD, patients most commonly die of respiratory or cardiac failure. Cardiac most common manifestations are dilated cardiomyopathy and arrhythmias, but patients are relatively asymptomatic due to physical inactivity. Respiratory complications include respiratory muscle fatigue, mucus plugging, atelectasis, pneumonia and respiratory failure. Cardiorespiratory complications are the principal cause of morbidity and mortality in DMD patients, leading to premature death in their late teens to early 20s[68]. However, recent advances in respiratory support have increased life expectancy until the late 30s[69]. Another symptom of DMD is the development of orthopaedic complications, especially scoliosis, which progresses significantly after loss of ambulation and impacts on respiratory vital capacity. Joint contractures are also frequent, mainly at the hips, knees, ankle joints and iliotibial bands[67]. DMD patients also present some degree of intellectual impairment, which unlike muscular and cardiac

symptoms, has not been shown to be progressive. These boys present an increased incidence of autism, attention deficit hyperactivity disorder, obsessive-compulsive disorder and specific language, reading and learning disabilities[65–67].

DIAGNOSIS

The early and accurate diagnosis of DMD is a crucial aspect of care[50,70]. The diagnostic process typically begins in early childhood when the first symptoms manifest. The initial diagnostic test is usually the analysis of serum creatine kinase (CK) levels, which are markedly raised in DMD patients, usually 50 to 100 times normal values. Serum CK concentrations are elevated even at birth, providing the opportunity for newborn screening[52,66]. Although not a specific finding, the concentrations of serum alanine aminotransferase (ALT) and aspartate aminotransferase (AST) are also elevated due to muscle damage[66,71]. Molecular genetic testing forms the mainstay of diagnosis. Deletions and duplications in the dystrophin gene can be detected by multiplex-ligation-dependent probe amplification (MLPA) or comparative genomic hybridization array. If deletion or duplication testing is negative, then genetic sequencing is required to detect point mutations. Finally, if genetic testing does not confirm a clinical diagnosis of DMD, it would be necessary to perform a muscle biopsy to determine the absence of dystrophin by immunohistochemistry or western blot analysis[50].

CURRENT MANAGEMENT OF DMD

Currently, there is no cure for DMD. Conventional treatment strategies focus on supportive therapy that partially reduces symptoms of DMD[55]. Standard of care includes the use of corticosteroids to prolong ambulation and to delay the onset of secondary complications like scoliosis and cardiomyopathy. However, long-term treatment with corticosteroids produces side effects such as obesity, immunosuppression, behavioural changes and skeletal fractures[72]. Supportive interventions also include surgery, physiotherapy and management of the cardiomyopathy and the pulmonary disease, among others[55]. Notably, therapy to treat

cardiomyopathy and the use of assisted non-invasive ventilation have contributed to the improved health-related quality of life and prolonged life expectancy of DMD patients from late adolescence to late thirties[69,73]. However, such therapies do not reverse the phenotype nor directly target the disease mechanism responsible for the pathology.

EMERGING THERAPIES FOR DMD

Over the past few years, different therapeutic approaches have emerged to target or compensate the primary defect of DMD, that is, the absence of dystrophin. These strategies include gene-based, cell-based and pharmacological therapies.

Gene therapies

Different strategies have been developed to restore the expression of functional dystrophin including gene replacement, exon skipping, suppression of premature stop codons and more recently, CRISPR-Cas9 genome editing[74–77].

Gene replacement. This therapy aims to restore dystrophin by replacing the mutant *DMD* gene with a synthetic substitute using recombinant adeno-associated virus (AAV) vectors. However, this strategy is limited because the AAV vector cannot carry the entire *DMD* gene due to its large size. This problem was overcome by the use of micro-dystrophins which are truncated but functional forms of dystrophin. Current challenges of gene replacement include improving methods for systemic gene delivery, increasing viral transduction efficiency and reducing innate and acquired immune responses to allow repeated AAV-dystrophin delivery[78].

Exon skipping. This strategy is one of the most promising therapeutic approaches, and it consists in the use of antisense oligonucleotides (AONs) to splice one or multiple exons in pre-mRNA to restore the reading frame of dystrophin, leading to a truncated form of dystrophin that is partially functional and produces a milder phenotype[79,80]. Multi-exon skipping, which involves the exclusion of multiple contiguous exons, increases the applicability of the treatment to patients with different mutational defects[81].

Suppression of premature stop codons. This approach involves the use of small molecules that promote the readthrough of premature termination codon mutations by interfering with the ability of the ribosome to recognize these stop signals, allowing to continue the translation of the dystrophin protein. Theoretically, a single small molecule drug that reads through nonsense mutations can address all the mutations within the entire coding region of the gene[82].

CRISPR-Cas9 genome editing. The bacterial Clustered Regularly Interspaced Short Palindromic Repeats (CRISPR)/CRISPR-associated (Cas) system has recently emerged as a new promising and effective genome-editing tool[83,84]. This system allows for sequence-specific cleavage of target loci across the genome leading to permanent gene correction, thus overcoming the transient mRNA correction associated with exon skipping and readthrough therapies that imply continuous drug administration[85].

Cell therapies

Cell therapy is based on the delivery of cells that will contribute to the regeneration of muscle fibres and tissue repair[86]. These cells can be either MuSCs, myoblasts, or muscle precursor cells that have the ability to differentiate into muscle cells such as muscle-resident and circulating progenitors, mesenchymal stem cells, embryonic stem cells and induced pluripotent stem (iPS) cells. Cell therapy can be a form of gene therapy itself if the functional *DMD* gene or dystrophin is directly delivered using cells as vectors. The major limitations to overcome are the poor survival of cells, the lack of dispersion from the injection site and the immunological rejection by the host[87].

Pharmacological upregulation of utrophin

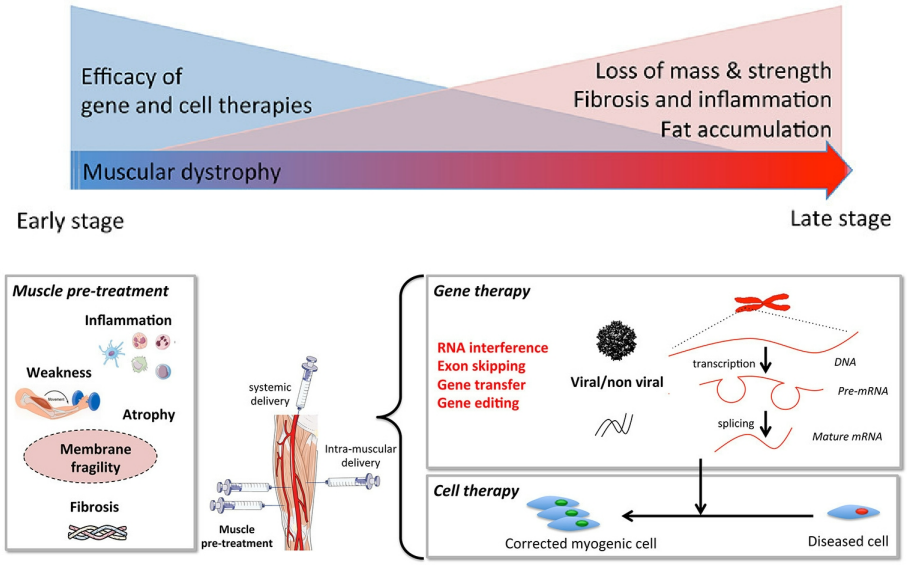
Utrophin is a structural and functional autosomal paralogue of dystrophin which shares 80% of homology with dystrophin and has functional redundancy[88]. Both utrophin and dystrophin have structurally similar N-terminal, cysteine-rich and C-terminal domains and share many binding partners including F-actin binding site[89]. Unlike dystrophin, utrophin is ubiquitously expressed. In skeletal muscle, utrophin is only expressed at

the neuromuscular and myotendinous junctions, whereas dystrophin is expressed throughout the sarcolemma. However, utrophin was found to be expressed across the entire sarcolemma in early development, regenerating muscle and in the skeletal muscle of DMD patients[90]. Due to the strong similarities between dystrophin and utrophin, utrophin was proposed to act as a surrogate to compensate for the lack of dystrophin in DMD. Utrophin upregulation leads to the functional replacement of dystrophin at the sarcolemma improving muscle function and ameliorating muscular dystrophy, independently of the mutation[74,90–92].

COMBINED THERAPIES FOR DMD

Emerging therapeutic approaches to treat DMD, such as gene-based and cell-based therapies, are limited by poor targeting and low efficiency in dystrophic muscle[93]. Dystrophic muscle is characterized by wasting, degeneration and inflammation, which leads to disruption of the sarcolemma integrity, resulting in loss of the therapeutic agent. At advanced stages, dystrophic muscles present exacerbated fibrosis and fat accumulation that produce a hostile environment that compromises the efficiency of single therapies by limiting its accessibility to the muscle[64]. Thereby, there is an increasing interest in the development of combined therapies, which consist in the use of one therapy to correct the genetic defect and a second one to improve the status of the recipient muscle, thus ensuring the maximal efficiency of the single target therapies[94]. To improve the dystrophic environment of the recipient tissue, different muscle conditioning treatments are being developed[94,95]. These treatments act synergistically by improving the muscle phenotype *per se* and optimizing the efficiency of single therapies (Scheme 10). One of the most promising strategies is to stimulate muscle growth and regeneration since regenerative therapies allow dystrophin to reach therapeutic expression levels necessary to restore function, which is not possible if muscle wasting has already progressed[95]. Treatment with IGF-1[96] or myostatin inhibitors[97] has shown beneficial effects in this context. Another approach is to control fibrosis and inflammation, which are the most important complications associated with DMD as they limit the accessibility of the single therapies to

the dystrophic muscle. In this sense, TGF-β[98] and NF-κB[99] inhibitors emerge as potential anti-fibrotic and anti-inflammatory therapies for muscle conditioning, respectively.



Scheme 10. Combined therapies for DMD treatment. Progression of DMD decreases the effectiveness of therapies intended to correct the genetic defect. Muscle pre-condition can increase the efficiency of gene- and cell-therapy. From Cordova G et al. Combined therapies for Duchenne muscular dystrophy to optimize treatment efficacy. *Front Genet*. 2018;9:114. Licensed under Creative Commons.

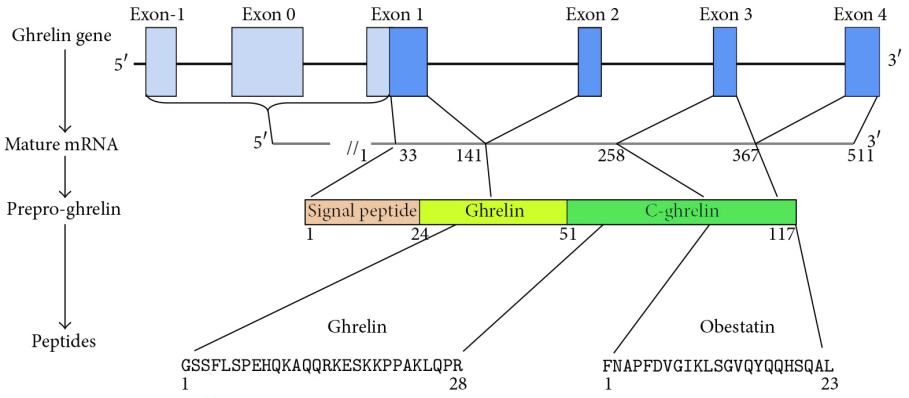
THE OBESTATIN/GPR39 SYSTEM

OBESTATIN

In 2005, Zhang et al. discovered, based on a bioinformatic prediction, a new peptide encoded by the ghrelin gene called obestatin- a contraction of obese, from the Latin *"obedere"*, meaning to devour, and *"statin"*, denoting suppression. It was firstly isolated from the stomach and was described as a

physiological opponent of ghrelin on food intake, body weight and gastric emptying[100]. However, its opposite function to ghrelin has been questioned and, since its discovery, several studies tried to resolve the controversy related to its physiological functions and its receptor.

Obestatin is a 23-amino acid hormone derived from preproghrelin, a polypeptide encoded by the ghrelin gene *(GHRL)* which is located on chromosome 3, band p25-26 and contains five exons and three introns. Preproghrelin is composed of 117 amino acids, with a 23-amino acid signal peptide and a 94-amino acid peptide called proghrelin. After translation, the signal sequence is eliminated in the endoplasmic reticulum and then a proteolytic processing occurs giving two mature peptides: ghrelin and obestatin. Obestatin is post-translationally modified with a C-terminal amide group on Leu[23] (Scheme 11). As with many regulatory peptides, the presence of a C-terminal amide group is essential for its biological activity[101,102]. In addition, the mass spectrometric data obtained by Zhang et al. indicate that obestatin may be processed to a 13 amino acid peptide, obestatin (11-23), which is biologically active[100].



Scheme 11. The ghrelin gene *(GHRL)* and its products. Schematic representation of the ghrelin gene and the processes leading to the synthesis of ghrelin and obestatin. Dark blue boxes represent preproghrelin-coding exons while light blue boxes show untranslated exonic regions. Horizontal lines represent introns. Adapted from Delporte C. Structure and physiological actions of Ghrelin. *Scientifica*. 2013;2013:518909. Licensed under Creative Commons.

There is evidence of the species-specific activity of the obestatin. The study of its structure-activity relationship revealed that mouse and human obestatin exhibit clear conformational differences beyond their differences in primary structure. In fact, mouse analogue adopts a distinct three-dimensional structure which cannot activate human GPR39, the canonical receptor of obestatin[103].

With regard to its distribution, obestatin was found to be mainly produced by the rat stomach[100], in cells of rat and human gastric mucosa, as well as in gastric myenteric cholinergic neurons[104]. Obestatin expression has been also shown in the endocrine pancreas, adipose tissue, skeletal muscle, liver, lung, thyroid, mammary gland and male reproductive system, suggesting autocrine/paracrine activities in peripheral tissues and organs[105–110].

OBESTATIN RECEPTOR: GPR39

Obestatin was originally described as the endogenous ligand of the G-protein 39-coupled receptor (GPR39), a G-protein-coupled receptor (GPCR) first cloned in 1997 from a foetal brain cDNA library by hybridization[111]. GPR39 was considered an orphan GPCR until the discovery of the obestatin in 2005 when, based on the obtained data of radiolabelled ligand binding assays, Zhang et al. proposed the obestatin as the cognate ligand of GPR39[100].

GPR39 is a 435-amino acid seven transmembrane GPCR that belongs to the same family as ghrelin (GHSR1a), motilin (GPR38) and neurotensin (NTSR1) receptors. Its gene is located on chromosome 2, band q21-q22, consisting of two exons[111]. The first exon encodes residues 1 to 285, corresponding to the N-terminal region and the first five transmembrane helices, and the second exon encodes residues 286 to 435, corresponding to the last two transmembrane helices and the C-terminal region. Between the two exons, there is an intron of 200 kb whose analogue appears in the genes of the ghrelin and the motilin receptors. The second exon also shares a segment of DNA with the antisense gene LYPD. The two-exon structure and LYPD1 gene-overlapping pattern are conserved among several species[112]. Two splice variants of the GPR39 receptor were identified:

GPR39 1-a is the full-length receptor and is the canonical form; and GPR39 1-b, a truncated form of the receptor that was originally considered biological inactive until very recently[112]. It was also shown that GPR39 has a high constitutive signalling activity through the serum response element (SRE)[113].

Regarding its expression, GPR39 is widely expressed throughout the body[114]. It is mainly expressed in the digestive system, but it is also expressed in adipose tissue, liver, spleen, thyroid, lung, heart, reproductive tissues, brain and skeletal muscle[109,114]. The expression of GPR39 in a wide range of tissues suggests its important role in the regulation of different physiological functions, like gastrointestinal mobility, hormone secretion, cell death, adipogenesis and myogenesis[109,114,115].

The controversy around GPR39 as obestatin receptor

GPR39 was considered an orphan receptor until the discovery of obestatin, which was described as its selective ligand[100]. However, several groups have questioned this conclusion, and the action of obestatin through GPR39 has always been controversial.

First, different studies from independent groups were unable to demonstrate any binding or stimulatory function of obestatin on GPR39[116–118]. This fact was reinforced by Zhang´s group inability to reproduce its original result regarding obestatin binding to GPR39[119]. However, all these results might be questionable. De Spiegeleer´s group demonstrated that the quality of the obestatin peptides supplied by several companies was insufficient for *in vitro* and *in vivo* experiments[120]. Actually, Zhang et al. observed that the inconsistent binding of obestatin to GPR39 could be due to loss of obestatin bioactivity after its poly-iodination[119], and later, they were able to demonstrate that mono-iodinated obestatin was capable of binding to human embryonic kidney 293 (HEK) cells transiently transfected with plasmids encoding GPR39[121].

On the other hand, Granata et al. proposed the glucagon-like peptide-1 (GLP-1) receptor (GLP-1R) as a mediator of the effects of obestatin, based on binding displacement assays of radiolabelled GLP-1 by obestatin in

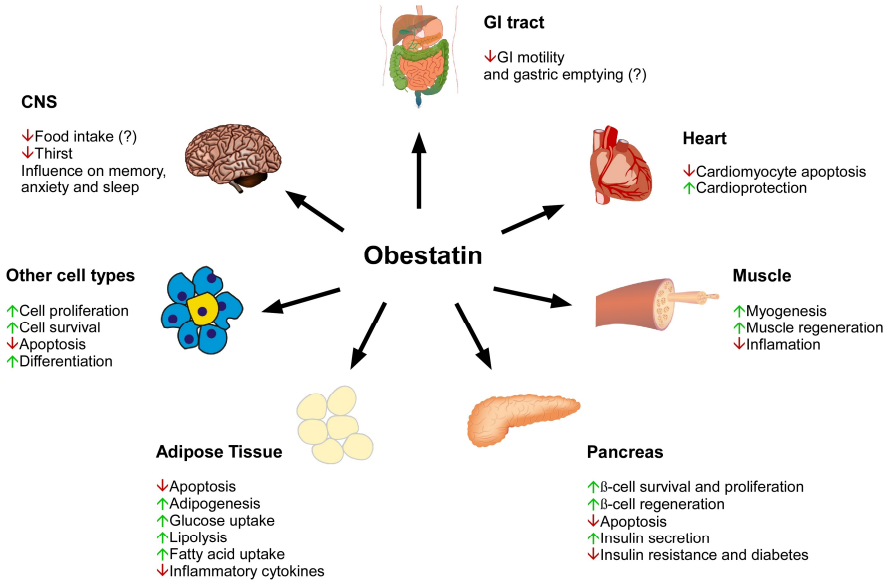
pancreatic β-cells[106]. However, this was questioned based on the results obtained from INS-1β and HEK cells overexpressing GLP-1R in which obestatin was not able to displace radiolabelled GLP-1 binding[122] and the fact that this work is prior to the report about the quality of obestatin peptides[120]. Furthermore, different groups propose zinc ions (Zn^{+2}) as the endogenous ligand of GPR39[123], considering GPR39 as Zn^{+2}-sensing receptor (ZnR) and not the obestatin receptor[124].

Despite this controversy, several studies evidence the action of obestatin through GPR39. Besides obestatin binding to GPR39, Zhang´s group demonstrated that obestatin induce the expression of c-fos (a transcription factor marker of gastrointestinal activity) in wild-type (WT) mice, but not in GPR39 null mice[121]. Previously, the *in vivo* effects of obestatin depending on GPR39 were confirmed using GPR39 null mice[125]. Moreover, studies on bone metabolism[126] and term pregnancy[127] have shown the correlation of expression levels of both GPR39 and obestatin. Furthermore, knockdown of GPR39 by siRNA experiments proved the GPR39 mediated actions of obestatin in several cell lines by inhibiting obestatin signalling[109,115,128–130]. Finally, coimmunoprecipitation experiments demonstrated the binding of obestatin to GPR39 in cultured C2C12 myoblasts[131].

OBESTATIN BIOACTIVITY

Obestatin was originally identified as a physiological opponent of ghrelin[100], suppressing food intake, slowing gastric emptying and jejunal motility and reducing body weight[100,121,132]. However, its action regarding food intake was soon discarded by different groups[133–137]. Although obestatin central effects are still unclear, several studies have described remarkable results regarding obestatin bioactivity in both central and peripheral tissues along these years (Scheme 12).

In peripheral cells and tissues, obestatin displays a variety of cellular effects by regulating metabolic and cell differentiation functions, increasing cell survival and proliferation[106,130,138] and inhibiting apoptosis and inflammation[139–141]. In particular, obestatin regulates adipogenesis, pancreatic homeostasis, cardiovascular function and myogenesis[142,143].



Scheme 12. Relevant physiological actions of obestatin. Obestatin exerts diverse actions in both central and peripheral tissues. CNS, central nervous system; GI, gastrointestinal. Adapted from Trovato L et al. Obestatin: is it really doing something? *Front Horm Res*. 2014;42:175–185. With permission from Karger Publishers.

Different groups have evidenced the important actions of obestatin in adipogenesis, playing a regulatory role in the expression of master regulators of the adipocyte fate and, consequently, lipid accumulation[115]. The relevance of obestatin as a regulator of adipocyte metabolism was further supported by glucose transporter type 4 (GLUT4) translocation and increased glucose uptake[115,139], being a mediator for insulin-induced adipogenesis[144].

In addition to its action in adipogenesis, obestatin exerts an autocrine/paracrine role in pancreatic β-cells, enhancing proliferation and inhibiting apoptosis[106]. Further studies revealed its role in pancreatic regeneration by promoting β-cell formation[145] and its protective function due to anti-inflammatory effects[141].

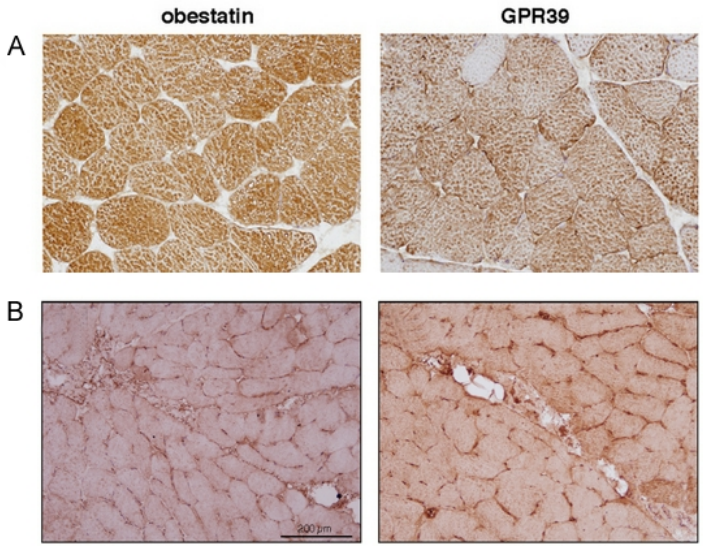
On the other hand, recent findings suggest that obestatin acts as a homeostatic regulator of the cardiovascular system, improving cardiac

function, displaying cardioprotective effects[146,147], inhibiting apoptosis in cardiomyocytes[146,148], and regulating blood pressure[149].

At the central level, obestatin was found to inhibit thirst and influence memory, anxiety and sleep, likely through indirect action on vagal neurons or by regulating secretion of other hormones[150–152].

ROLE OF THE OBESTATIN/GPR39 SYSTEM IN MYOGENESIS

Several studies have demonstrated that the obestatin/GPR39 system acts as an autocrine signal involved in muscle regeneration and myogenesis. It is expressed in healthy skeletal muscle (Scheme 13), and this expression increases upon muscle injury. *In vitro*, obestatin expression is up-regulated during the early stages of myogenesis being sustained throughout terminal differentiation[109].



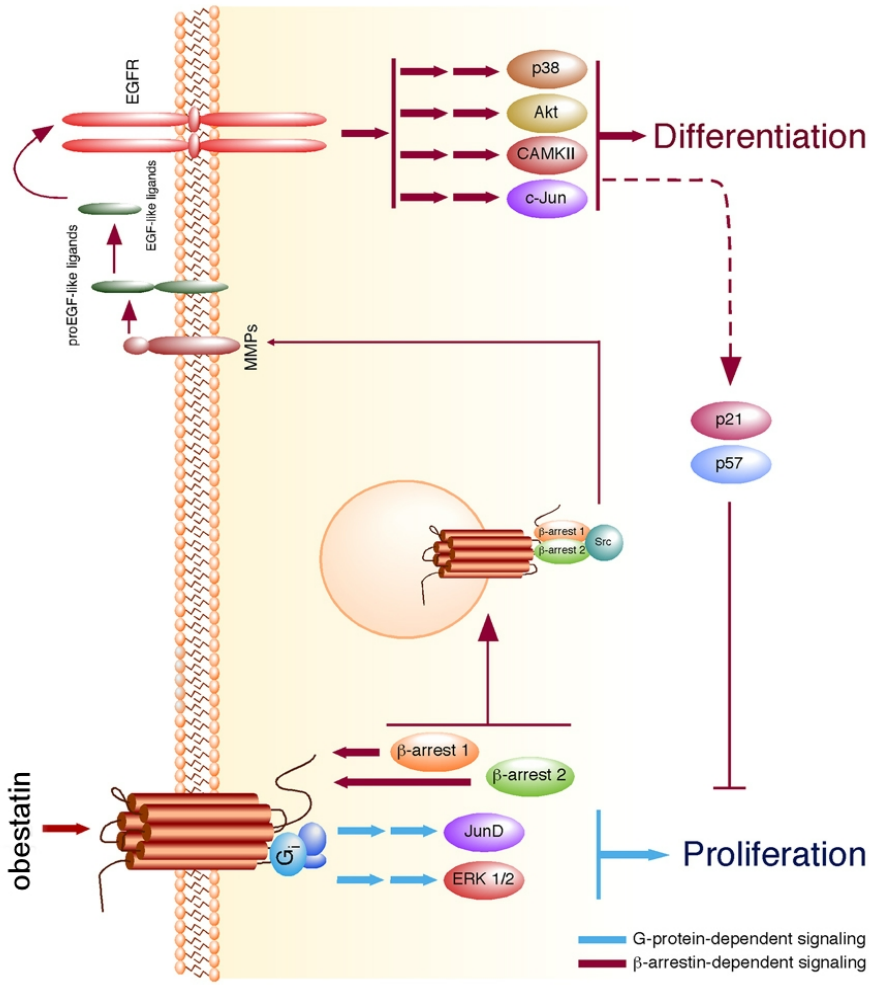
Scheme 13. The obestatin/GPR39 system is expressed in skeletal muscle. Immunohistochemical detection of obestatin and GPR39 in rat (A) and human (B) gastrocnemius muscle. From (A) Gurriarán-Rodríguez U et al. The obestatin/GPR39 system is up-regulated by muscle injury and functions as an autocrine regenerative system. *JBC*. 2012; 287(45):38379-89. Permitted by The American Society for Biochemistry and Molecular Biology, Inc.; and (B) Santos-Zas I et al. β-Arrestin scaffolds and signaling elements essential for the obestatin/GPR39 system that determine the myogenic program in human myoblast cells. *Cell. Mol. Life Sci*. 2016. 73(3):617-635. With permission from Springer Nature.

The intramuscular injection of obestatin or its overexpression in skeletal muscle improves regeneration after muscle injury by regulating multiple steps of myogenesis: myoblast proliferation, cell cycle exit, differentiation, and recruitment to fuse and form multinucleated hypertrophic myotubes[131]. This action is coordinated by the interplay between G protein-dependent and β-arrestin-dependent mechanisms[128]. In addition to the myogenic action, obestatin administration results in an increased expression of vascular endothelial growth factor (VEGF)/vascular endothelial growth factor receptor 2 (VEGFR2) and the consequent microvascularization, with no significant effect on collagen deposition in developing skeletal muscle[131]. Recently, it was demonstrated that obestatin signalling controls oxidative phenotype of muscle fibre through both class II HDAC/MEF2 and PGC-1α mechanisms[153].

The functional properties of the obestatin/GPR39 system suggest its potential clinical application in skeletal muscle. Indeed, in cell transplantation therapy, e.g. myoblast-based therapy by xenotransplanting primary human myoblasts into immunodeficient mice, obestatin not only enhances the efficiency of engraftment, but it also facilitates an even distribution of myoblasts within the host muscle[154]. On the other hand, obestatin counteracts deregulations in proteostasis, e.g. those associated with glucocorticoid-induced myotube atrophy, and to restore efficient basal homeostasis[155].

OBESTATIN SIGNALLING

Myogenesis is a multistep process by which myoblasts first proliferate, then withdraw from the cell cycle, and finally differentiate and fuse to form the multinucleated mature myotubes[13,156]. In particular, the obestatin/GPR39 system exerts its action in myogenesis by the coordinated interplay between G protein-dependent and β-arrestin-dependent mechanisms, controlling the specificity, efficiency and capacity of the signals to direct the progression of the myogenic program (Scheme 14)[128].



Scheme 14. Proposed model for the G-protein- and β-arrestin-mediated activation of myogenesis through the obestatin/GPR39 system. Obestatin binding to GPR39 receptor results in the activation of Gi/o protein-dependent pathway, leading to the activation of ERK1/2 and JunD signalling nodes that regulates myoblast proliferation. Simultaneously, GPR39/β-arrestins/Src complex initiates the transactivation of EGFR through MMPs and subsequent downstream Akt, p38, CAMKII and JNK/c-Jun signalling to regulate cell cycle exit (p21 and p57), recruitment and fusion of myoblast to form myotubes. From Santos-Zas I et al. β-Arrestin scaffolds and signaling elements essential for the obestatin/GPR39 system that determine the myogenic program in human myoblast cells. *Cell. Mol. Life Sci*. 2016;73(3):617-635. With permission from Springer Nature.

The obestatin-associated mitogenic action is determined by G protein-dependent activation defining the intricate pathways related to the extracellular signal-regulated kinase-1/2 (ERK1/2) and JunD axis, activating the first proliferation step of the myogenic process[128]. ERK1/2 pathway plays a fundamental role in cellular proliferation, migration and fusion[157]. In the context of obestatin-induced activity, ERK activity initially increases, consistent with the initial proliferation of myoblasts, and then is followed by a decrease, which is necessary for differentiating myoblasts to overcome its inhibitory effect. Indeed, ERK was shown to inhibit differentiation by preventing the nuclear accumulation of members of MEF2[158], and the expression of certain myogenic factors, including MyoD[159] and the cyclin-dependent kinase (CDK) inhibitor p21[160]. On the other hand, obestatin exerts its myogenic action through the β-arrestin-dependent transactivation of epidermal growth factor receptor (EGFR), triggering the cell cycle exit and the development and progression of differentiation through a kinase hierarchy determined by the Akt, Ca^{2+}/calmodulin-dependent protein kinase II (CaMKII), c-Jun, and p38 axes. Upon obestatin stimulus, β-arrestins are recruited to the membrane, where they functionally interact with GPR39 leading to Src activation and signalplex formation to EGFR transactivation by matrix metalloproteinases. This signalplex regulates the mitotic arrest by p21 and p57 expression and the mid-to-late stages of differentiation through JNK/c-Jun, CAMKII, Akt and p38 pathways to form multinucleated myotubes. Thus, the activation of β-arrestin-dependent signalosome promotes the expression of myogenic regulatory factors (i.e., myogenin) and MHC[128].

OBJECTIVES

USC
UNIVERSIDADE
DE SANTIAGO
DE COMPOSTELA

There is a growing need of therapeutic approaches for the treatment of disorders of skeletal muscle. The final aim of therapy for several skeletal muscle diseases, such as DMD, is gene replacement; however, this remains a challenging problem with many obstacles remaining on the path to the clinic. In this sense, much attention has recently been given to the understanding of the molecular and cellular mechanisms underlying skeletal muscle regeneration in different contexts, as a manner to identify and develop new therapeutic approaches to counteract and/or ameliorate significant hallmarks of these diseases. Ideally, this type of therapy would activate MuSCs to enhance their regenerative potential. Although this mode of action does not treat the genetic basis of the structural myofibre instability, it is sufficient to maintain a stable level of regeneration and reduce the severity of dystrophic symptoms. Furthermore, the development of this kind of approach would be also required for combinatorial therapies with gene- or cell-based strategies. In this context, our group has demonstrated that the obestatin/GPR39 system regulates muscle homeostasis acting as an autocrine/paracrine signal, making obestatin a promising therapeutic candidate for the treatment of conditions related to muscle regeneration. Thus, the specific aims of the present work are:

1. To determine the role of the obestatin/GPR39 in the regulation of MuSCs.

2. To investigate the therapeutic potential of the obestatin/GPR39 system for focal treatment of dystrophic muscles using the dystrophin deficient *mdx* mouse model and *in vitro* cell culture models of human DMD skeletal muscle cells.

USC
UNIVERSIDADE
DE SANTIAGO
DE COMPOSTELA

MATERIALS AND METHODS

USC
UNIVERSIDADE
DE SANTIAGO
DE COMPOSTELA

MATERIALS

Rat/mouse obestatin was obtained from BCN Peptides (Barcelona, ES). Human obestatin was purchased from Biomedal (Sevilla, ES). Insulin was obtained from Novo Nordisk (Bagsvaerd, DK). STO-609, Compound C and Rapamycin were supplied by Santa Cruz Biotechnology (Texas, USA). All other chemical reagents were from Sigma Chemical (Missouri, USA).

ANTIBODIES

Table 2. Primary Antibodies

Primary antibody	Use	Dilution	Supplier	Reference
Actin	WB	1:4000	Abcam	ab1801
Akt	WB	1:2000	Novus Biologicals	NB100-92467
p-Akt (S473)	WB	1:1000	Cell Signaling	92710
p-Akt (S473)	IF	1:50	Cell Signaling	92710
AMPK	WB	1:1000	Cell Signaling	2603
p-AMPK(T172)	WB	1:1000	Cell Signaling	2535
p-CAMKII (T286)	WB	1:1000	Cell Signaling	3361
Cleaved Caspase-3	WB	1:500	Abcam	ab2302
Cleaved Caspase-3	IF	1:50	Abcam	ab2302
Cathepsin L	WB	1:2000	Abcam	ab133641
Collagen 1	WB	1:2000	Abcam	ab34710
CPT1	WB	1:100	Santa Cruz Biotechnology	sc-514555
CTGF	WB	1:2000	Abcam	ab6992

Note: Relation of the primary antibodies used in the different analyses performed in this work. IF, immunofluorescence; WB, western blot.

Table 2. Primary antibodies *(Cont.)*

Primary antibody	Use	Dilution	Supplier	Reference
Cytochrome C	WB	1:100	Santa Cruz Biotechnology	sc-7159
EGFR	IF	1:50	Cell Signaling	4267
FoxO1	WB	1:500	Cell Signaling	2880
FoxO3a	WB	1:1000	Cell Signaling	12829
FoxO4	WB	1:500	Cell Signaling	9472
p-FoxO1(T24)/ FoxO3a(T32)/FoxO4(T28)	WB	1:500	Cell Signaling	2599
GAPDH	WB	1:2000	Abcam	ab9485
GPR39	WB	1:2000	Novus Biologicals	NLS139
GPR39	IF	1:100	Novus Biologicals	NLS139
GSK3	WB	1:1000	Santa Cruz Biotechnology	sc-56913
p-GSK3(S21/9)	WB	1:1000	Cell Signaling	9331
HDAC4	WB	1:1000	Cell Signaling	7628
p-HDAC4(S246) /HDAC5(S259)/HDAC7(S155)	WB	1:1000	Cell Signaling	3443
Ki67	IF	1:200	Abcam	ab15580
Laminin	IF	1:200	Dako	Z0097
LC3 I/II	WB	1:1000	Cell Signaling	12741S
LC3 B	IF	1:500	Cell Signaling	2775
MAFbx	WB	1:500	Santa Cruz Biotechnology	sc-166806

Note: Relation of the primary antibodies used in the different analyses performed in this work. IF, immunofluorescence; WB, western blot.

Table 2. Primary antibodies *(Cont.)*

Primary antibody	Use	Dilution	Supplier	Reference
Mef2A	WB	1:1000	Cell Signaling	9736
Mef2C	WB	1:100	Santa Cruz Biotechnology	sc-365862
MuRF-1	WB	1:500	Santa Cruz Biotechnology	sc-32920
MHC	IF	1:200	DSHB	MF20
MHC	WB	1:500	DSHB	MF 20
MHC I	IF	2ug/mL	DSHB	BA-F8
MHC IIa	IF	2ug/mL	DSHB	SC-71
MHC IIb	IF	2ug/mL	DSHB	BF-F3
MHC IIx	IF	2ug/mL	DSHB	6H1
slow-MHC	WB	1:2000	Sigma	SAB4200670
fast-MHC	WB	1:2000	Sigma	A4335
mTOR	WB	1:1000	Cell Signaling	2983
p-mTOR (S2448)	WB	1:1000	Cell Signaling	2971
mtTFA	WB	1:100	Santa Cruz Biotechnology	sc-166965
Myf5	IF	1:50	Novus Biologicals	MAB4027
Myogenin	WB	1:500	DSHB	F5D
Myogenin	IF	Undiluted	Dako	IR067
MyoD	IF	1:50	Santa Cruz Biotechnology	sc-304
MyoD	IF	1:50	Dako	M3512

Note: Relation of the primary antibodies used in the different analyses performed in this work. IF, immunofluorescence; WB, western blot.

Table 2. Primary antibodies *(Cont.)*

Primary antibody	Use	Dilution	Supplier	Reference
NFATc1	WB	1:500	R&D systems	AF5640
NFATc1	IF	1:200	R&D systems	AF5640
p-NFATc1 (S172)	WB	1:500	R&D systems	MAB5640
NICD	IF	1:100	Cell Signaling	4147
NOS1	WB	1:100	Santa Cruz Biotechnology	sc-5302
Obestatin	IF	1:200	Abcam	ab41704
Obestatin	WB	1:500	Abcam	ab41704
Par-3	IF	1:100	Millipore	07-330
Pax7	IF	Undiluted	DSHB	Pax7
PGC1α	WB	1:2000	Abcam	ab191838
p-PKD (S916)	WB	1:1000	Cell Signaling	2051
Preproghrelin	WB	1:200	Santa Cruz Biotechnology	sc-10368
p62	WB	1:1000	Cell Signaling	5114S
S6	WB	1:1000	Cell Signaling	2217
p-S6 (S240/244)	WB	1:2000	Cell Signaling	2215
p-S6 (S235/236)	IF	1:50	Cell Signaling	2211
S6K1	WB	1:500	Santa Cruz Biotechnology	sc-230
p-S6K1(T389)	WB	1:1000	Cell Signaling	9234
Troponin I-FS	WB	1:500	Santa Cruz Biotechnology	sc-30486

Note: Relation of the primary antibodies used in the different analyses performed in this work. IF, immunofluorescence; WB, western blot.

Table 2. Primary antibodies *(Cont.)*

Primary antibody	Use	Dilution	Supplier	Reference
Troponin I-SS	WB	1:500	Santa Cruz Biotechnology	sc-20645
UCP3	WB	1:100	Santa Cruz Biotechnology	sc-7756
ULK1	WB	1:250	Santa Cruz Biotechnology	sc-390904
p-ULK1 (S758)	WB	1:500	GeneTex	GTX132654
p-ULK1 (S317)	WB	1:500	Abgent	AP19250c
Utrophin	IF	1:10	Novocastra	NCL-DRP2
Utrophin	WB	1:100	Novocastra	NCL-DRP2
Vangl2	IF	1:50	Santa Cruz Biotechnology	sc-46561
α-bungarotoxin	IF	1:500	Invitrogen	B13422
α-SMA	WB	Undiluted	Dako	IR611
α -syntrophin	WB	1:100	Santa Cruz Biotechnology	sc-166634
α7-integrin	WB	1:1000	Abcam	ab203254
α7-integrin	IF	1:200	Abcam	ab203254
β-catenin	IF	1:50	Millipore	05-665
β-dystroglycan	WB	1:100	Santa Cruz Biotechnology	sc-33702
β1D-integrin	WB	1:1000	Abcam	ab8991
β1D-integrin	IF	1:400	Abcam	ab8991
4E-BP1	WB	1:1000	Cell Signaling	9452

Note: Relation of the primary antibodies used in the different analyses performed in this work. IF, immunofluorescence; WB, western blot.

Table 2. Primary antibodies *(Cont.)*

Primary antibody	Use	Dilution	Supplier	Reference
p-4E-BP1 (T37/46)	WB	1:1000	Cell Signaling	9459
p-4E-BP1 (T70)	WB	1:1000	Cell Signaling	9455

Note: Relation of the primary antibodies used in the different analyses performed in this work. IF, immunofluorescence; WB, western blot.

Table 3. Secondary Antibodies

Secondary antibody	Use	Dilution	Supplier	Reference
Goat Anti-Mouse IgG (H&L) Alexa Fluor 488	IF	1:1000	Invitrogen	A11029
Goat Anti-Mouse IgG1 Alexa Fluor 594	IF	1:1000	Invitrogen	A21125
Goat Anti-Rabbit IgG (H&L) Alexa Fluor 594	IF	1:1000	Invitrogen	A11012
Goat Anti-Rabbit IgG Fc Alexa Fluor 488	IF	1:1000	Abcam	ab150089
Goat Anti-Rabbit IgG (H&L) Alexa Fluor 750	IF	1:1000	Invitrogen	A21039
Peroxidase AffiniPure Goat Anti-Rabbit IgG (H+L)	WB	1:10000	Jackson ImmunoResearch	111-035-003
Peroxidase AffiniPure Goat Anti-Mouse IgG (H+L)	WB	1:10000	Jackson ImmunoResearch	115-035-003
Peroxidase AffiniPure Donkey Anti-Goat IgG (H+L)1	WB	1:10000	Jackson ImmunoResearch	705-035-003

Note: Relation of the secondary antibodies used in the different analyses performed in this work. IF: immunofluorescence; WB: western blot.

PRIMERS

Table 4. Primers

Primer	Fw (5'-3')	Rv (5'-3')
AchRα	CCACAGACTCAGGGGAGAAG	AACGGTGGTGTGTGTTGATG
AchRε	CAATGCCAATCCAGACACTG	CCCTGCTTCTCCTGACACTC
AchRδ	CATCGAGTGGATCATCATTGAC	CGGCGGATGATAAGGTAGAA
Musk	TGAGAACTGCCCCTTGGAACT	GGGTCTATCAGCAGGCAGCTT
Erbb1	GACCTTCACATCCTGCCAGT	GCATGGAGGTCAGTCCAGTT
RPS20	CCATGGCATTTAAAGATACCG	AACCTTCTCCAGCGACTTCAC

Note: Sequences of the primers used in this study. Primers were purchased from Eurofins Genomics (Ebersberg, DE). Fw, forward; Rv, reverse.

METHODS

Animals. Mouse strains used in this study included female Swiss mice and male C57BL/10ScSn-Dmd*mdx*/J mice (*mdx* mice). Female Swiss mice were obtained from the breeding animal facilities of the University of Santiago de Compostela (Santiago de Compostela, ES) and used for isolation/culture of single myofibres. Male *mdx* mice were obtained from The Jackson Laboratory (Maine, USA). For protein expression assays, 4-, 8- and 18-week-old male *mdx* mice were used. To examine the effects of exogenous obestatin in dystrophic muscles, 8-week-old male *mdx* mice were employed. Experiments were performed in accordance with the University of Santiago de Compostela guidelines for animal handling and animal care as determined by the University of Santiago de Compostela Animal Care Committee (Procedure number 15010/17/005) according to the guidelines of the Spanish Royal Decree 53/2013, Directive 2010/63/EU and FELASA Guidelines.

Single myofibre isolation and culture. Single myofibres were isolated from gastrocnemius muscle of 8-week-old female Swiss mice as described earlier[161]. Gastrocnemius muscles were dissected and then incubated in a 0.2% collagenase I (Worthington; New Jersey, USA) in DMEM (Lonza; Basel, CH) solution for 1 h at 37°C. Myofibres were isolated using a glass pipette to flush the muscle with medium to release the single fibres, and cultured in floating conditions in plating medium consisting of 15% foetal bovine serum (FBS) (GE Healthcare Life Science; Utah, USA), 1% chick embryo extract (Sera Laboratories; Sussex, UK) and 50 µg/mL gentamicin (Gibco, Thermo Fisher Scientific; Massachusetts; USA) in DMEM, in presence or absence of obestatin (5 nM). FBS-coated plates were used to prevent fibre attachment.

Small interfering RNA (siRNA) silencing of gene expression assays in single myofibres. MuSCs were transfected on myofibres cultured in floating conditions using Lipofectamine 2000 reagent (Invitrogen, Thermo Fisher Scientific; Massachusetts, USA) as per manufacturer's instructions. Two transfections were performed at 2- and 24-hours (h) after isolation of the fibres to ensure maximal efficiency, as described earlier[40]. Chemically synthesized double-stranded siRNA duplexes targeting GPR39, β-catenin or EGFR were selected from ON-TARGETplus SMARTpool siRNA from Dharmacon (Colorado, USA): GPR39, CCUGUAAGCUCCACACGUU, GCACAC-GACUUCCGGUACA, CAGGAAGUAUGAAUGGCAA, GGGAAAGGCAGAUGCGU-AU. β-catenin, GUGAAAUUCUUGGUAUUA, GCGCUUGGCUGAACCAUCA, CA-GCAAAUCAUGCGCCUUU, AAGCUGACCUGAUGGAGUU. EGFR, GAAACUACG-UGGUGACAGA, GGGAGUGCGUGGAGAAAUG, AAUAAUACGUGGCAGAACA, UUACGACCUUUCCUUCUUA). An ON-TARGETplus non-targeting siRNA was used as a control for all siRNA experiments.

Cell cycle analysis in single myofibres. The monitoring of the cell cycle entry of MuSCs was performed by 5-ethynyl-2´-deoxyuridine (EdU) incorporation on cultured myofibres using the Click-IT EdU imaging kit (Invitrogen, Thermo Fisher Scientific; Massachusetts, USA). EdU (10 µM) was added to culturing medium in the presence or absence of obestatin (5 nM), and single myofibres where then fixed at 2-, 10- and 20-h after plating. EdU was detected according to the manufacturer's instructions.

Obestatin dosing in *mdx* mice. To examine the effects of exogenous obestatin in dystrophic muscles, 8-week-old male *mdx* mice were employed. The experimental protocol used in the present work was previously described[153]. Animals were assigned to one of the following experimental groups (n=5 per group): (1) control group (vehicle administration: PBS); and, (2) obestatin-treated group. Obestatin treatment was performed via intramuscular injection of 20 µL of obestatin solution in PBS (pH 6.3) (500 nmol/kg body weight) into the *tibialis anterior* (TA) muscle every 72 h during 30 days. Control group was treated with 20 µL of PBS under the same conditions. Injections were performed inserting the needle of a 0.3 mL/29 gauge syringe (Terumo Myjector V-100 insulin syringe) at 1 mm in the distal part of the muscle, in a region that is not taken into account for histological analysis, as previously described[131]. After 30 days, mice were anaesthetized by intraperitoneal injection of 2.2 mg ketamine/0.4 mg xylazine per 10 g of animal body weight. Muscle force was measured and blood samples collected from tail bleeds in all animals. Animals were sacrificed by cervical dislocation under anaesthesia and TA muscles from different groups were excised, weighed and processed for subsequent analyses. For immunoblot and RT-PCR analysis, muscles were snap-frozen in liquid nitrogen. For histologic analysis, muscle tissue samples were mounted in tissue freezing medium (tragacanth paste) and frozen in isopentane, while livers and kidneys were fixed by immersion in 4% (w/v) buffered paraformaldehyde (PFA)-PBS for 24 h, dehydrated and embedded in paraffin by standard procedure.

Measurements of muscle force *in vivo* in *mdx* mice. Muscle force was measured in a living animal as previously described[153]. TA muscle contractile performance was measured *in vivo* in anaesthetized mice using 1305A Whole Animal System (Aurora Scientific Inc.; Ontario, CA). TA contractions were evoked by electrical stimulation of the common peroneal nerve using one electrode placed on the popliteal fossa. The force-frequency curves were determined by stepwise increasing stimulation frequency, pausing 120 s between stimuli to avoid effects due to fatigue. Developed force was expressed as specific force.

Blood measurements in *mdx* mice. Blood samples were collected from tail bleeds under general anaesthesia at the end of the treatment. The blood was collected in heparinized tubes, serum was isolated, and creatine kinase (CK), aspartate aminotransferase (AST), alanine aminotransferase (ALT), alkaline phosphatase, bilirubin and urea levels were performed by the Central Laboratory at Hospital Clínico Universitario de Santiago de Compostela (Santiago de Compostela, ES).

RNA extraction, cDNA synthesis and real-time PCR. Total RNA was extracted from control and obestatin-treated TA muscle of *mdx* mice using TRIzol reagent according to the manufacturer's instructions (MRC; Ohio, USA). After DNAse I treatment (Thermo Fisher Scientific; Massachusetts, USA), 0.5 µg of total RNA was reverse transcribed using High-Capacity cDNA Reverse Transcription Kits (Thermo Fisher Scientific; Massachusetts, USA). Real-time PCR was carried out in Applied Biosystems StepOnePlusTM Real-Time PCR System (Thermo Fisher Scientific; Massachusetts, USA) using Luminaris HiGreen qPCR Master Mix (Thermo Fisher Scientific; Massachusetts, USA). The 2−ΔΔCt method was used to analyse the relative changes in each gene's expression normalized against the housekeeping 40S ribosomal protein S20 (RPS20) RNA expression[162]. Sequences of the primers used in this study are listed in Table 4.

Cell culture and differentiation of human immortalized DMD myoblasts. Immortalized human DMD myoblasts were obtained from MyoBank-AFM bank of tissues for research, a partner in the EU network EuroBioBank[86]. Cell lines employed in this study were: (i) DMD6: derived from the biopsy of the deltoid muscle of a 6-year-old male patient suffering from DMD with a duplication of exon 2 (Ref. M-56994); and, (ii) DMD14: derived from the biopsy of the paravertebral muscle of a 14-year-old male patient suffering from DMD with a duplication of exon 2 (Ref. 5-13515). Myoblasts were cultivated in growth medium (GM) containing medium 199:DMEM (1:4, v/v; Lonza) supplemented with 20 % FBS (v/v), 25 µg/µL fetuin, 5 ng/mL hEGF, 0.5 ng/mL bFGF, 0.2 µg/mL dexamethasone (Sigma-Aldrich; Missouri, USA) and 50 µg/mL gentamycin (Invitrogen, Thermo Fisher Scientific; Massachusetts, USA). Differentiation into myotubes was initiated at 90%

confluence by switching to differentiation medium (DM; DMEM supplemented with 50 µg/mL gentamycin in absence or presence of 10 nM obestatin or 1.72 µm insulin) for 3 days unless otherwise stated. For simplicity, the results presented in this work correspond to DMD6 cells as no significant differences were found between both DMD cell lines.

Immunoblot analysis. Protein was isolated from cells or tissue using ice-cold RIPA buffer [50 mmol/l Tris–HCl (pH 7.2), 150 mmol/l NaCl, 1 mmol/l EDTA, 1% (v/v) NP-40, 0.25% (w/v) Na-deoxycholate, protease inhibitor cocktail (Sigma Chemical; Missouri, USA), phosphatase inhibitor cocktail (Sigma Chemical; Missouri, USA)]. The lysates were clarified by centrifugation (14,000 ×g for 15 minutes at 4°C) and the protein concentration was quantified using the QuantiProTM BCA assay kit (Sigma Chemical; Missouri, USA). For immunoblotting, equal amounts of protein were fractionated by SDS–PAGE and transferred onto nitrocellulose membranes. Primary and secondary antibodies were incubated according to the manufacturer's instructions. Immunoreactive bands were detected by enhanced chemiluminescence (Pierce ECL Western Blotting Substrate, Thermo Fisher Scientific; Massachusetts, USA). The image processing was performed using ImageJ64 analysis software (National Institutes of Health; Maryland, USA).

Histological analysis of skeletal muscle. Muscle samples were mounted in tissue freezing medium (tragacanth paste) and snap frozen in nitrogen-cooled isopentane. The sections, 10-µm thick, were mounted on Histobond Adhesion Microslides (Marienfeld; Lauda-Königshofen, DE). For the haematoxylin/eosin (HE), succinate dehydrogenase (SDH), and Masson's trichrome stains, serial cryostat sections were stained following standard protocols. Compiled images were used to reconstruct a view of the entire TA muscle. This compilation was used for quantification of centrally located nuclei (CLN), number of myofibres and cross-sectional area using ImageJ64 analysis software. Formalin-fixed kidneys and livers were paraffin-embedded, 4-µm longitudinal and sagittal sections cut and stained with HE following a standard protocol. Digital images were acquired with a Zeiss Axio Vert.A1 microscope using Zen software (Carl Zeiss; Oberkochen, DE).

Immunofluorescence analysis of single myofibres. Single myofibres were stained as described elsewhere[30]. Myofibres were fixed in 4% (w/v) buffered PFA-PBS, quenched with glycine solution (0.1M in PBS), and permeabilized and blocked in PBS containing 1% BSA, 5% goat serum, and 0.2% Triton X-100 at room temperature. Myofibres were then incubated with primary antibodies overnight at 4ºC and finally with corresponding secondary antibodies for 1 h at room temperature. 4',6-diamidino-2-phenylindole (DAPI) was used to counterstain the cell nuclei (Life Technologies, Thermo Fisher Scientific; Massachusetts, USA). Digital images were acquired with a Zeiss Axio Vert.A1 microscope using Zen software. For quantification of different MuSCs populations, ImageJ64 analysis software was used.

Immunofluorescence analysis of skeletal muscle. Muscle samples were mounted in tissue freezing medium (tragacanth paste) and snap frozen in nitrogen-cooled isopentane. The sections, 10-µm thick, were mounted on Histobond Adhesion Microslides. Muscle sections were permeabilized and blocked with 10% normal goat serum blocker reagent (Life Technologies, Thermo Fisher Scientific; Massachusetts, USA) for 10 minutes. Muscle sections were then incubated with primary antibodies diluted in blocker reagent overnight at 4ºC and finally with a mixture of appropriate secondary antibodies for 1 h at room temperature. DAPI was used to counterstain the cell nuclei. Digital images were acquired with a Leica TCS-SP8 spectral confocal microscope (Leica Microsystems; Heidelberg, DE). Compiled images were used to reconstruct a view of the entire TA muscle for the quantification of fibre types using ImageJ64 analysis software.

Immunofluorescence analysis in DMD cells. DMD cells were cultured on coverslips and differentiated into myotubes in DM or DM supplemented with obestatin or insulin for 3 days. Differentiated cells were fixed with ethanol 96% for 10 minutes, permeabilized and blocked with PBS-T (0.25% Triton X-100 and 1% BSA in PBS) for 30 minutes (Sigma Chemical; Missouri, USA). Cells were then incubated with the primary antibody diluted in PBS-T overnight at 4ºC and finally with the appropriate secondary antibody for 1 h at room temperature. DAPI was used to counterstain the cell nuclei. Five

fields from three independent experiments were randomly selected for each treatment. The differentiation grade was evaluated based on the myotube area and the number of nuclei per MHC positive cells (≥3 nuclei) for 20–50 myotubes). Digital images of the cell cultures were acquired with Zeiss Axio Vert.A1 microscope using Zen software. For quantification of myotube area and fluorescence intensity of selected proteins for each cell, ImageJ64 software was used.

Statistical analysis. All values are presented as mean ± standard error of the mean (SEM). Statistical analyses were performed using GraphPad Prism (version 5.0b; GraphPad Software; California, USA). ROUT test with a Q=5% was performed to statistically detect the presence of outliers. Kolmogorov-Smirnov test with Dallal-Wikilnson-Lilief P value was performed to evaluate the normality of each data set. Unpaired Student t-test was used to compare means for data sets with a normal distribution. Mann-Whitney test was used to compare medians for data sets with non-normal distribution. For multiple comparisons, ANOVA was employed. Values of $P<0.05$ were considered to be statistically significant (*).

USC UNIVERSIDADE DE SANTIAGO DE COMPOSTELA

USC
UNIVERSIDADE
DE SANTIAGO
DE COMPOSTELA

RESULTS

USC
UNIVERSIDADE
DE SANTIAGO
DE COMPOSTELA

CHAPTER 1:

ROLE OF THE OBESTATIN/GPR39 SYSTEM IN THE REGULATION OF SATELLITE CELLS

USC
UNIVERSIDADE
DE SANTIAGO
DE COMPOSTELA

The obestatin/GPR39 system is differentially expressed during MuSCs activation

The obestatin/GPR39 system is expressed in healthy skeletal muscle and this expression strikingly increased upon muscle injury[109]. *In vitro*, obestatin is preferentially expressed by myotubes, whereas GPR39 is equally expressed in both myoblast and myotube cells. Expression of both obestatin and GPR39 is coordinately up-regulated during the early stages of myogenesis, and their levels remained sustained throughout terminal differentiation[128,154]. To test this differential expression in MuSCs, we examined skeletal muscle fibres extracted from gastrocnemius muscles and fixed immediately following isolation. Under these conditions, MuSCs are in their native environment and are immunodetected with antibodies against Pax7 and Myf5 as "stem" $Pax7^+/Myf5^-$, or "committed" $Pax7^+/Myf5^+$ MuSCs[30]. We observed the presence of GPR39 on $Pax7^+/Myf5^-$ and $Pax7^+/Myf5^+$ MuSCs (Figure 1.1a and 1.1c). Obestatin was specifically expressed in MuSCs that contains detectable levels of Myf5, $Pax7^+/Myf5^+$ (Figure 1.1b and 1.1c).

For functional assessment, single myofibres were cultured in suspension under growth conditions. Within 24- or 48-h, when MuSCs express MyoD and proliferate to give rise to transient-amplifying cells, obestatin was detected on $Pax7^+/MyoD^+$ cells (Figure 1.2). Obestatin expression was detected in MuSCs descendants on fibres cultured for 72 h, when cells activate myogenin to differentiate ($myogenin^+$ cells; Figure 1.2). Taken together, these results demonstrate that GPR39 is expressed in both quiescent and activated MuSCs. However, obestatin is up-regulated in committed/proliferating MuSCs and myoblasts.

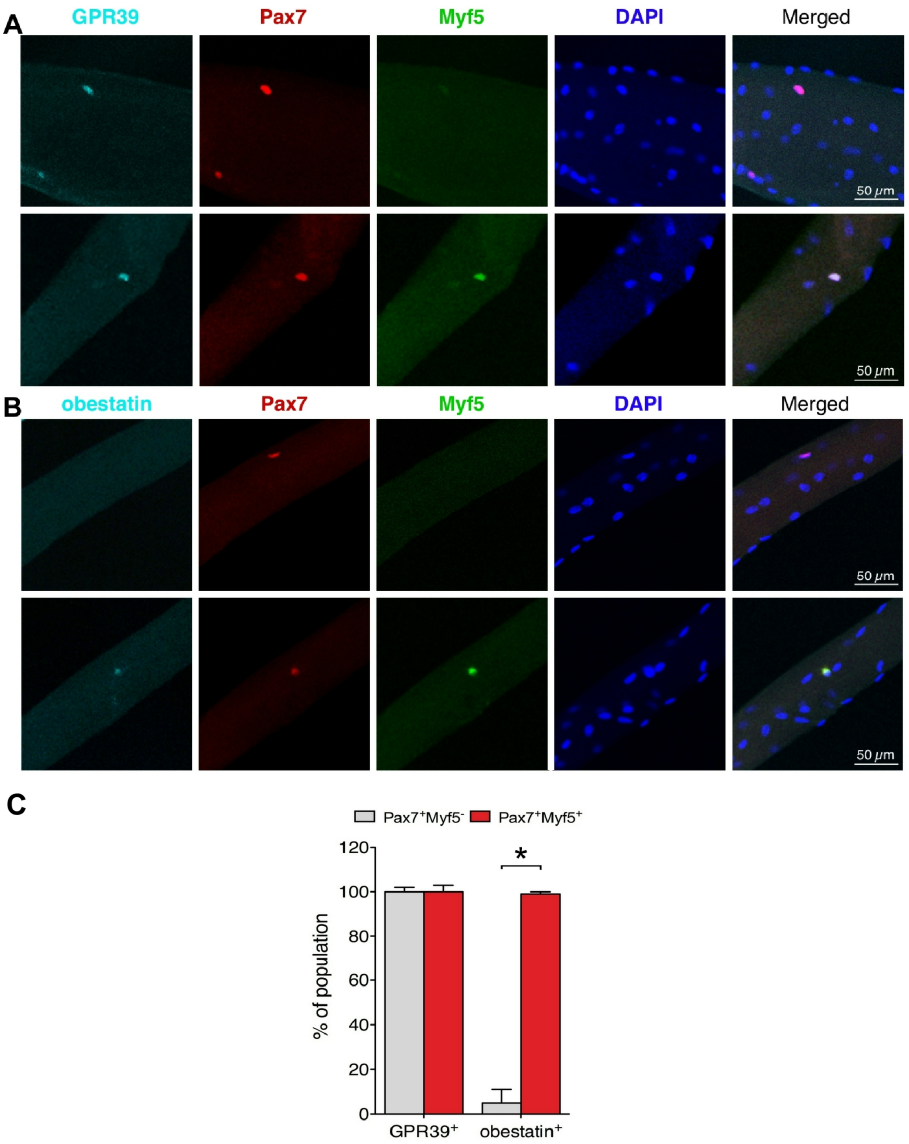


Figure 1.1. Expression of the obestatin/GPR39 system in MuSCs of freshly isolated myofibres. Immunofluorescence detection of GPR39 (A) and obestatin (B) in quiescent ($Pax7^+/Myf5^-$) and activated ($Pax7^+/Myf5^+$) MuSCs in freshly isolated myofibres from gastrocnemius muscle. (C) Quantification by immunofluorescence of GPR39 and obestatin in quiescent ($Pax7^+/Myf5^-$) and activated ($Pax7^+/Myf5^+$) MuSCs, expressed as % of MuSC population (n=3 mice, ≥100 cells/mouse; mean±SEM; * $P < 0.05$ *versus* control values).

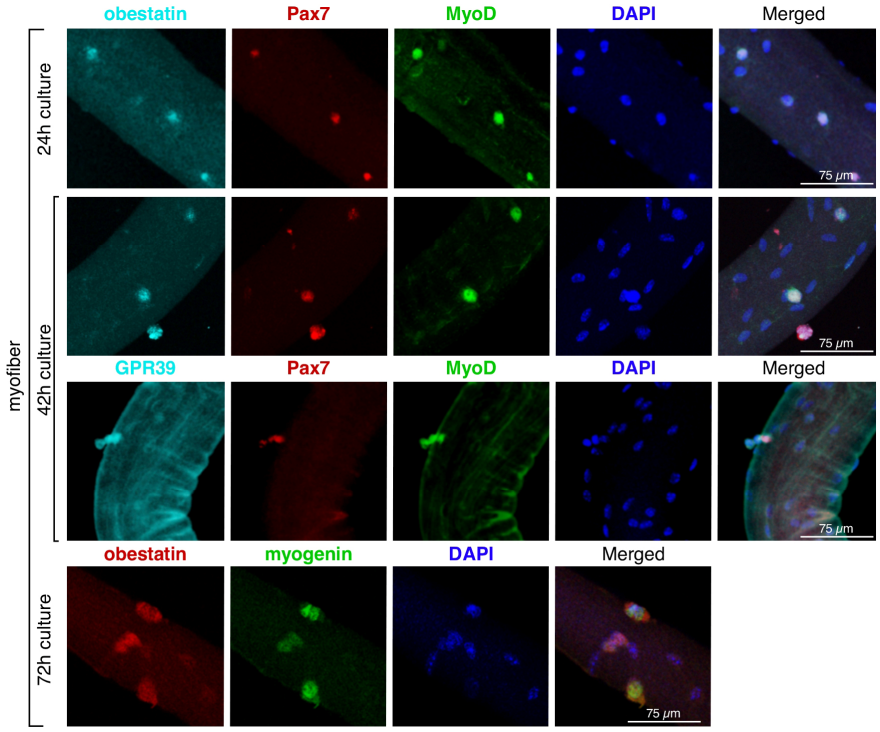


Figure 1.2. Expression profile of the obestatin/GPR39 system in proliferating MuSCs and myogenic precursor cells. Immunofluorescence analysis of obestatin and GPR39 in activated ($Pax7^+/MyoD^+$) and differentiating ($myogenin^+$) MuSCs in isolated myofibres from gastrocnemius muscle cultured in floating conditions (n=3 mice, ≥100 cells/mouse).

GPR39 signalling drives MuSCs expansion

We next asked whether MuSC division requires the presence of GPR39. To that end, we performed siRNA-mediated knockdown of GPR39 (siGPR39) in isolated myofibres from gastrocnemius muscle (Figure 1.3a). siGPR39 caused 68.0±15.3% reduction of $Pax7^+$ cell number per myofibre when compared with the scrambled siRNA (siControl) at 42 h after isolation (Figure 1.3b). At this time point, siGPR39 resulted in a 48.0±16.8% decrease in $MyoD^+$ cell number (Figure 1.3c). The number of $myogenin^+$ cell per myofibre further decreased by 45.0±17.0% at 72 h in culture (Figure 1.3d). The analysis of active-caspase3, which labels apoptotic cells, in $Pax7^+$ cells

revealed an increase in the active-caspase 3^+/$Pax7^+$ cell number at 42 h in culture (Figure 1.4). These results demonstrate that GPR39 participates in the control of MuSCs survival following activation.

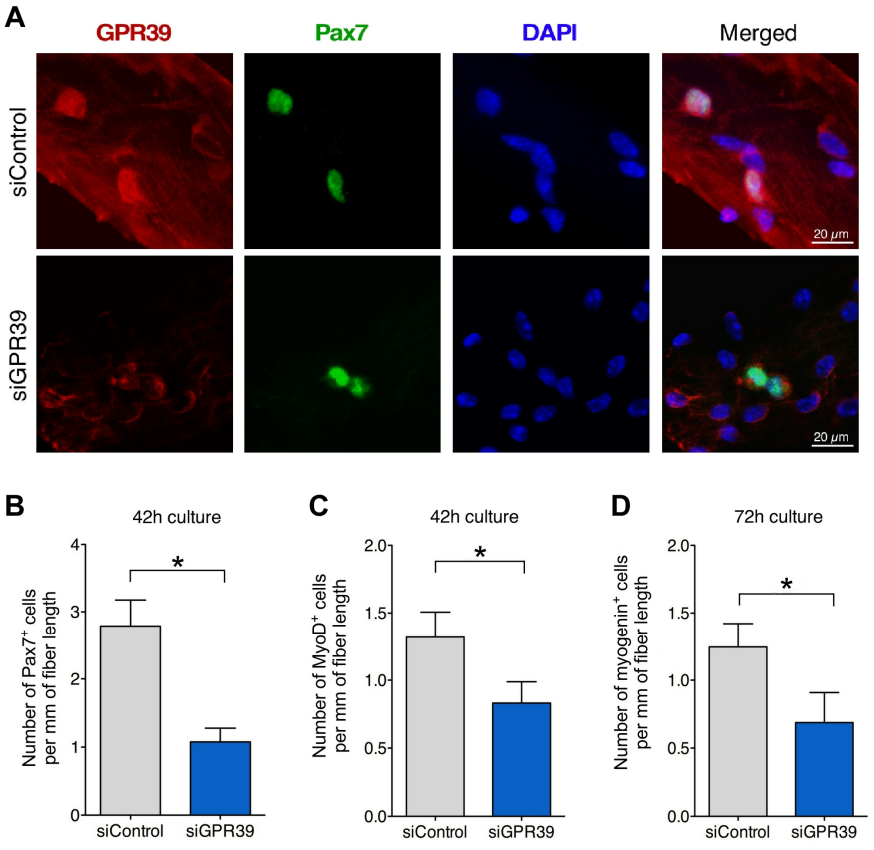


Figure 1.3. GPR39 signalling drives MuSCs expansion. (A) GPR39 immunostaining on single gastrocnemius fibres isolated and cultured in floating conditions after siRNA-mediated knockdown of GPR39 (siGPR39). (B) Effect of siGPR39 on total number of $Pax7^+$ cells per myofibre after 42 h of culture. (C) Effect of siRNA depletion of GPR39 on $MyoD^+$ cells per myofibre after 42 h of culture. (D) Effect of acute GPR39 deficiency on $myogenin^+$ cells on myofibres after 72 h of culture. In b, c and d, cells were enumerated and normalized against myofibre length (mm). Data were expressed as mean±SEM (n=3 mice per group, ≥100 cells/mouse; * $P < 0.05$ *versus* control values).

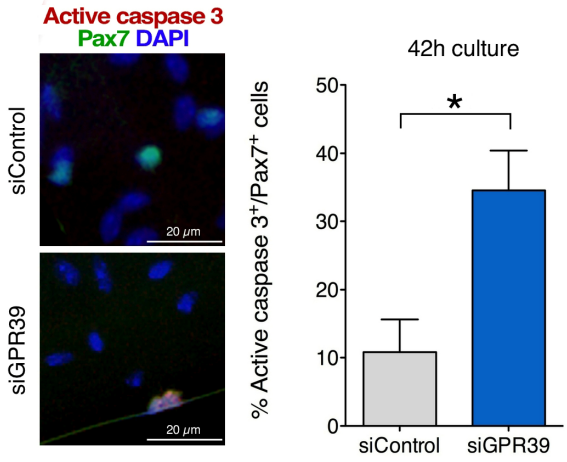


Figure 1.4. GPR39 signalling controls survival in MuSCs. *Left panel*, Pax7 and active caspase 3 immunostaining on single myofibres in the presence of siGPR39 after 42 h of culture. *Right panel*, quantification of active caspase 3^+ MuSCs on myofibre after 42 h of culture. Cells were enumerated and normalized against myofibre length (mm). Data were expressed as mean±SEM (n=3 mice per group, ≥100 cells/mouse; * $P < 0.05$ *versus* control values).

The balance between proliferation and differentiation of MuSCs is regulated by the obestatin/GPR39 system

Cultured myofibres, isolated from gastrocnemius muscles, were stimulated with obestatin (5 nM) to determine the kinetic of cell-cycle entry. We found that MuSCs showed a markedly increased propensity to enter the cell cycle when compared to control MuSCs, as measured by the number of $Pax7^+$ cells that co-expressed Ki67, a protein expressed in all cell cycle phases except G_0, at 24 h after stimulation (Figure 1.5a and 1.5b). Similarly, the proportion of 5-ethynyl-2'-deoxyuridine (EdU; S-phase marker on the cell cycle)-labeled $Pax7^+$ was significantly higher in obestatin-treated myofibres when compared to control cultures. Specifically, 40.0±4.0% of obestatin-treated myofibres had incorporated EdU (EdU^+) within 20 h compared to 21.0±4.4% of EdU^+ MuSCs in control myofibres at the same time (Figure 1.6a and 1.6b). Consistent with these observations, the population of $Pax7^+$ cells increased by 55.0±18.9% in obestatin-treated cultured myofibres at 24 h (Figure 1.5c).

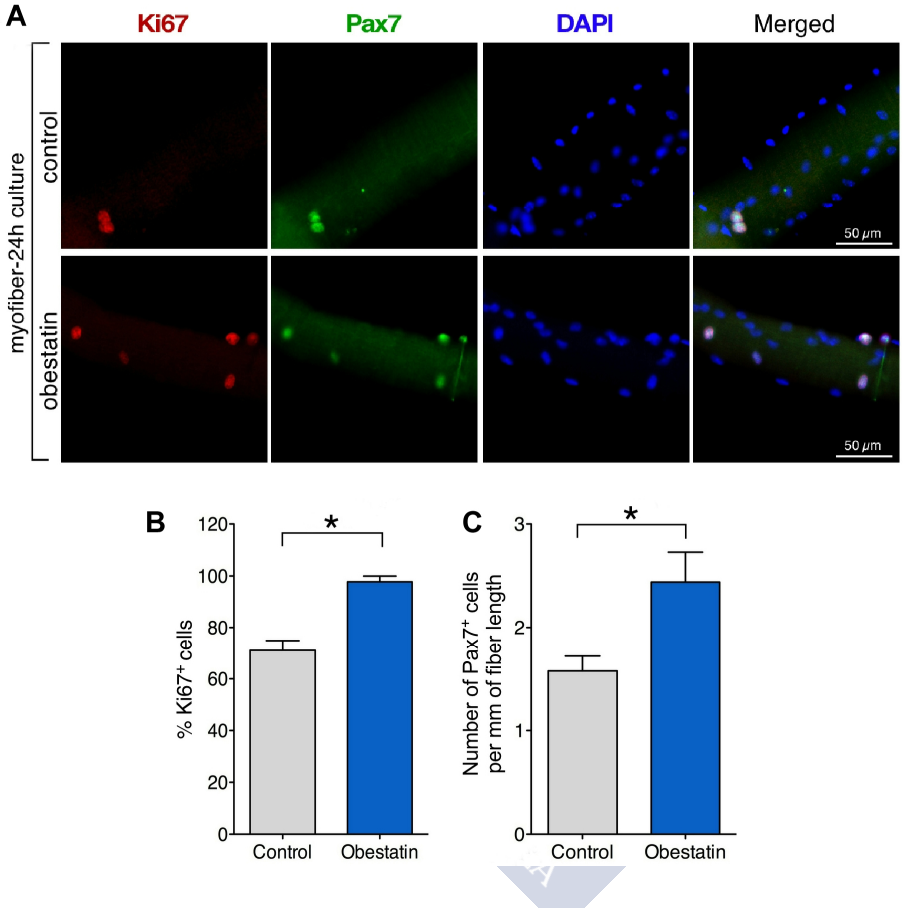


Figure 1.5. Obestatin accelerates MuSCs cell cycle entry. (A) Representative immunofluorescence images of Ki67-stained MuSCs from obestatin- (5 nM) or vehicle-treated myofibres isolated from gastrocnemius muscles and cultured in floating conditions in the first 24 h. (B) Obestatin stimulation increases the number of Ki67$^+$ MuSCs at 24 h. Data are presented as the percentage of Pax7$^+$ cells that are Ki67$^+$. (C) Immunofluorescence analysis of Pax7$^+$ cells in myofibres isolated and stimulated *in vitro* with obestatin (5 nM, 24 h) or vehicle (control). Pax7$^+$ cells were enumerated and normalized against myofibre length (mm). Data are presented as mean±SEM (n=4 mice per group, ≥100 cells/mouse; * $P < 0.05$ *versus* control values).

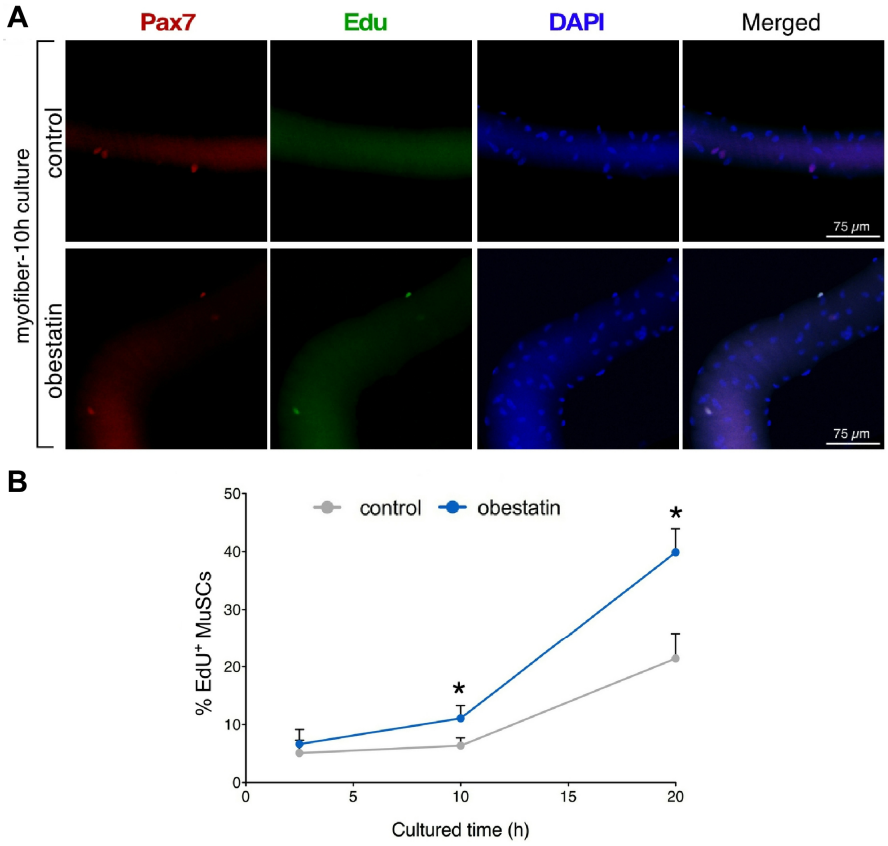


Figure 1.6. Obestatin leads to early MuSCs exit from quiescence. (A) Representative immunofluorescence images of EdU-stained MuSCs from obestatin- (5 nM) or vehicle-treated myofibres cultured in floating conditions at 10 h. (B) Cell cycle entry of MuSCs analysed by EdU incorporation from obestatin- (5 nM) or vehicle-treated myofibres at 2.5-, 10- and 20-h post-stimulation. Data are presented as mean±SEM (n=4 mice per group, ≥100 cells/mouse; * $P < 0.05$ *versus* control values).

We also found that a higher frequency of Pax7^{+} cells was positive for phosphorylated Akt at S473 [pAkt(S473); Figure 1.7a and 1.7b] and S6 at S240/244 [pS6(S240/244); Figure 1.8a and 1.8b] in myofibres treated with obestatin. Thus, obestatin-treated MuSCs displayed accelerated cell cycle entry and time required to complete the first cell division compared to control MuSCs.

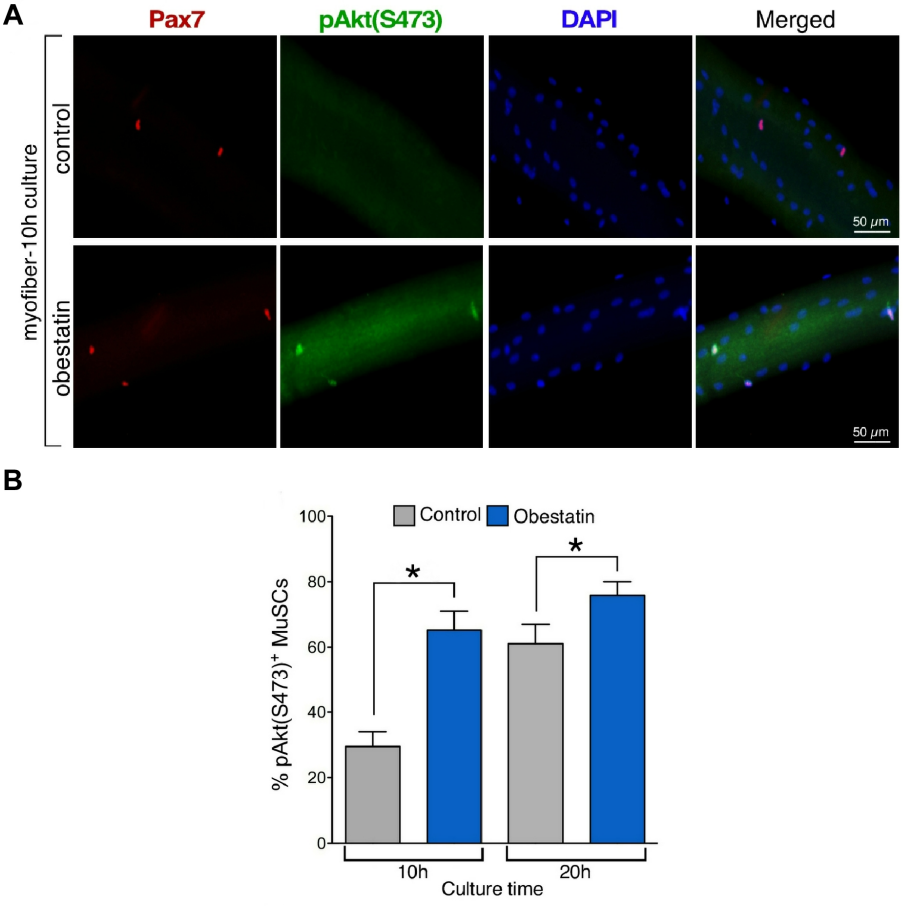


Figure 1.7. Obestatin activates Akt in MuSCs. (A) Representative immunofluorescence images of pAkt(S473) in $Pax7^+$ MuSCs from obestatin- (5 nM) or vehicle-treated myofibres in the first 10 h. (B) Percentages of $Pax7^+$ cells that are $pAkt(S473)^+$ on myofibres at 10- and 20-h post stimulation. Data are presented as mean±SEM (n=4 mice per group, ≥100 cells/mouse; * $P < 0.05$ *versus* control values).

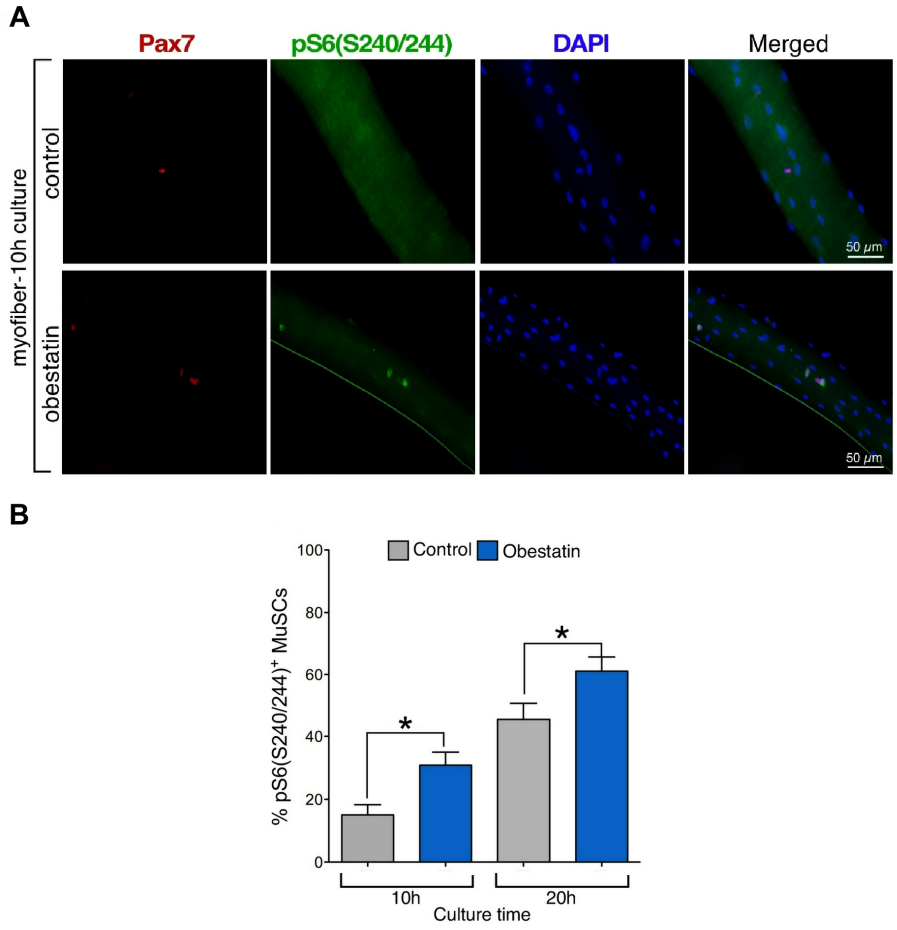


Figure 1.8. Obestatin activates S6 in MuSCs. (A) Representative immunofluorescence of pS6(S240/244) in Pax7^{+} MuSCs from obestatin- (5 nM) or vehicle-treated myofibres at 10 h. (B) Percentages of Pax7^{+} cells that are pS6(S240/244)$^{+}$ on myofibres at 10- and 20-h post stimulation. Data are presented as mean±SEM (n=4 mice per group, ≥100 cells/mouse; **P*<0.05 *versus* control values).

Obestatin/GPR39 signalling in MuSCs fate

MuSCs undergo symmetric cell division, which generates two identical daughter stem cells, and asymmetric cell division, which generates two daughter cells with distinct fates. We then analysed the distribution of Pax7/Myf5 in the plan of division of MuSCs. In obestatin-treated isolated myofibres (5 nM), 64.0±3.3% of cell doublets displayed an asymmetric distribution of Myf5, a marker of activated MuSCs, in apicobasal cell division events contrasting with a 27.0±3.9% observed in control myofibres at 42 h (Figure 1.9a and 1.9b).

Consistent with these observations, a significant proportion of cell doublets (63.0±11.7%) displayed a uniform dispersion of the planar cell polarity effector Vangl2 in the presence of obestatin (Figure 1.9c and 1.9d). However, the majority of cell doublets analysed (74.0±6.9%) in untreated myofibres exhibited polarized localization of Vangl2 on opposite poles of the daughter cells (Figure 1.9c and 1.9d). The PAR complex, composed of partitioning defective 3 (Par-3), partitioning defective 6 (Par-6), and an atypical protein kinase C λ (PKC λ), participates in the asymmetric distribution of intracellular proteins and the positioning of the plane of cell division[41,163]. At 42 h, the majority of $Pax7^+$ cells analysed (69.3±3.3%) in obestatin-treated cultures displayed an asymmetric distribution of Par-3. The remaining $Pax7^+$ cells showed symmetrical Par-3 distribution (12.0±3.3%) or low Par-3 levels (Figure 1.9e and 1.9f). Conversely, Par-3 appeared asymmetric in 21.2±4.0% and symmetric 42.3±5.0% of untreated myofibre-associated $Pax7^+$ cells during the first cell division following explant (Figure 1.9e and 1.9f). Thus, obestatin signalling controls MuSC fate determination, in particular asymmetric *versus* symmetric commitment.

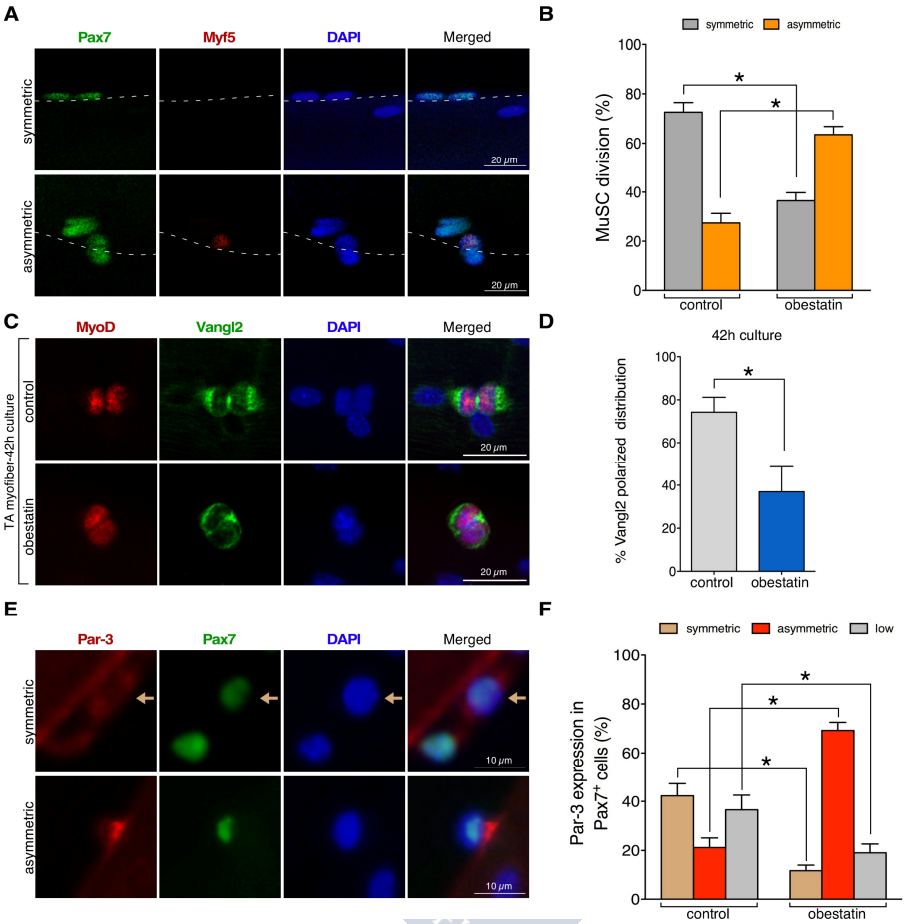


Figure 1.9. Obestatin signalling leads asymmetric MuSC division. (A) Representative immunofluorescence images of symmetric and asymmetric cell division. (B) Quantification of symmetric and asymmetric cell divisions in obestatin- (5 nM, 42 h) and vehicle-treated myofibres. Asymmetric distribution of Myf5 was taken as reference. (C) Representative immunofluorescence of Vangl2 cellular localization on myofibres. (D) Quantification of cell doublets displaying polarized location of Vangl2 at 42 h in obestatin- (5 nM) and vehicle-treated myofibres. (E) Representative immunofluorescence of Par-3 localization in MuSCs on myofibres at 42 h. Arrow indicates symmetric location of Par-3. (F) Quantification of cell doublets displaying symmetric or asymmetric location, or low levels of Par-3 following obestatin (5 nM, 42 h) or vehicle treatment. Data are presented as mean±SEM (n=4 mice per group, ≥100 cells/mouse; * $P < 0.05$ *versus* control values).

Obestatin activity controls Notch and β-catenin signalling pathways in MuSCs

The temporal balance between proliferation and differentiation of MuSCs is regulated by Notch and Wnt/β-catenin signalling pathways[164,165]. At 12 h of culture *ex vivo*, most of the fibre-associated Pax7$^+$ cells were positive for the active intracellular domain of Notch1 (NICD1), a marker of Notch activity (83.0±3.8%; Figure 1.10a and 1.10b). Strikingly, we found that NICD1 co-localized with approximately 17.0±4.3% of Pax7$^+$ cells in obestatin-treated myofibres (5 nM; Figure 1.10a and 1.10b).

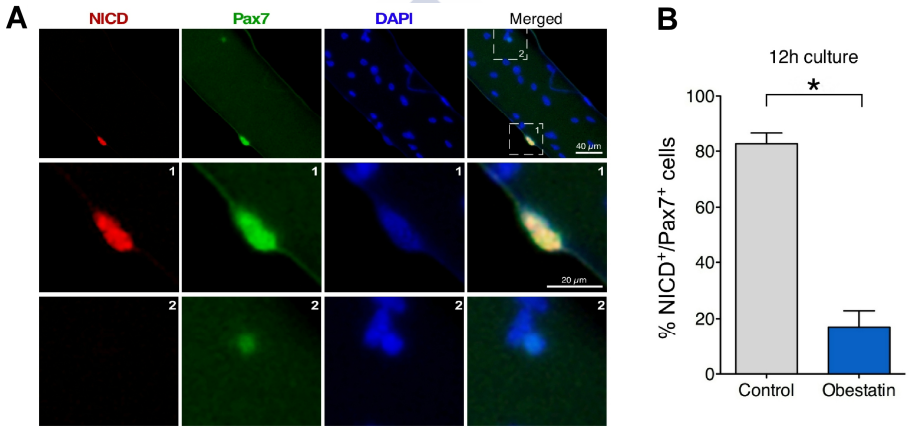


Figure 1.10. Obestatin inhibits Notch signalling in MuSCs. (A) Representative immunofluorescence of NICD cellular localization in Pax7$^+$ cells on myofibres 12 h after isolation. (B) Percentages of Pax7$^+$ cells that are NICD$^+$ on myofibres after obestatin (5 nM, 12 h) or control treatment. Data are presented as mean±SEM (n=3 mice per group, ≥100 cells/mouse; * $P < 0.05$ *versus* control values).

Given the role of Notch signalling in the regulation of progenitor status[166], the loss of Notch signalling in response to obestatin could promote the decision of progenitor cells to differentiate. Indeed, we found that the proportion of MyoD$^+$ cells was significantly increased by 21.0±14.2% in obestatin-treated myofibres at 42 h (Figure 1.11a). Similarly, an increase in the proportion of myogenin$^+$ cells was observed at 72 h after obestatin stimulation (27.0±16.4%; Figure 1.11b).

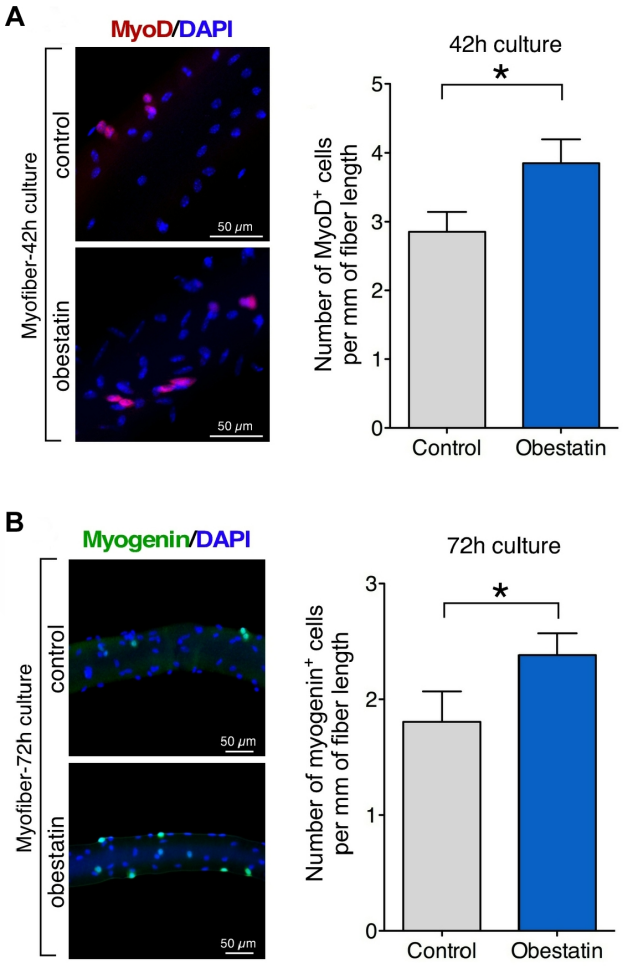


Figure 1.11. Obestatin increases the population of myogenic progenitors. (A) *Left panel.* Representative immunofluorescence of MyoD$^+$ cells on obestatin- and control-treated myofibres (5 nM, 42 h). *Right panel.* Quantification of MyoD$^+$ cells on obestatin- and control-treated myofibres (5 nM, 42 h). (B) *Left panel.* Representative immunofluorescence of myogenin$^+$ cells on obestatin- and control-treated myofibres (5 nM, 72 h). *Right panel.* Quantification of myogenin$^+$ cells on obestatin- and control-treated myofibres (5 nM, 72 h). Cells were enumerated and normalized against myofibre length (mm). Data are presented as mean±SEM (n=3 mice per group, ≥100 cells/mouse; * $P < 0.05$ *versus* control values).

We next questioned whether the inhibition of Notch signalling would facilitate the activation of β-catenin signalling. We thus analysed the distribution of β-catenin at 42 h culture. The majority of MyoD$^+$ cells analysed (73.0±6.4%) harboured nuclear localization of β-catenin in obestatin-treated myofibres unlike untreated myofibres (28.0±9.2%; Figure 1.12a and 1.12b). Additionally, siRNA-mediated knockdown of β-catenin (siβ-catenin) decreased by 45.0±4.0% the total number of MyoD$^+$ cells per myofibre following obestatin stimulation when compared with the siControl at 42 h culture (Figure 1.13a and 1.13b). Thus, the temporal switch from Notch to β-catenin signalling associated to the obestatin/GPR39 system regulates cell fate determination and assures the production of myogenic progenitors during myogenesis.

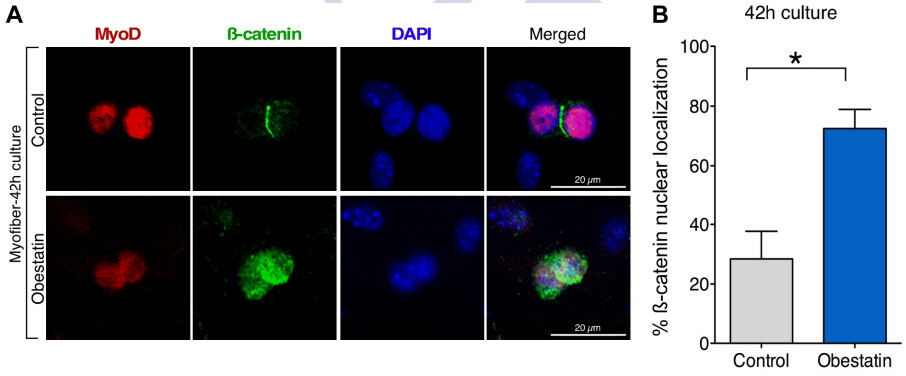


Figure 1.12. Obestatin promotes nuclear localization of β-catenin in MuSCs. (A) Representative immunofluorescence of β-catenin cellular localization in MyoD$^+$ cells on myofibres at 42 h after obestatin (5 nM) or control treatment. (B) Quantification of cell doublets displaying nuclear location of β-catenin at 42 h in obestatin- (5 nM) and vehicle-treated myofibres. Data are presented as mean±SEM of the percentage of total MyoD$^+$ cells (n=3 mice per group, ≥120 cells/mouse; * $P < 0.05$ *versus* control values).

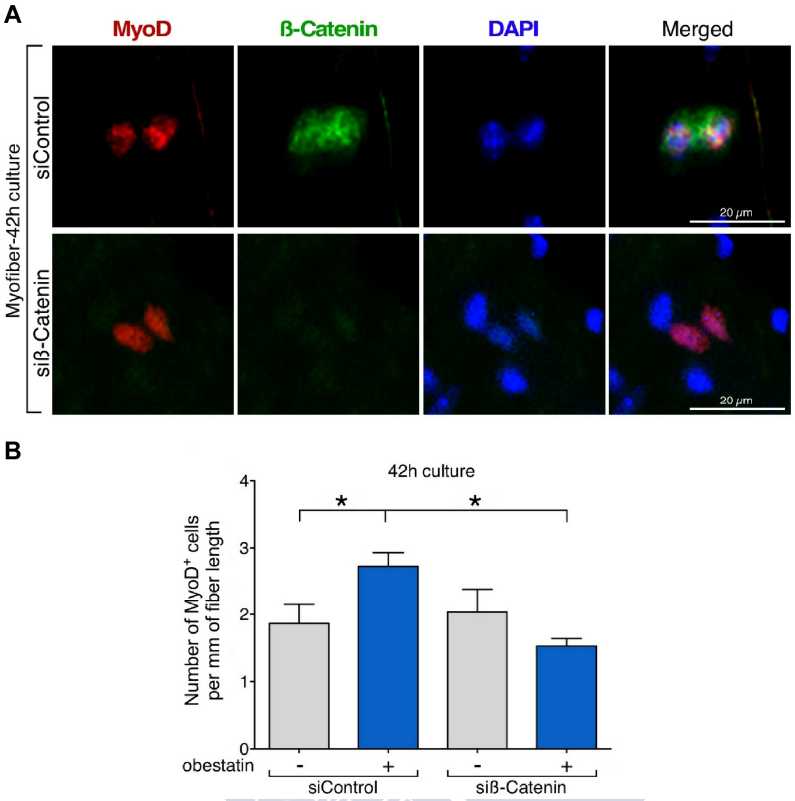


Figure 1.13. Obestatin controls cell fate of MuSCs trough β-catenin signalling. (A) β-catenin immunostaining on single gastrocnemius fibres isolated and cultured in floating conditions after siRNA-mediated knockdown of β-catenin (siβ-Catenin, 42 h culture). (B) Effect of siRNA depletion of β-Catenin on MyoD$^+$ cells per myofibre after 42 h of obestatin (5 nM) or control treatment. Data are presented as mean±SEM of the percentage of total MyoD$^+$ cells (n=4 mice per group, ≥100 cells/mouse; * $P < 0.05$ *versus* control values).

EGFR regulates the obestatin activity in MuSCs

Given that the transactivation of EGFR by the obestatin/GPR39 system is essential for the cell cycle exit and differentiation in myoblasts[128], we next focused on how the differentiation state of MuSCs is affected by loss of EGFR. siRNA-mediated knockdown of EGFR (siEGFR) was performed on isolated myofibres. Immunostaining of treated fibres demonstrated extensive silencing of EGFR expression after 42 h (Figure 1.14a).

Importantly, the ability of obestatin to induce MyoD$^+$ cells was significantly decreased by siEGFR (61.0±6.1%) when compared to scrambled siRNA (Figure 1.14b). These results demonstrate the implication of the transactivation of EGFR by GPR39 in the obestatin signalling to regulate myogenic lineage progression and differentiation also in MuSCs.

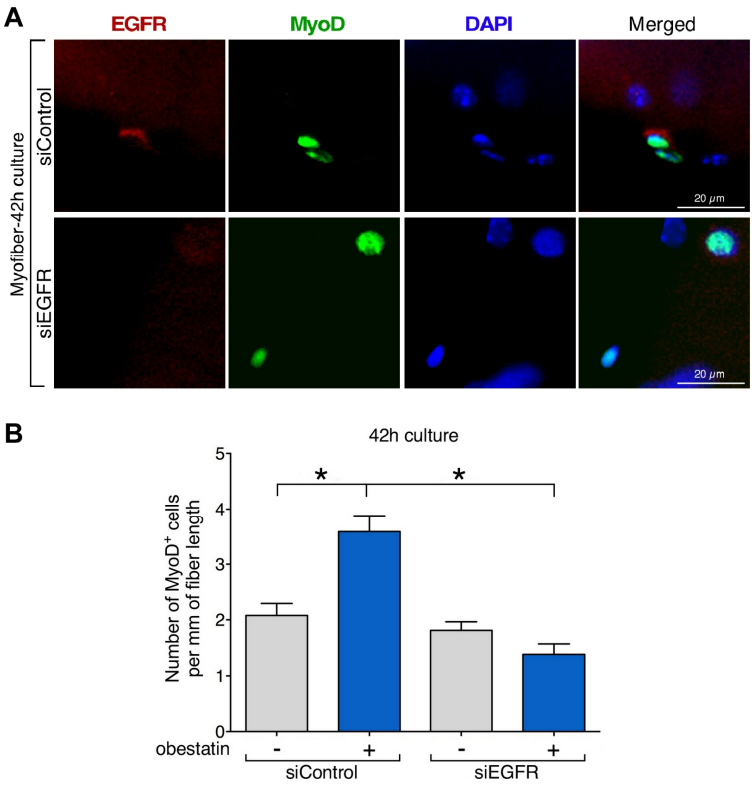


Figure 1.14. The transactivation of EGFR by GPR39 regulates myogenic lineage progression in MuSCs. (A) EGFR immunostaining on myofibres isolated and cultured in floating conditions after siRNA-mediated knockdown of EGFR (siEGFR, 42 h culture). (B) Effect of siEGFR on MyoD$^+$ cells per myofibre after 42 h of obestatin (5 nM) or control treatment. Data are presented as mean±SEM of the percentage of total MyoD$^+$ cells (n=4 mice per group, ≥100 cells/mouse; * $P < 0.05$ *versus* control values).

CHAPTER 2:

EFFECT OF OBESTATIN TREATMENT ON *mdx* MICE

USC
UNIVERSIDADE
DE SANTIAGO
DE COMPOSTELA

Obestatin treatment improves muscle strength in *mdx* mice

As a first step, we investigated the protein expression of preproghrelin, as precursor of obestatin, and GPR39 in the *tibialis anterior* (TA) muscles of *mdx* mice at different ages (4-, 8- and 18-week-old *mdx* mice) by immunoblot analysis. As shown in Figure 2.1, we found an inverse relationship between muscle preproghrelin and GPR39 protein expression with ageing. The age-related changes prompted us to examine the effects of exogenous obestatin in 8-week-old *mdx* mice. Obestatin treatment was performed via intramuscular injection into the TA muscles every 72 h during 30 days [500 nmol/kg body weight (n=5); referred as obestatin group; Figure 2.2] with sampling at 12 weeks of age, as previously described[153]. Results from this group were compared with control vehicle-treated *mdx* mice [phosphate buffered saline (PBS); n=5; now referred as control group] under the same conditions.

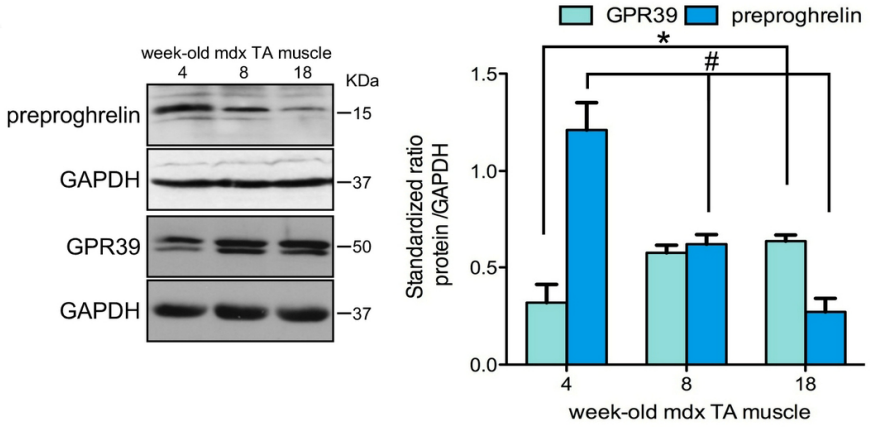


Figure 2.1. Expression of the obestatin/GPR39 system in relation to age in *mdx* mice. Protein levels of preproghrelin, precursor of obestatin, and GPR39 in the TA muscles of *mdx* mice of different ages (4-, 8- and 18-week-old *mdx* mice; n=3 per age-group). Protein levels were analysed by immunoblot and data were expressed as arbitrary units (mean±SEM; $^{*,\#}P< 0.05$ *versus* control values) obtained from intensity scans.

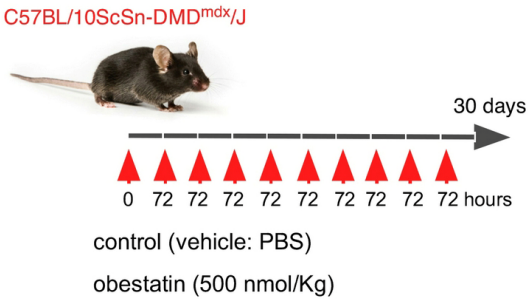


Figure 2.2. Schematic diagram of treatment administration. Obestatin [500 nmol/kg body weight; n=5] or vehicle (PBS, control; n=5) was administered intramuscularly each 72 h in TA from *mdx* mice during 30 days.

As functional strength is one of the measurable outcomes frequently used for DMD patients, we investigated force production in the TA muscles. No significant differences in twitch force were found between the obestatin-treated and control groups (20.0±1.5 and 20.5±1.7 mN/mm^2, respectively; Figure 2.3a). By contrast, the mean tetanic specific force was higher in obestatin-treated TA regarding control TA muscles (51.8±0.4 and 39.0±3.2 mN/mm^2, respectively; Figure 2.3b), representing a 33.0±1.5% increase in relation to control muscles. The force-frequency curves for TA muscle displayed improved force generation beginning at 140 Hz and continuing through 200 Hz relative to PBS (Figure 2.4).

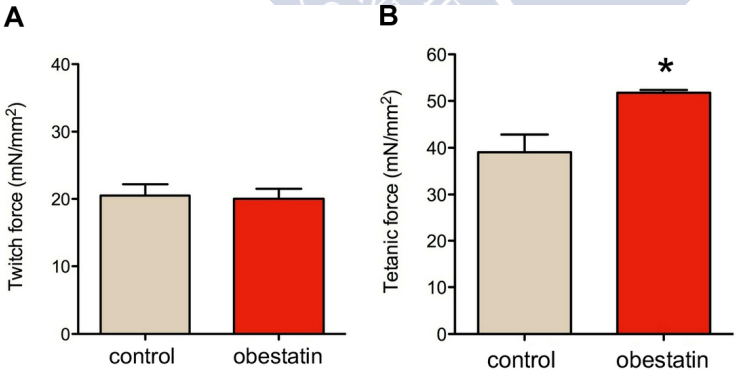


Figure 2.3. Obestatin treatment increases tetanic force in *mdx* TA muscle. (A) Effect of intramuscular injection of obestatin or vehicle on the twitch force at 30 days. (B) Effect of intramuscular injection of obestatin or vehicle on the tetanic force at 30 days. Data are represented as mean±SEM (n=5 animals per group; * $P < 0.05$ *versus* control values).

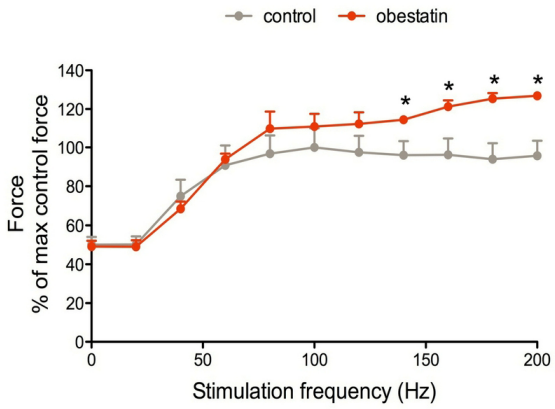


Figure 2.4. Obestatin treatment increases strength in *mdx* TA muscle. Force-frequency curve of TA muscles in obestatin- or vehicle-treated groups at 30 days. Data are represented as mean±SEM (n=5 animals per group; * $P < 0.05$ *versus* control values).

The wet-weights of TA muscles were measured. Interestingly, we did not observe significant differences in the average muscle mass of the TA treated with obestatin relative to control (Figure 2.5a). Furthermore, we analysed the serum levels of creatine kinase (CK), a skeletal muscle enzyme released during fibre degeneration (Figure 2.5b). We observed a significant decrease in the average CK levels of *mdx* mice treated with obestatin relative to control mice (16180.0±5968.0 and 39290.0±7979 U/L, respectively), suggesting a decrease in the level and severity of muscle damage.

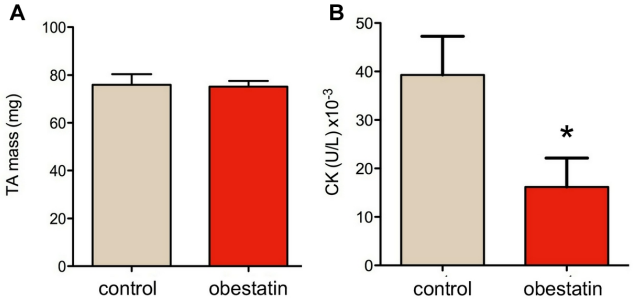


Figure 2.5. Obestatin treatment reduces serum CK levels in *mdx* mice. (A) TA muscle weight after 30 days of treatment with vehicle or obestatin. (B) Serum CK levels after 30 days of treatment with vehicle or obestatin. Data are represented as mean±SEM (n=5 animals per group; * $P < 0.05$ *versus* control values).

The TA muscles from obestatin-treated or control *mdx* mice were stained with haematoxylin and eosin (HE) (Figure 2.6a) and analysed for the presence of centrally located nuclei (CLN; Figure 2.6b), myofibre number (Figure 2.7a) and cross-sectional area (CSA; Figure 2.7b and 2.7c). A 10±1.2% decrease in CLN percentage was observed in the obestatin-treated *mdx* TA muscle compared to control (Figure 2.6b).

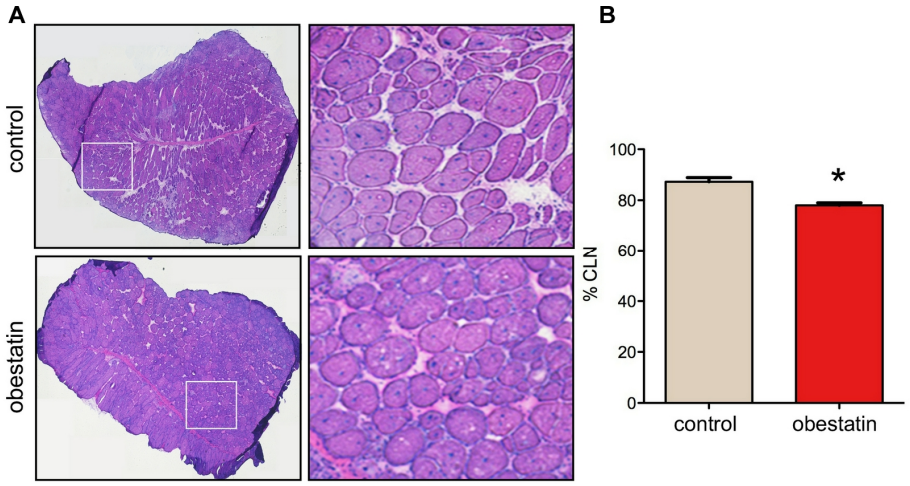


Figure 2.6. Obestatin treatment decreases the percentage of CNL in *mdx* mice. (A) Representative HE staining from vehicle- and obestatin-treated TA muscles at 30 days. (B) Quantitation of myofibres with CNL from vehicle- and obestatin-treated TA muscles at 30 days. Data are shown as % of myofibres with CLN. Data are represented as mean±SEM (n=5 animals per group; * $P < 0.05$ *versus* control values).

We found the average number of myofibres in the obestatin treated *mdx* mice (2067.0±40.5) was only slightly lower compared to control animals (2191.0±68.0) (Figure 2.7a), but this difference was not statistically significant. CSA was 23.5±3.2% larger in control mice compared to obestatin-treated mice (Figure 2.7b): mice treated with obestatin presented an increase in the percentage of small myofibres between 5-20x10^2 μm^2 (Figure 2.7c). Together, these data show that *mdx* mice treated with obestatin present an improvement in functional outcome measures (muscle strength) and a small increase in the number of small diameter fibres.

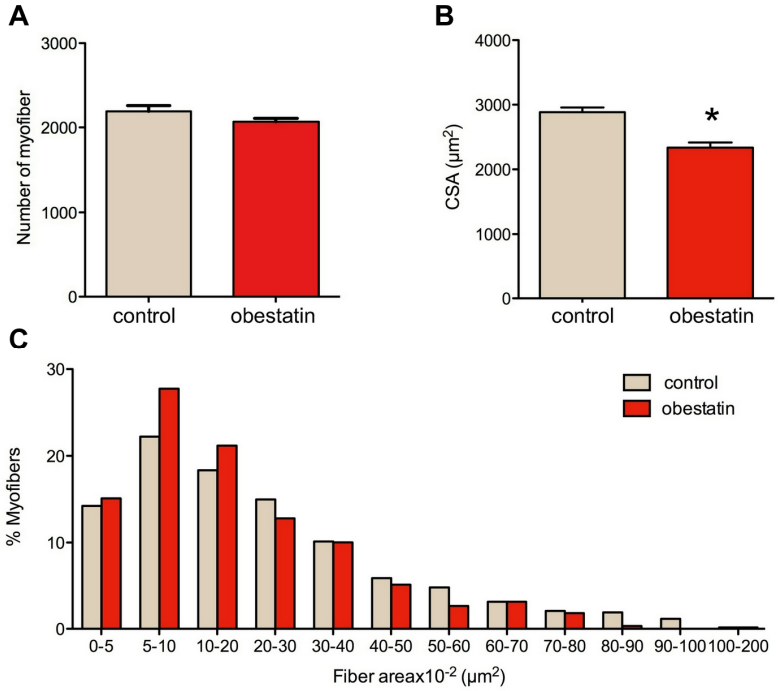


Figure 2.7. Obestatin treatment increases the number of small diameter fibres in *mdx* mice. (A) Quantification of the number of myofibres in TA muscles after 30 days of treatment with vehicle or obestatin. (B) Cross-sectional area of muscle fibres from TA muscles after intramuscular injection of obestatin or vehicle at 30 days. (C) Distribution of fibre diameter from vehicle- and obestatin-treated mice. Data are expressed as % of myofibres and represented as mean±SEM (n=5 animals per group; * $P < 0.05$ *versus* control values).

Obestatin regulates oxidative fibre expression

On histological examination of TA (fast/glycolytic muscle) from obestatin-treated animals, we observed a marked increase in the relative density of succinate dehydrogenase (SDH) positive fibres (SDH^+, oxidative fibres), compared with control *mdx* mice, with a corresponding decrease in SDH negative fibres (SDH^-, Figure 2.8a and 2.8b). Quantitation of the total fibre number revealed an increase of 23.0±1.9% in SDH^+ fibres, oxidative fibre type, in the obestatin-treated group relative to the control group. On the other hand, the number of SDH^- fibres was decreased by 23.0±6.5% in obestatin-treated TA muscles relative to control muscles.

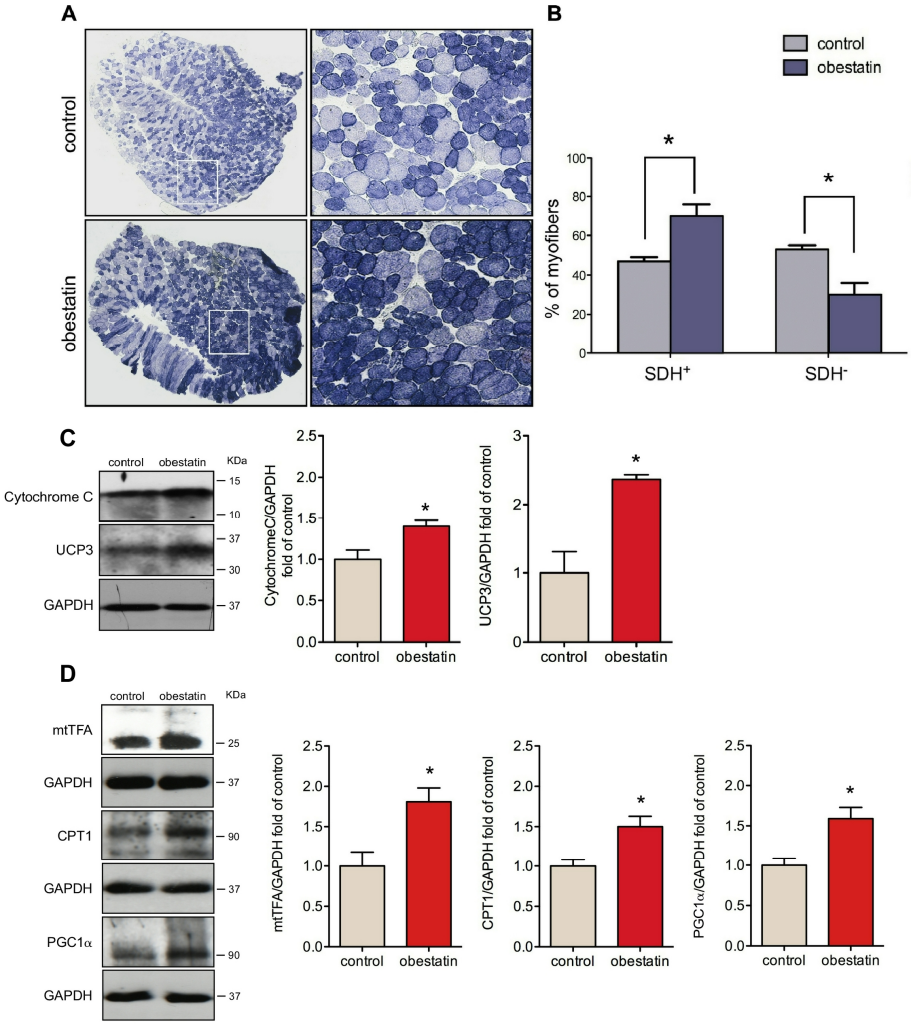


Figure 2.8. Obestatin treatment increases oxidative fibre density. (A) Representative SDH staining from TA from control muscles and obestatin-treated muscles at 30 days. (B) Quantitation of SDH^+ and SDH^- muscle fibres from TA muscles. (C) Immunoblot analysis of cytochrome C and UCP3 in TA muscles after intramuscular injection of obestatin or vehicle at 30 days. (D) Immunoblot analysis of mtTFA, CPT1 and PGC1α in TA muscles after intramuscular injection of obestatin or vehicle at 30 days. Data were expressed as mean±SEM (n=5 animals per group) obtained from intensity scans (* $P < 0.05$ *versus* control values).

This oxidative fibre-type switch was associated with significant increase in the expression of proteins involved in the mitochondrial biogenesis pathway, such as cytochrome C (40.3±7.0%), mitochondrial uncoupling protein 3 (UCP3; 136.5±7.1%), mitochondrial transcription factor A (mtTFA; 81.1±17.0%), peroxisome-proliferator-activated receptor-γ coactivator-1 (PGC-1α; 58.5±14.0%) and carnitine palmitoyltransferase-1 (CPT1; 50.36±13.1%) in obestatin-treated *mdx* mice as compared to control animals (Figure 2.8c and 2.8d).

The slow type I and the fast type IIa, IIb and IIx constitute the four basic fibre types, classically identified based on their MHC isoform content[4,167]. Muscle fibre-type assessment by immunofluorescence (Figure 2.9a) revealed that obestatin increased by 25.2±1.7% the number of type I fibres relative to controls (Figure 2.9b). These TA muscles had a reduction in type IIx fibres compared with control while no significant differences were observed in type IIa and IIb fibres (Figure 2.9b). The CSA of type I fibres was significantly increased in obestatin-treated TA muscles compared to control mice (4-fold increase; Figure 2.9b). Interestingly, type IIb fibres had a significantly larger CSA in obestatin-treated mice than control mice, whereas no significant differences were observed in type IIa and IIx (Figure 2.9b).

Slow and oxidative myofibre identity is regulated by the balance between positive and negative signalling by MEF2 and the class II HDAC proteins, respectively[168]. Indeed, immunoblot analysis of obestatin-treated TA muscles demonstrated the up-regulation of MEF2A and MEF2C protein expression (92.0±16.0 and 52.0±7.0%, respectively; Figure 2.10a). However, the activity of MEF2 is tightly regulated through association with HDACs, which act as signal-dependent repressors of gene expression. HDAC phosphorylation in response to differentiation signals or motor innervation provides docking sites for the 14-3-3 chaperone protein that leads to nuclear export of HDACs enabling MEF2 to activate the slow myofibre gene program[169–171]. Consistent with this, obestatin treatment resulted in markedly elevated levels of HDAC5 [pHDAC5(S259); 149.2±29.5%] and HDAC7 [pHDAC7(S155); 93±32.0%] phosphorylation but no significant differences were observed in HDAC4 phosphorylation (Figure 2.10b).

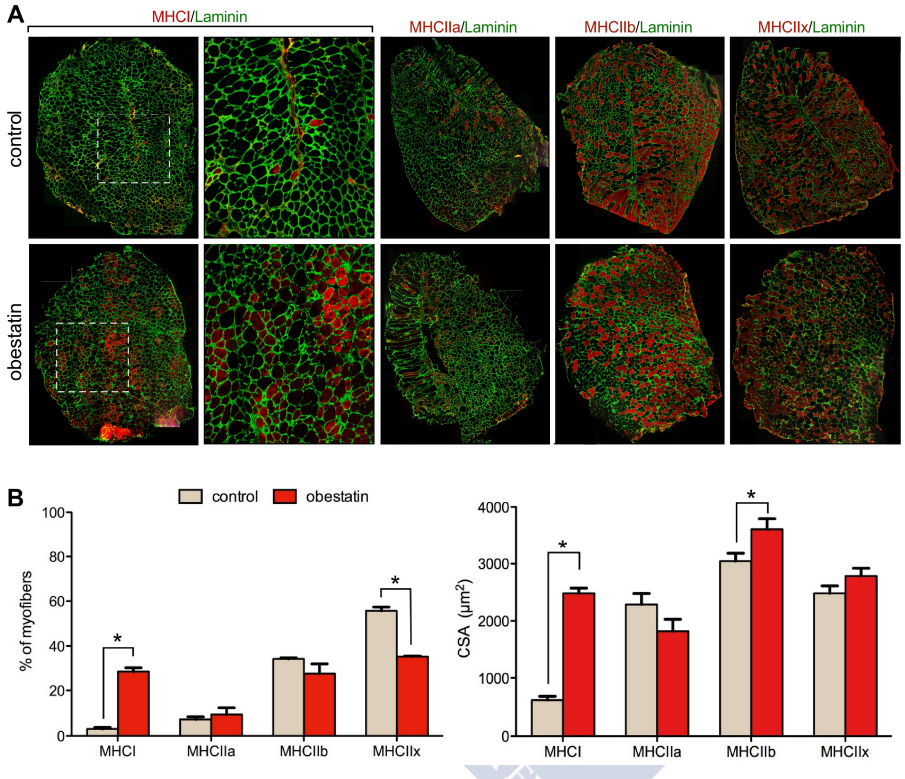


Figure 2.9. Obestatin stimulates fast to slow twitch fibre type shifting in *mdx* mice. (A) Representative images of control- and obestatin-treated TA muscles showing MHC expression. Mice muscle serial cross-section incubated with a primary antibody against MHCI, MHCIIa, MHCIIb or MHCIIx, followed by incubation with appropriate fluorescent-conjugated secondary antibody. (B) Quantitation of fibre types *(left panel)* and CSA *(right panel)*. Data are shown as mean±SEM of 5 animals per group (* $P < 0.05$ *versus* control values).

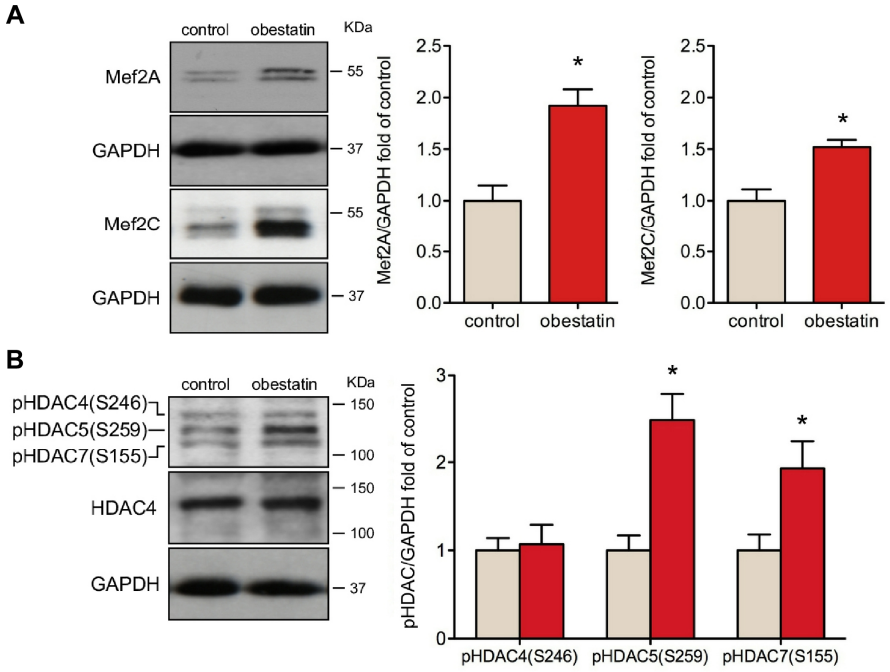


Figure 2.10. Obestatin controls slow fibre type program through MEF2 and HDACs. (A) Immunoblot analysis of MEF2A and MEF2C in TA muscles after intramuscular injection of obestatin or vehicle at 30 days. (B) Immunoblot analysis of pHDAC4(S246), pHDAC5(S259), pHDAC7(S155) and HDAC4 in TA muscles after intramuscular injection of obestatin or control at 30 days. Data were expressed as mean±SEM (n=5 per group) obtained from intensity scans (* *P*< 0.05 *versus* control values).

Consistent with the role of MEF2 as a transcriptional regulator of the slow-fibre phenotype, the expression of slow troponin I (troponin I-SS) was much higher in obestatin-treated muscles (147.0±27%) than in control muscles whereas fast troponin I (troponin I-FS) expression was decreased (51.0±4.0%; Figure 2.11). Therefore, the phosphorylation of HDAC5/7 potentially regulated by obestatin signalling provides a mechanism for the modulation of MEF2 target genes to promote slow and oxidative myofibres.

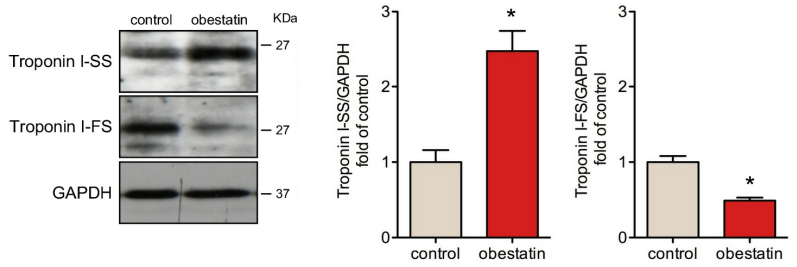


Figure 2.11. Obestatin increases troponin I-SS expression. Expression of the slow-fibre–specific troponin I-SS and fast-fibre-specific troponin I-FS in TA muscles after intramuscular injection of obestatin or vehicle at 30 days. Data were expressed as mean±SEM (n=5 per group) obtained from intensity scans (* *P*< 0.05 *versus* control values).

Obestatin modulates molecular markers of protein synthesis and degradation

In terms of protein degradation, obestatin treatment led to a 43.6±7.6 and 42.8±14.0% decrease in the expression of the ubiquitin E3-ligases MuRF1 and MAFbx, respectively (Figure 2.12a). One mechanism by which obestatin reduces the expression of the ubiquitin E3-ligases is the phosphorylation and subsequent nuclear exclusion of FoxO family members[155]. As shown in Figure 2.12b, obestatin-treated mice showed a striking increase in FoxO1 phosphorylation at T24 [pFoxO1(T24); 130.4±18.0%] and FoxO4 phosphorylation at T28 [pFoxO4(T28); 378.6±59.5%] related to control mice but did not change basal FoxO3a phosphorylation at T32 [pFoxO3(T32)]. This suggests that post-translational modifications of FoxO4 and FoxO1 could play a role in directing FoxO activity in response to obestatin and, thus, to control the E3-ubiquitin ligases MuRF1 and MAFbx.

The down-regulation of MuRF1 and MAFbx expression was concomitant with the activation of positive regulators of protein synthesis. Obestatin increased S6K1 phosphorylation at S371 [pS6K1(S371)] and its downstream target, the ribosomal protein S6 phosphorylation at S240/244 [pS6(S240/244)] by 152.9±39.0 and 109.0±23.4% respectively, compared to control mice (Figure 2.13a and 2.13b). Furthermore, obestatin markedly promoted 4E-BP1 hyperphosphorylation at T70 [p4E-BP1(T70)], especially

concerning the γ form (71.2±11.4%), altering the basal phosphorylation of β and γ forms at T37/T46 [p4E-BP1(T37/46); 49.4±7.8 and 25.5±9.2%, respectively] (Figure 2.13c). Consequently, obestatin signalling regulates critical components of the anabolic machinery for protein synthesis, S6K1 and 4E-BP1[172], in dystrophic conditions.

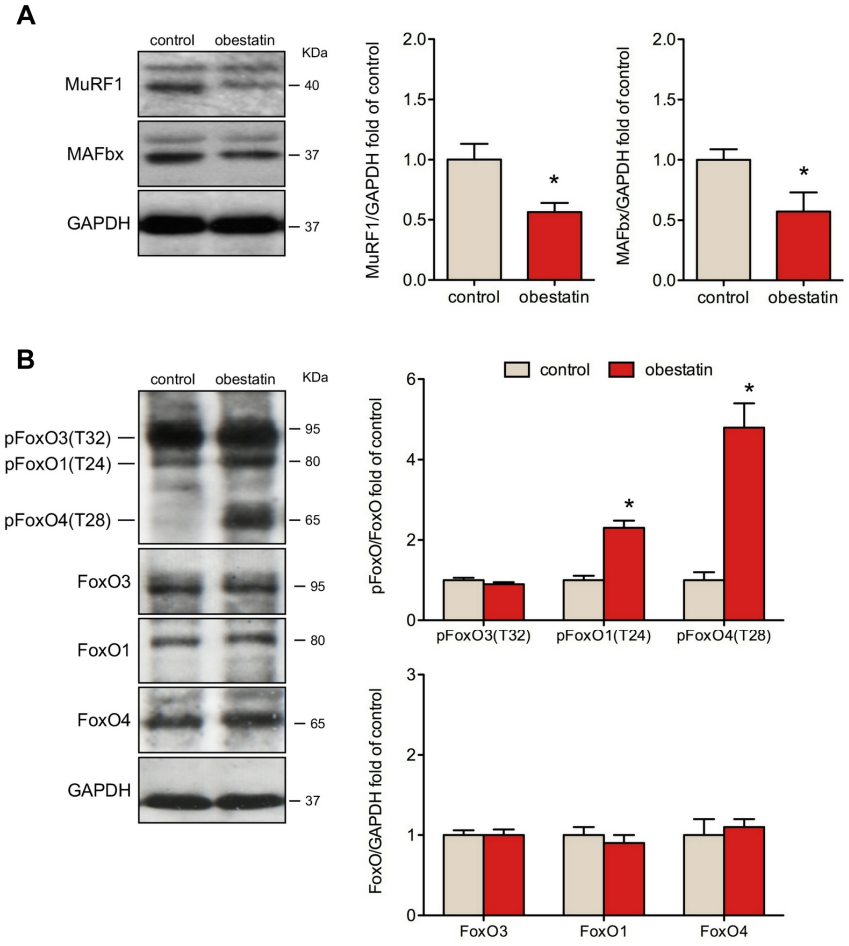


Figure 2.12. Obestatin treatment protects from atrophy. (A) Immunoblot analysis of MuRF1 and MAFbx in TA muscles after intramuscular injection of obestatin or vehicle. (B) Immunoblot analysis of the phosphorylation partner of FoxO3, FoxO1 and FoxO4 in TA muscles after intramuscular injection of obestatin or vehicle at 30 days. Data were expressed as mean±SEM (n=5 animals per group; * *P*< 0.05 *versus* control values).

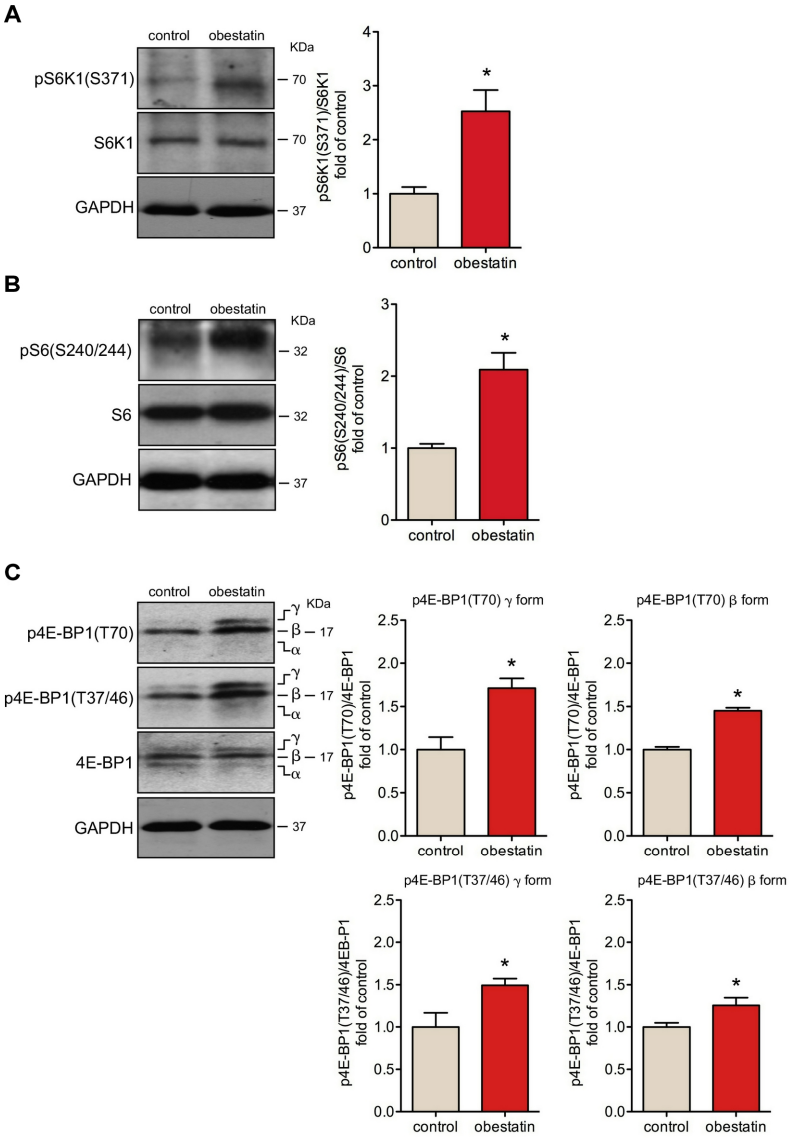


Figure 2.13. Obestatin treatment induces protein synthesis signalling. (A) Immunoblot analysis of pS6K1(S6371) and S6K1 in TA muscles after intramuscular injection of obestatin or vehicle at 30 days. (B) Immunoblot analysis of pS6(S240/244) and S6 in TA muscles after intramuscular injection of obestatin or vehicle. (C) Immunoblot analysis of p4E-BP1(T70), p4E-BP1(T37/46) and 4E-BP1 in TA muscles after intramuscular injection of obestatin or vehicle. Data were expressed as mean±SEM obtained from intensity scans (n=5 animals per group; * $P< 0.05$ *versus* control values).

Obestatin-treated *mdx* mice have increased sarcolemma adhesion protein components

The improvements in *mdx* mice under obestatin treatment could be associated with restoration or increased abundance of sarcolemma adhesion protein components. Analysis by immunoblot of some of these proteins showed that obestatin treatment increased the expression of utrophin by 74.0±20.3% compared to control mice (Figure 2.14). This up-regulation was concomitant with increased expression of α-syntrophin and β-dystroglycan compared to control mice (38.8±6.9 and 96.1±26.0%, respectively; Figure 2.14) but did not change basal neuronal nitric oxide synthase (NOS1) expression. In addition, obestatin treatment led to increased levels of α7- and β1D -integrin (35.2±4.8 and 37.9±5.8% compared to control mice, respectively; Figure 2.14).

Confocal imaging analysis of histological sections from obestatin-treated TAs showed a noticeable increase in the expression of utrophin in the extrasynaptic sarcolemma (Figure 2.15). By contrast, utrophin was expressed at low levels on the extrasynaptic sarcolemma, being mainly restricted to neuromuscular junction (NMJ) in control muscles (Figure 2.15a). Importantly, we found an increase in α7- and β1D-integrin proteins at the sarcolemma in obestatin-treated mice when compared with control (Figure 2.15b). These data, together with the significant decrease in CK, suggest that obestatin treatment protects the fibres by reducing the degradation of the sarcolemma adhesion components in skeletal muscle of *mdx* mice, thereby increasing membrane stability.

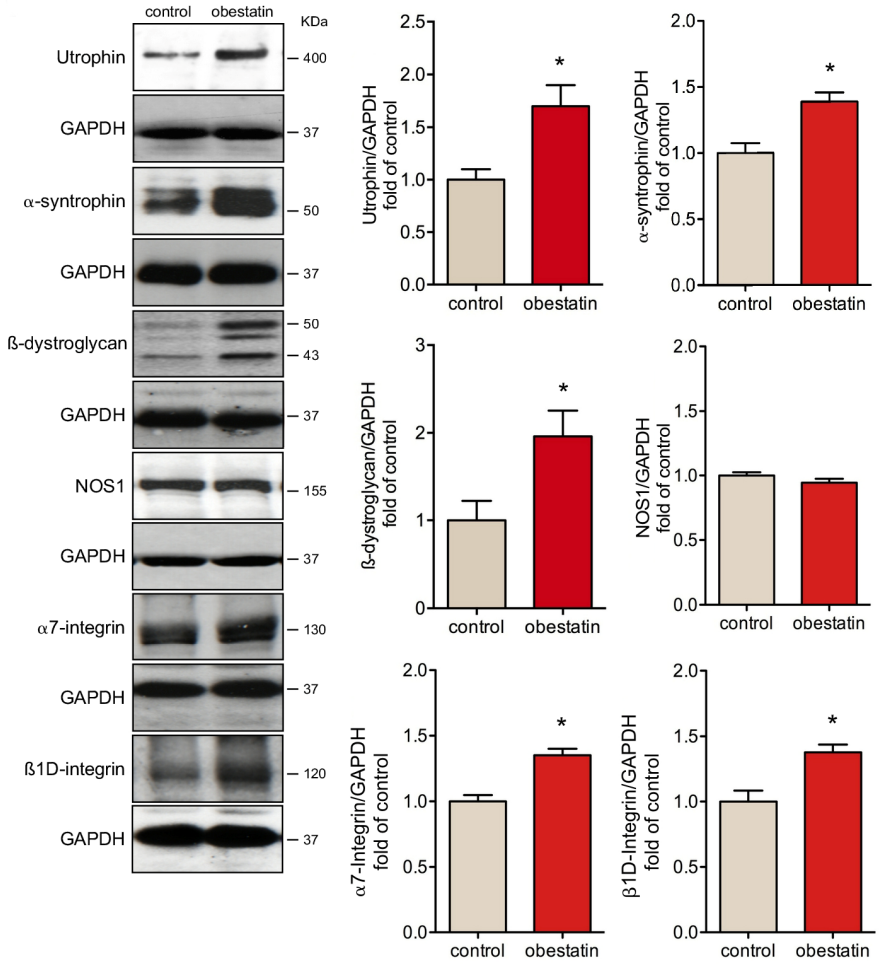


Figure 2.14. Obestatin increases the expression of sarcolemma adhesion protein components. Immunoblot analysis of utrophin, α-syntrophin, β-dystroglycan, NOS1, α7-integrin and β1D-integrin in TA muscles after intramuscular injection of obestatin or vehicle at 30 days. Data were expressed as mean±SEM (n=5 animals per group; * $P < 0.05$ *versus* control values).

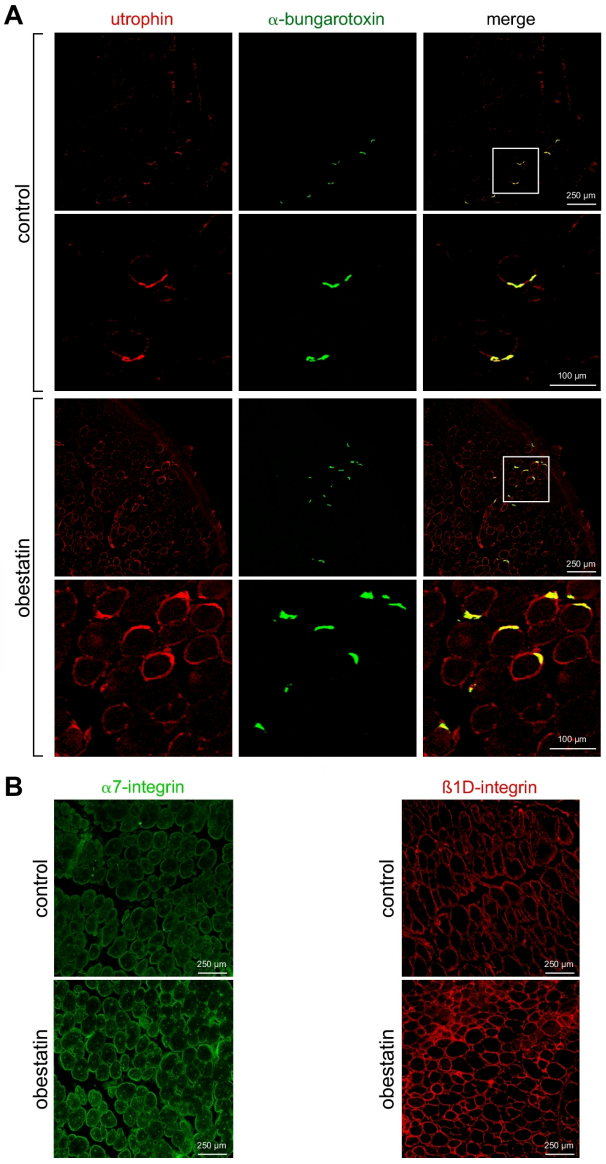


Figure 2.15. Obestatin increases the expression of utrophin in the extrasynaptic sarcolemma. (A) Representative immunofluorescence images of obestatin-treated or control TA muscles at 30 days showing utrophin and neuromuscular junctions (α-bungarotoxin) expression. (B) Representative immunofluorescence images from obestatin-treated or control TA muscles showing α7-integrin *(left panel)* and β1D-integrin *(right panel)* expression at 30 days (n=5 animals per group).

Obestatin enhances AchRα gene

We further tested whether obestatin regulates the NMJ gene expression, based on the regulatory role of PGC-1α in the NMJ program[173]. To test this hypothesis, we measured the expression levels of acetylcholine receptor (AchR) α subunit (AchRα), ε subunit (AchRε), δ subunit (AchRδ), muscle-specific receptor tyrosine kinase (MuSK) and receptor tyrosine-protein kinase erbb-1 (ErbB1) by quantitative RT-PCR. We detected increased levels of AchRα (165.0±73%) but not AchRε, AchRδ, MuSK or ErbB1 in obestatin-treated mice relative to controls (Figure 2.16).

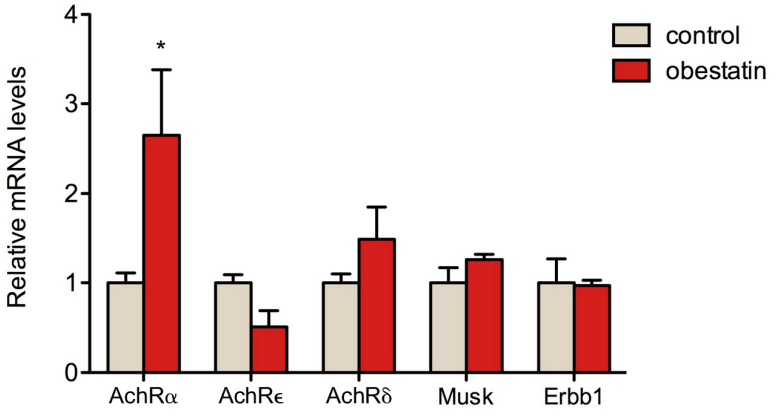


Figure 2.16. Obestatin increases the expression of AchRα gene. Relative mRNA levels of acetylcholine receptor (AchR) subunits α, δ, ε and Musk, Erbb1 in obestatin-treated or control TA muscles at 30 days. Data were expressed as mean±SEM (n=5 animals per group; * *P*< 0.05 *versus* control values).

Obestatin alleviates the phenotype of muscular dystrophy

We determined the rate of interstitial fibrotic regions by Masson's trichrome staining. While fibrosis typically only becomes prominent in older *mdx* mice, even the mild degree of tissue fibrosis developed at 12 weeks of age was reduced in TAs of obestatin-treated mice (Figure 2.17a). Consistent with this, the expression of fibrosis-associated molecules, connective tissue growth factor (CTGF), α-smooth muscle actin (α-SMA) and collagen type I

(Coll I) proteins were decreased by 45.0±5.0, 33±6.0 and 26.5±8.4% in obestatin-treated muscles, compared to control mice, respectively (Figure 2.17b).

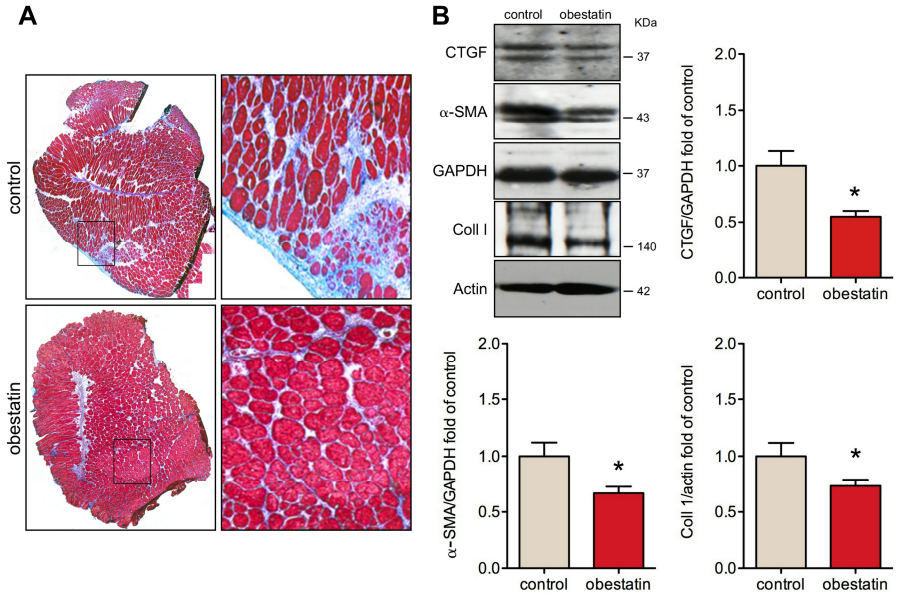


Figure 2.17. Obestatin regulates muscle tissue fibrosis in *mdx* mice. (A) Representative images of the histological analysis from sections stained with Masson's trichrome staining are shown from obestatin-treated or control TA muscles at 30 days. (B) Expression analysis of CTGF, α-SMA and Coll I in TA muscles after intramuscular injection of obestatin or vehicle. Data were expressed as mean±SEM (n=5 animals per group; * *P*< 0.05 *versus* control values).

To further assess the extent of damaged myofibres, we quantified the number of IgG-positive damaged fibres by immunofluorescence and found a 16-fold decrease in the number of damaged fibres in obestatin-treated muscles (Figure 2.18a and 2.18b).

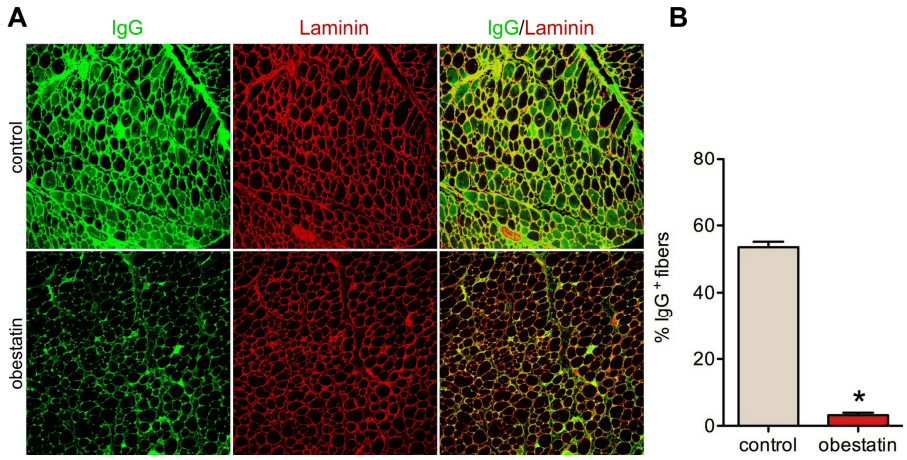


Figure 2.18. Obestatin reduces necrosis in *mdx* mice. (A) Representative images of IgG staining and laminin of obestatin- or vehicle-treated TA muscles. (B) Quantitation of IgG^+ fibres in obestatin-treated or control TA muscles at 30 days. Data were expressed as mean±SEM (n=5 animals per group; * $P< 0.05$ *versus* control values).

Toxicological analysis

In order to assess potential toxicity of obestatin treatment, plasma was collected from mice at the end of treatment and organs harvested for toxicological analysis. Compared with control *mdx* mice, histological HE staining of kidney and liver tissue sections of obestatin-treated mice showed no detectable effect on cells in those tissues nor any increase in the amount of infiltrating immune cells, suggesting the absence of any toxic effect (Figure 2.19a and 2.19b, respectively). Serum levels of urea, bilirubin and alkaline phosphatase showed no significant difference compared to *mdx* control mice (Figure 2.19b). Interestingly, serum levels of aspartate aminotransferase (AST) and alanine aminotransferase (ALT) liver enzymes were significantly reduced in obestatin-treated mice compared to controls (Figure 2.19b). Overall these results indicate that during the time-course of the experiment, obestatin did not induce any overt hepatic or renal toxicity in *mdx* mice.

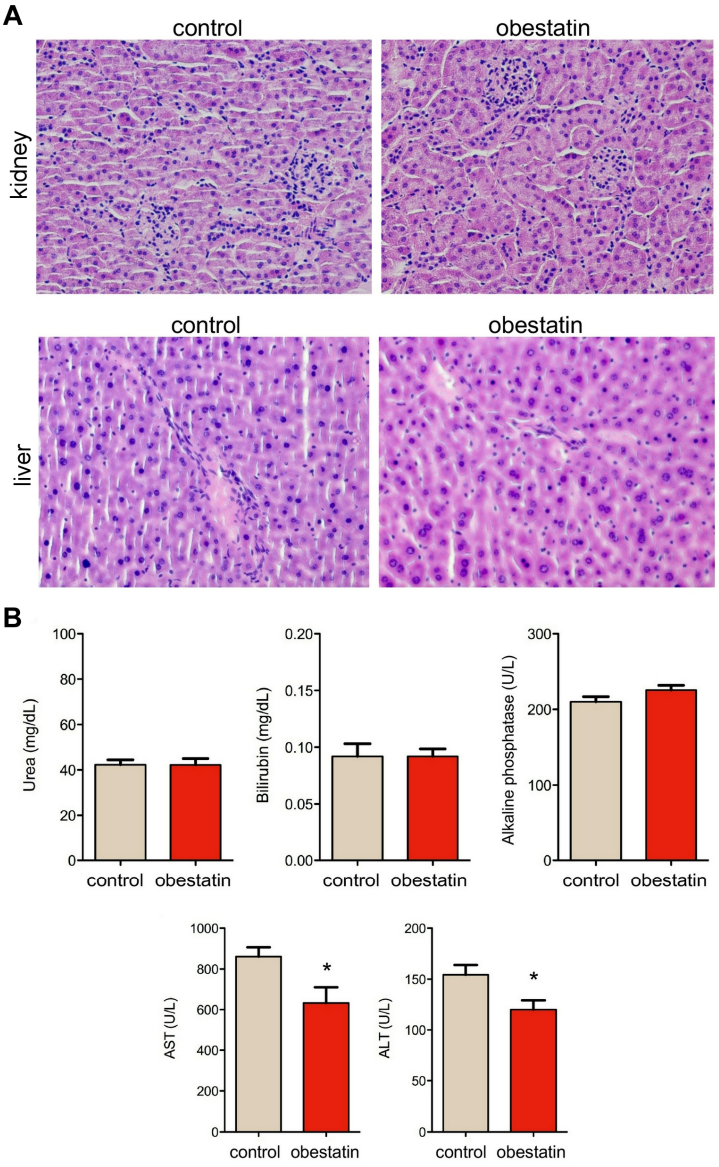


Figure 2.19. Obestatin treatment does not induce renal or hepatic toxicity. (A) Histological HE staining of kidney and liver tissue sections of *mdx* mice after intramuscular injection in TA of obestatin or vehicle. (B) Serum urea, bilirubin, alkaline phosphatase, AST and ALT levels were measured at the end of the treatment in *mdx* controls and *mdx* mice treated with obestatin. Data were expressed as mean±SEM (n=5 animals per group; * $P< 0.05$ *versus* control values).

Obestatin signalling regulates differentiation of human DMD cells

To validate whether obestatin signalling and effect are conserved between human and mouse, we used an *in vitro* cell culture model of human DMD skeletal muscle cells, which is the only model available to assess signalling in a human context. To assess the effect of human obestatin on differentiation, DMD myoblasts were switched to differentiation medium (DM) supplemented with obestatin at a range of concentrations (0.01-100 nM) for 3 days. As shown in Figure 2.20, the protein levels of myogenin were up-regulated at a maximal level in the presence of 10 nM obestatin. Insulin (1.72 µM) was used as the positive control based on its role in the control of skeletal muscle growth and in the regulation of muscle mass[128].

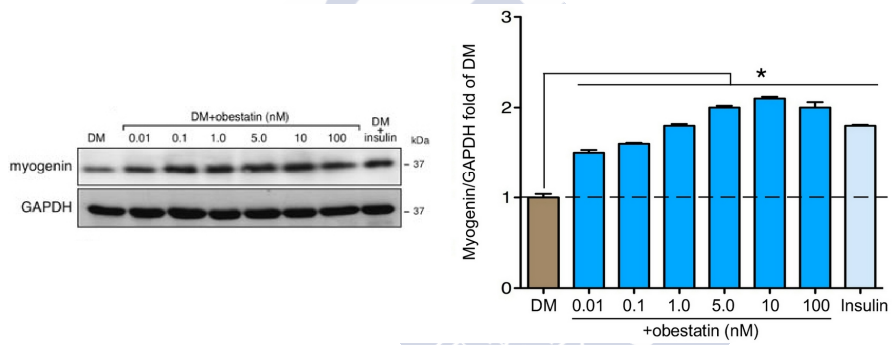


Figure 2.20. Dose–response effect of obestatin (0.01-100 nM) or insulin (1.72 µM) on differentiating human DMD cells. Levels of myogenin were represented as fold of DM. Immunoblots are representative of the mean value (n=3). Data were expressed as mean±SEM (* *P*< 0.05 *versus* DM values).

To investigate whether obestatin stimulated hypertrophic growth, DMD cells were treated with obestatin in DM during 72 h (Figure 2.21). The myotube area was larger in the obestatin-treated cells (DM+obestatin; 992.32±40.31 µm^2) as compared to untreated conditions (DM; 687.42±31.02 µm^2) or insulin-treated cells (DM+insulin; 879.76±44.40 µm^2) at 72 hours post-differentiation (hpd) (Figure 2.21b and 2.21c). Furthermore, the number of myonuclei per MHC$^+$ myotube was 20±1.79 in obestatin-treated cells *versus* 5±0.19 in control cells or 8±0.67 in insulin-treated cells (Figure 2.21d).

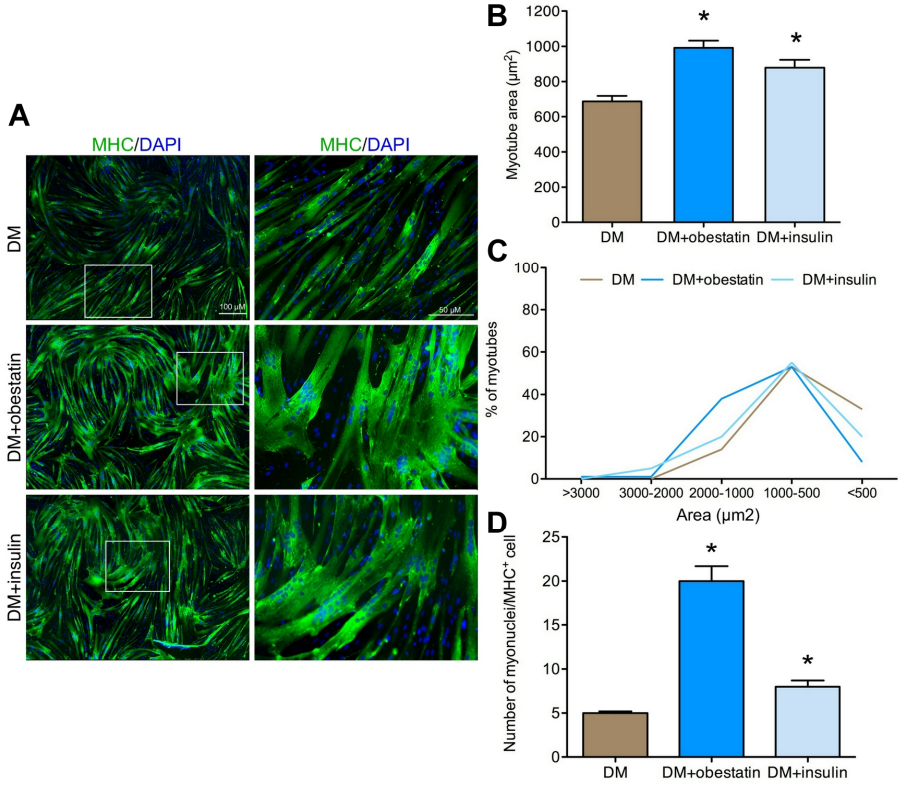


Figure 2.21. Obestatin enhances hypertrophic growth of human DMD myotubes. (A) Immunofluorescence detection of MHC and DAPI on human DMD myotubes under DM, DM+obestatin (10 nM) or DM+insulin (1.72 µM) during 72 h. (B, C) Evaluation of the differentiation grade based on the assessment of myotube area and distribution. (D) Quantification of the number of myonuclei in MHC^+ cells on human DMD myotubes under DM, DM+obestatin (10 nM) or DM+insulin (1.72 µM) during 72 h. Data were expressed as mean±SEM (* *P*< 0.05 *versus* DM values).

Immunoblot analysis of total-, slow- and fast-MHC demonstrated a robust increase in the protein levels of total- and slow-MHC in the presence of 10 nM obestatin (75.0±2.2 and 52±6.0% compared to untreated cells; Figure 2.22) with a significant decrease in the levels of fast-MHC (Figure 2.22).

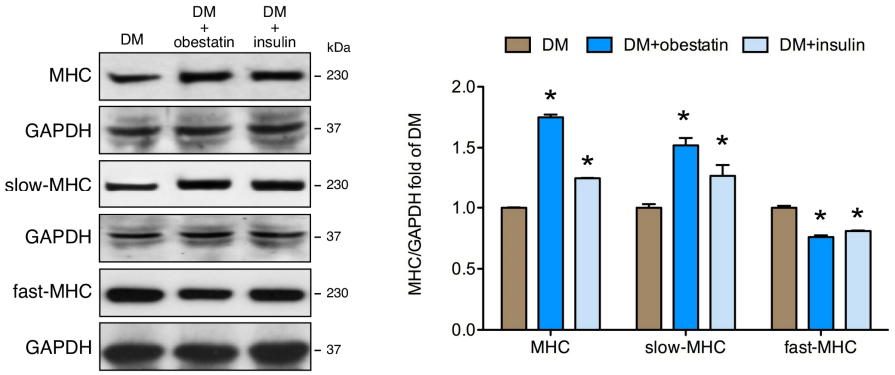


Figure 2.22. Obestatin favours slow-MHC expression on human DMD myotubes. Immunoblot analysis of MHC, slow-MHC and fast-MHC on human DMD myotubes after 72 h under DM, DM+obestatin (10 nM) or DM+insulin (1.72 µM). Protein level was expressed as fold of DM. Data were expressed as mean±SEM (n=3; * *P*< 0.05 *versus* DM values).

Immunoblot analyses of utrophin, α-syntrophin, and β-dystroglycan revealed elevated protein expression in obestatin-treated cells as compared to untreated cells at 72 hpd (36.7±3.0, 42.1±3.0, and 26.9±6.5%, respectively; Figure 2.23). The protein levels of NOS1, α7- and β1D-integrins were also up-regulated at 72 hpd (16.7±2.0, 30.5±3.0, and 32.7±2.0%; Figure 2.23). Thus, human DMD myotubes underwent a functional switch towards an oxidative fibre type orchestrated by obestatin signalling during *in vitro* myogenesis. In addition, the up-regulation of the expression of sarcolemma adhesion components is also confirmed in this system, thereby increasing membrane stability.

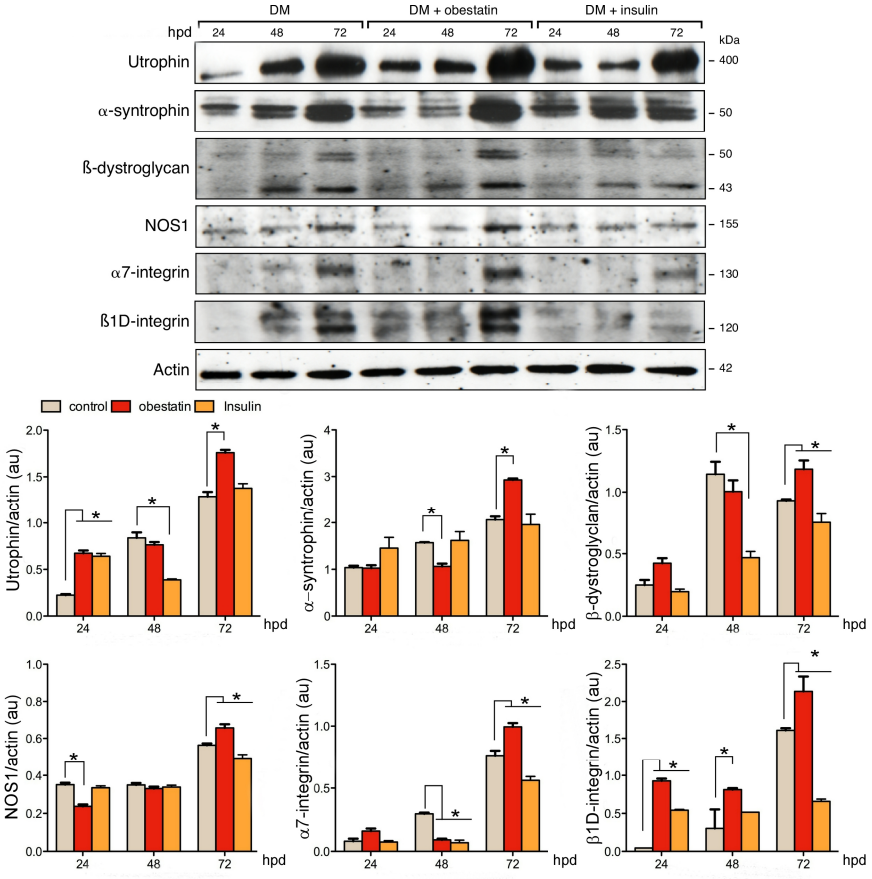


Figure 2.23. Obestatin regulates sarcolemma adhesion protein components on human DMD cells. Immunoblot analysis of obestatin effect (10 nM) on utrophin, α-syntrophin, β-dystroglycan, NOS1, α7-integrin and β1D-integrin expression on differentiating human DMD cells. Protein levels were expressed as optical density arbitrary units obtained from intensity scans. Data were expressed as mean±SEM (n=3; **P*< 0.05 *versus* control values).

USC
UNIVERSIDADE
DE SANTIAGO
DE COMPOSTELA

CHAPTER 3:

REGULATION OF UTROPHIN EXPRESSION AND AUTOPHAGY BY THE OBESTATIN/GPR39 SYSTEM IN DMD

USC
UNIVERSIDADE
DE SANTIAGO
DE COMPOSTELA

Obestatin-dependent modulation of utrophin expression by class II HDAC/ MEF2 and calcineurin/NFATc1 axis

We attempted to establish a correlation between the level of utrophin expression and key phenotype-bending signalling molecules linked to the obestatin/GPR39 system in human DMD myotubes. Specifically, we explored the stimulation of class II HDAC/MEF2 and calcineurin/NFAT signalling pathways as transcriptional targets involved in the specification of the slow myofibre phenotype and utrophin expression[174–176]. To this end, we gathered several DMD samples: in proliferating conditions (growth medium, GM: control); during the indicated time course within the 72 h of differentiation (differentiation medium, DM) under obestatin (10 nM) or insulin (1.72 μM) administration. As Figure 3.1 shows, utrophin protein is present in human DMD myoblast cells, and its expression profile is markedly different during the chronology of differentiation. In particular, obestatin increased the utrophin expression by 59.7±5.9% compared to untreated DMD myotubes at 72 hpd, a result superior to those reached with insulin (Figure 3.1). Slow and oxidative myotube identity is regulated by the balance between positive and negative signalling by MEF2 and the class II HDAC proteins, respectively[168]. In fact, immunoblot analysis of obestatin- and insulin-treated DMD cells demonstrated the up-regulation of MEF2A and MEF2C protein expression (Figure 3.1). However, the activity of MEF2 is tightly regulated through association with HDACs, which act as signal-dependent repressors of gene expression. HDAC phosphorylation in response to differentiation signals or motor innervation provides docking sites for the 14-3-3 chaperone protein that leads to nuclear export of HDACs enabling MEF2 to activate the slow myofibre gene program[171]. According to this point, obestatin treatment resulted in markedly elevated levels of phosphorylation of HDAC4 [pHDAC4(S246)], an effect observed in untreated and, to a lesser extent, in insulin-treated cells (Figure 3.1). We also observed an increased phosphorylation of HDAC5 [pHDAC5(S259)] and HDAC7 [pHDAC7(S155)], a common effect among experimental groups (Figure 3.1). Phosphorylation of HDACs in response to obestatin or insulin was accompanied by the activation of PKD [pPKD(S916)], kinase responsible for phosphorylation and nuclear export of class II HDACs (Figure 3.1)[177–179].

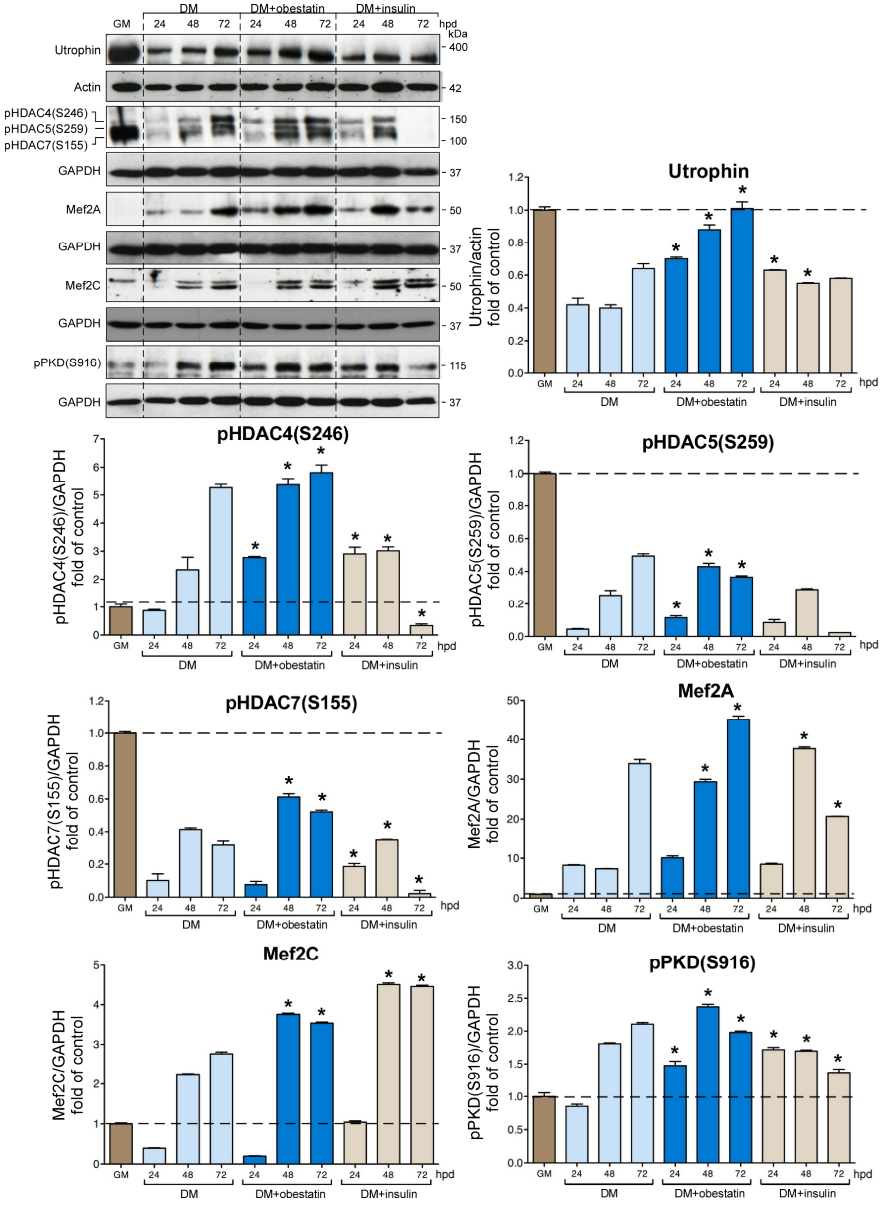


Figure 3.1. Obestatin increases utrophin expression. Immunoblot analysis of utrophin, pHDAC4(S246), pHDAC5(S259), pHDAC7(S155), MEF2A, MEF2C and pPKD(S916) on differentiating DMD cells under DM, DM+obestatin (10 nM) or DM+insulin (1.72 µM). Protein level was expressed as fold of control. Data were expressed as mean±SEM obtained from intensity scans (n=3; * *P*< 0.05 *versus* DM values).

Consistent with the role of MEF2 as a transcriptional regulator of the slow-myotube phenotype, analysis of total-, slow- and fast-MHC demonstrated an increase in the protein levels of total- and slow-MHC in the presence of obestatin (Figure 2.22). Furthermore, the expression of slow troponin I (troponin I-SS) was much higher in obestatin-treated cells than in untreated cells (Figure 3.2). The results achieved for MHC and troponin I-SS in response to obestatin were superior to those reached with insulin (Figure 2.22 and 3.2).

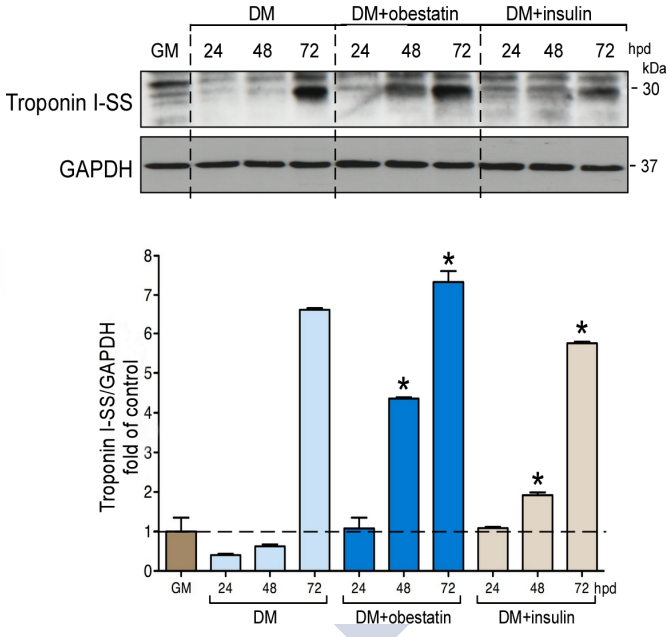


Figure 3.2. Obestatin favours slow-myotube phenotype on human DMD cells. Troponin I-SS expression on differentiating DMD cells under DM, DM+obestatin (10 nM) or DM+insulin (1.72 µM). Protein level was expressed as fold of control. Data were expressed as mean±SEM obtained from intensity scans (n=3; * *P*< 0.05 *versus* DM values).

This oxidative myotube-type switch was associated with significant increase in the expression of proteins involved in the mitochondrial biogenesis pathway, such as CPT1, PGC-1α, UCP3, and Cytochrome C (Cit C) in obestatin-treated DMD cells as compared to untreated cells (Figure 3.3). This up-regulation was also observed in insulin-treated cells although expression levels were differentially regulated (Figure 3.3).

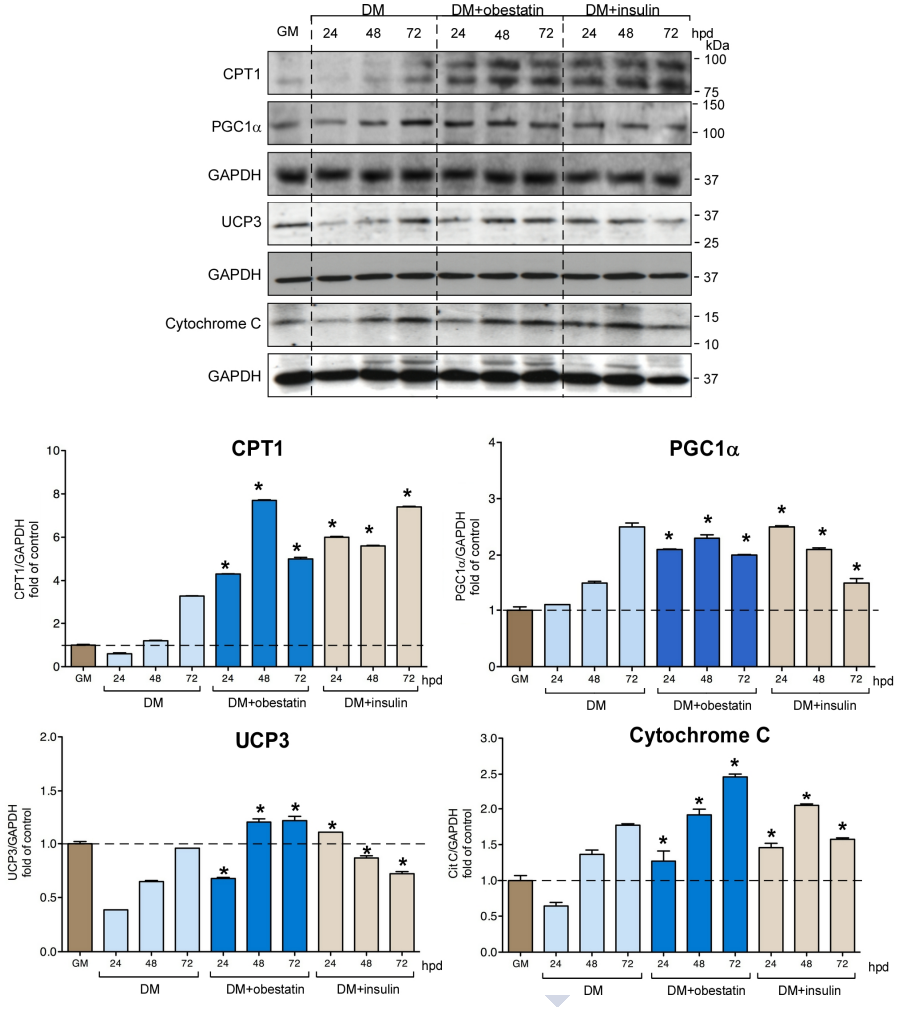


Figure 3.3. Obestatin regulates proteins of mitochondrial biogenesis. Immunoblot analysis of CPT1, PGC1α, UCP3 and Cytochrome C on differentiating DMD cells under DM, DM+obestatin (10 nM) or DM+insulin (1.72 μM). Protein level was expressed as fold of control. Data were expressed as mean±SEM obtained from intensity scans (n=3; * $P< 0.05$ *versus* DM values).

HDACs do not function in isolation to control MEF2 activity. Indeed, MEF2 is regulated by a plethora of signalling networks that include the calcineurin phosphatase. Calcineurin dephosphorylates members of the NFAT family of transcription factors, which enables them to translocate into

the nucleus, where they activate transcription in cooperation with other transcription factors, including MEF2 and GATA4[4,171,180–182]. As shown in Figure 3.4, obestatin-treated cells showed a striking decrease in NFATc1 phosphorylation at S172 [pNFATc1(S172)] related to untreated cells in which gradual increase of pNFATc1(S172) was observed during the differentiation process. This effect was also shown in insulin-treated cells (Figure 3.4). A number of protein kinases oppose calcineurin-mediated activation of NFATc1 by directly phosphorylating and promoting nuclear exit of NFATc1. Among them, GSK3β was identified as the principal cellular kinase responsible for the phosphorylation of NFATc1[183,184]. In untreated cells, levels of GSK3β phosphorylation at S9/21 [pGSK3β(S9/21)] were markedly decreased during the differentiation process (Figure 3.4). However, phosphorylation of the β form in response to obestatin or insulin was increased (Figure 3.4). The down-regulation of GSK3β by phosphorylation was concomitant with an increase in Akt activation, detected by the phosphorylation of its regulatory residue S473 [pAkt(S473)] in Akt family members (Akt1, Akt2 and Akt3) in obestatin-stimulated cells (Figure 3.4). In insulin-treated cells, pAkt1(S473) was significantly increased although Akt2 and Akt3 phosphorylation were markedly decreased during the differentiation process (Figure 3.4). The regulatory interplay between Akt/GSK3 and calcineurin/NFATc1 signalling cascades determines the subcellular localization of NFATc1. The localization of endogenous NFATc1 proteins was visualized by fluorescence microscopy in DMD myotubes at 72 hpd, and the percentage of nuclear NFATc1 was calculated (Figure 3.5). As depicted in the representative images, NFATc1 was mainly present in the cytoplasm in untreated cells but increased localization to the nucleus by 113.3±12.1% or 20.1±1.5% in response to obestatin or insulin signalling, respectively (Figure 3.5). These results suggested that obestatin signalling decreased NFATc1 phosphorylation, activation and nuclear inclusion allowing for NFATc1-dependent gene expression. Taken together, utrophin expression by obestatin signalling is related to the promotion of the slow oxidative myogenic program through the cooperative activation of the class II HDAC/MEF2 and calcineurin/NFATc1 pathways.

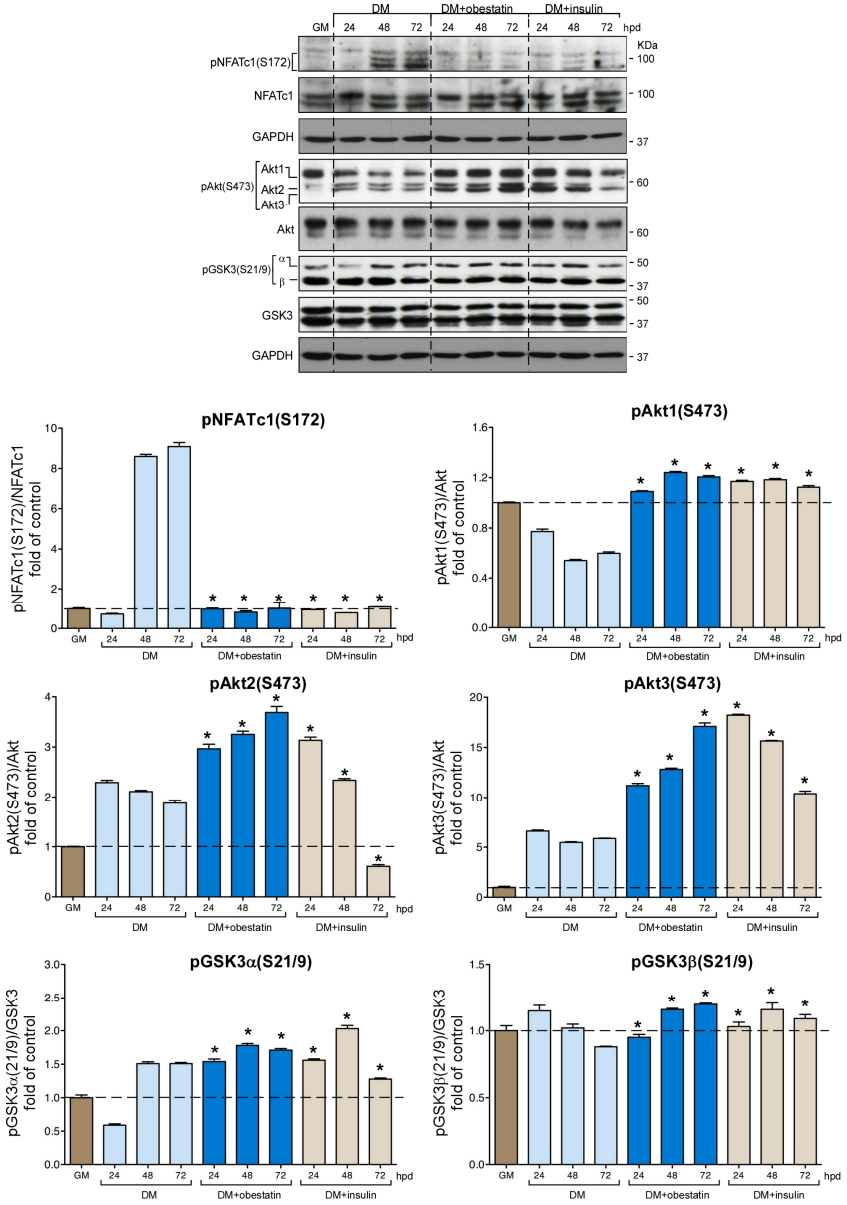


Figure 3.4. Obestatin modulates NFATc1 pathway on human DMD cells. Immunoblot analysis of pNFATc1(S172), pAkt1(S473), pAkt2(S473), pAkt3(S473), pGSK3α(S21/9) and pGSK3β(S21/9) on differentiating DMD cells under DM, DM+obestatin (10 nM) or DM+insulin (1.72 µM). Protein level was expressed as fold of control. Data were expressed as mean±SEM (n=3; * *P*< 0.05 *versus* DM values) obtained from intensity scans.

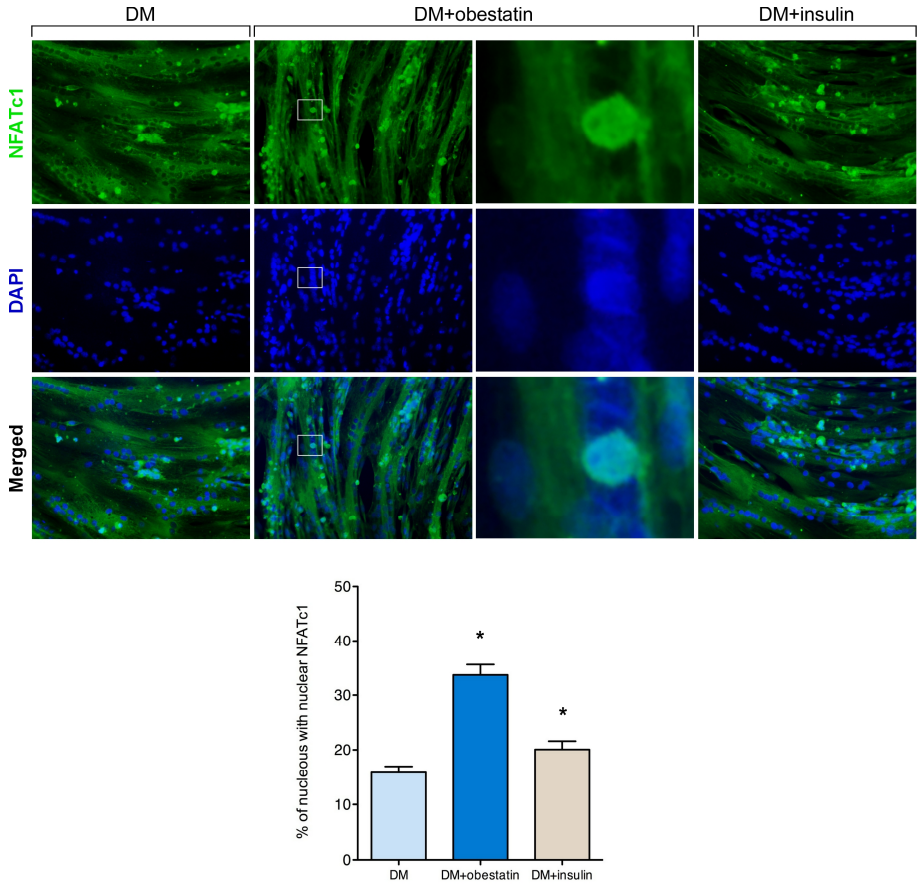


Figure 3.5. Obestatin promotes nuclear translocation of NFATc1 on human DMD cells. *Upper panel.* Immunofluorescence detection of NFATc1 on DMD myotubes obtained after 72 h under DM, DM+obestatin (10 nM) or DM+insulin (1.72 µM). DAPI was used to identify cell nucleus. *Lower panel.* Quantification of nuclear localization of NFATc1. Data were expressed as mean±SEM (n=5; * *P*< 0.05 *versus* DM values).

Obestatin enhances autophagy but does not stimulate the ubiquitin E3-ligases

Because autophagy has a role in the pathogenesis of DMD, we investigated the role of the obestatin/GPR39 system in this process. Both *mdx* and DMD muscles show evidence of impaired autophagy, which is accompanied by persistent activation of Akt axis, an intracellular target regulated by obestatin signalling[185]. To this end, we gathered several DMD samples: differentiated DMD myotubes (72 hpd) after 24 h of treatment with or without obestatin (10 nM) or insulin (1.72 μM). The p62 protein, also called sequestosome 1 (SQSTM1) protein, is an autophagy-specific substrate, the accumulation of which is used as a readout for autophagy impairment[186]. Interestingly, p62 was significantly decreased in obestatin-treated DMD myotubes compared to untreated- or insulin-treated myotubes (35.2±2.1% or 42.6±1.8%, respectively; Figure 3.6). Because reduction of p62 is a hallmark of enhanced autophagic flux, we next evaluated levels of the widely used microtubule-associated protein light chain 3 (LC3) autophagy marker in the soluble (LC3I) and autophagosome-associated (LC3II) forms[186]. The levels of LC3I were not different among groups; however, LC3II was significantly increased in obestatin-treated DMD myotubes as revealed by an increase in the LC3II/LC3I ratio compared to untreated cells (43.5±1.8%) and in contrast to insulin-treated cells (decreased by 17.0±4.2; Figure 3.6). Up-regulation of LC3II was associated with increased expression of the lysosomal enzyme Cathepsin L in obestatin-treated cells (59.4±6.8% compared to untreated cells), further supporting an enhanced autophagy (Figure 3.6). In insulin-treated cells, Cathepsin L appeared not to be altered in basal state. Autophagy flux was further monitored by treating DMD myotubes with chloroquine (20 μM, 24 h), an established lysosomal inhibitor that prevents the degradation of the autophagic content[186]. Chloroquine treatment led to the accumulation of p62 and LC3II levels in obestatin-treated DMD myotubes (83.9±2.9% and 71.0±2.5%, respectively), but not in untreated- or insulin-treated cells where common features of both markers were exhibited (Figure 3.6). In addition, obestatin stimulation was associated with a reduction in the Cathepsin L expression after chloroquine treatment (24.4±0.7%; Figure 3.6).

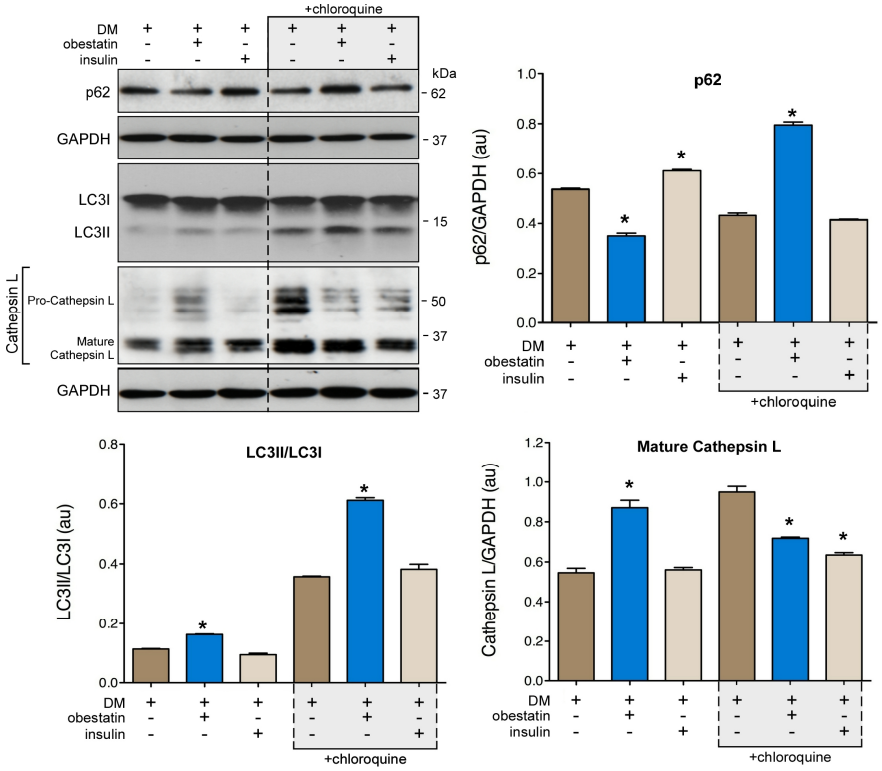


Figure 3.6. Obestatin promotes autophagy on human DMD cells. Immunoblot analysis of p62, LC3II and Cathepsin L on DMD myotubes under DM, DM+obestatin (10 nM, 24 h), DM+insulin (1.72 µM, 24 h), in presence or absence of chloroquine (20 µM, 24 h).). Data were expressed as arbitrary units obtained from intensity scans (mean±SEM; n=3; * *P*< 0.05 *versus* DM or DM+chloroquine values, respectively).

Using immunofluorescence analysis of LC3II in combination with chloroquine treatment, we found a higher autophagic flux in obestatin-treated cells than untreated (increase in mean fluorescence intensity (MFI): 119.4±5.7%) or insulin-treated DMD cells (MFI increased by 52.4±3.9%; Figure 3.7). Chloroquine treatment induced LC3II punctate (non-fused autophagosomes) accumulation in untreated and obestatin-treated cells maintaining the difference between groups (MFI increased by 116.2±1.4% in obestatin related to untreated cells), but not in insulin-treated cells (Figure 3.7). These results supported a role of the obestatin/GPR39 signalling in the regulation of autophagic activity in DMD cells.

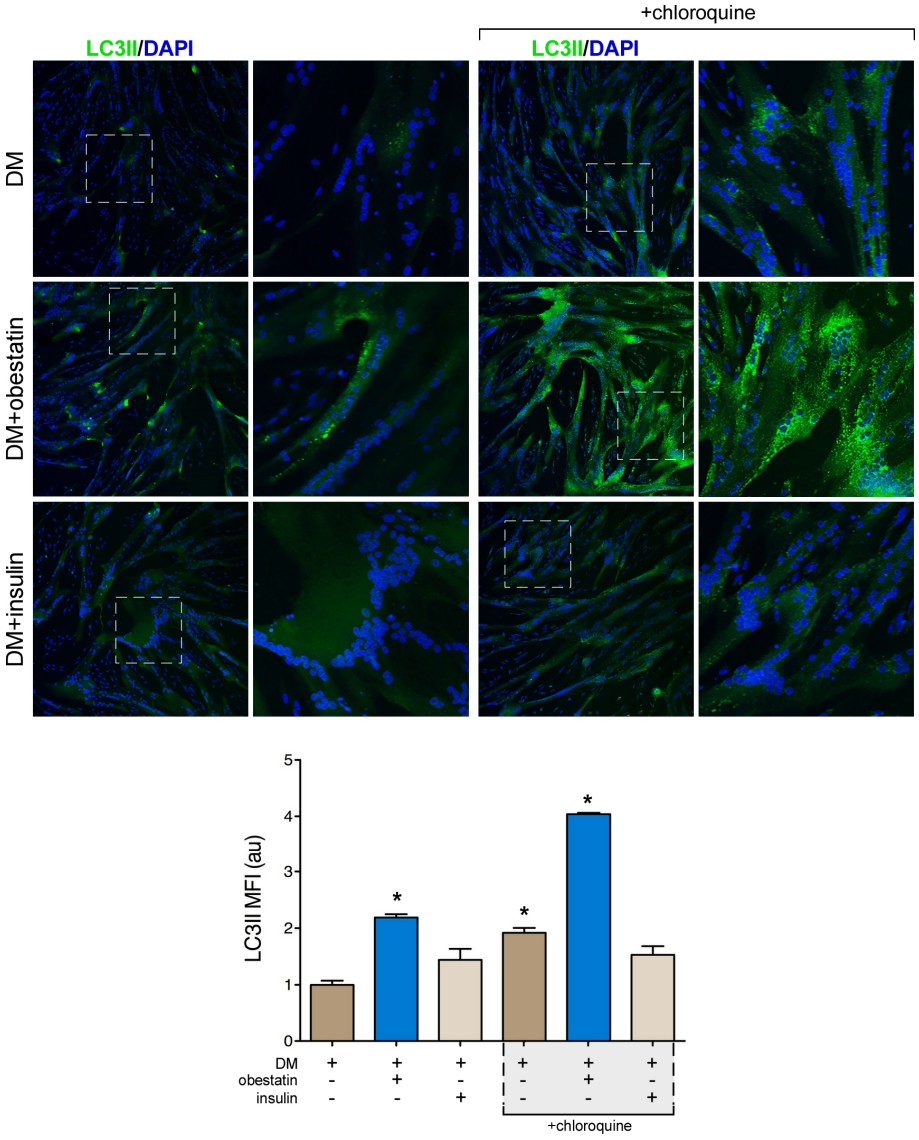


Figure 3.7. Obestatin enhances autophagic flux on human DMD cells. *Upper panel.* Immunofluorescence detection of LC3II on DMD myotubes under DM, DM+obestatin (10 nM, 24 h) or DM+insulin (1.72 µM, 24 h), in presence or absence of chloroquine (20 µM, 24 h). *Lower panel.* The change in mean fluorescence intensity (MFI) of LC3II on DMD cells is shown. Data were expressed as mean±SEM (n=5; * $P < 0.05$ *versus* DM or DM+chloroquine values, respectively).

In the light of Akt/mTOR axis being considered as critical for the repression of autophagy-lysosome proteolysis[187], we were surprised by the Akt [pAkt(S473)] and mTOR [pmTOR(S2448)] activation observed in obestatin-treated DMD myotubes (Figure 3.8). Akt activation was further supported by inhibition of FoxO-dependent ubiquitin E3-ligases MuRF1 and MAFbx, which correlated with increased phosphorylation of FoxO4 at T28 [pFoxO4(T28)] and, to a lesser extent, FoxO1 at T24 [pFoxO1(T24)] (Figure 3.9). The implication of the mTOR pathway was demonstrated by the activation of the ribosomal protein S6 at S240/244 [pS6(S240/244)] and by 4E-BP1 hyperphosphorylation at T70 [p4E-BP1(T70)] and at T37/T46 [p4E-BP1(T37/46)] (Figure 3.10). Added to this seemingly contradicting finding, our experimental data revealed concurrent activation of AMPK [pAMPK(T172)] by obestatin signalling in DMD cells (Figure 3.8). Akt/mTOR and AMPK are often perceived as antagonists that suppress or induce autophagy under nutrient sufficiency or shortage, respectively[188]. Indeed, insulin led to activation of the Akt/mTOR pathway and inactivation of AMPK (Figure 3.8 and 3.10) with subsequent inhibition of protein degradation via inactivation of autophagy-lysosome and ubiquitin-proteasome pathways (Figure 3.7 and 3.9, respectively). However, it has been noted that autophagy is also required to provide amino acids and metabolite intermediates for biosynthetic processes[189]. Indeed, the inhibition of autophagic degradation by chloroquine markedly decreased the levels of MHC protein in obestatin-treated DMD myotubes with no major changes in pAkt(S473), pmTOR(S2448) and pAMPK(T172) (Figure 3.8). In agreement, pS6(S240/244) and 4E-BP1 hyperphosphorylation, were not significantly affected by chloroquine treatment at least in measured time (72 hpd, 24 h treatment; Figure 3.8 and 3.10). Intriguingly, we found that prevention of lysosome degradation by chloroquine inhibited MHC protein level in insulin-treated DMD cells (Figure 3.8), an effect not related to apoptosis activation as cleaved caspase-3 levels remained unchanged (Figure 3.10).

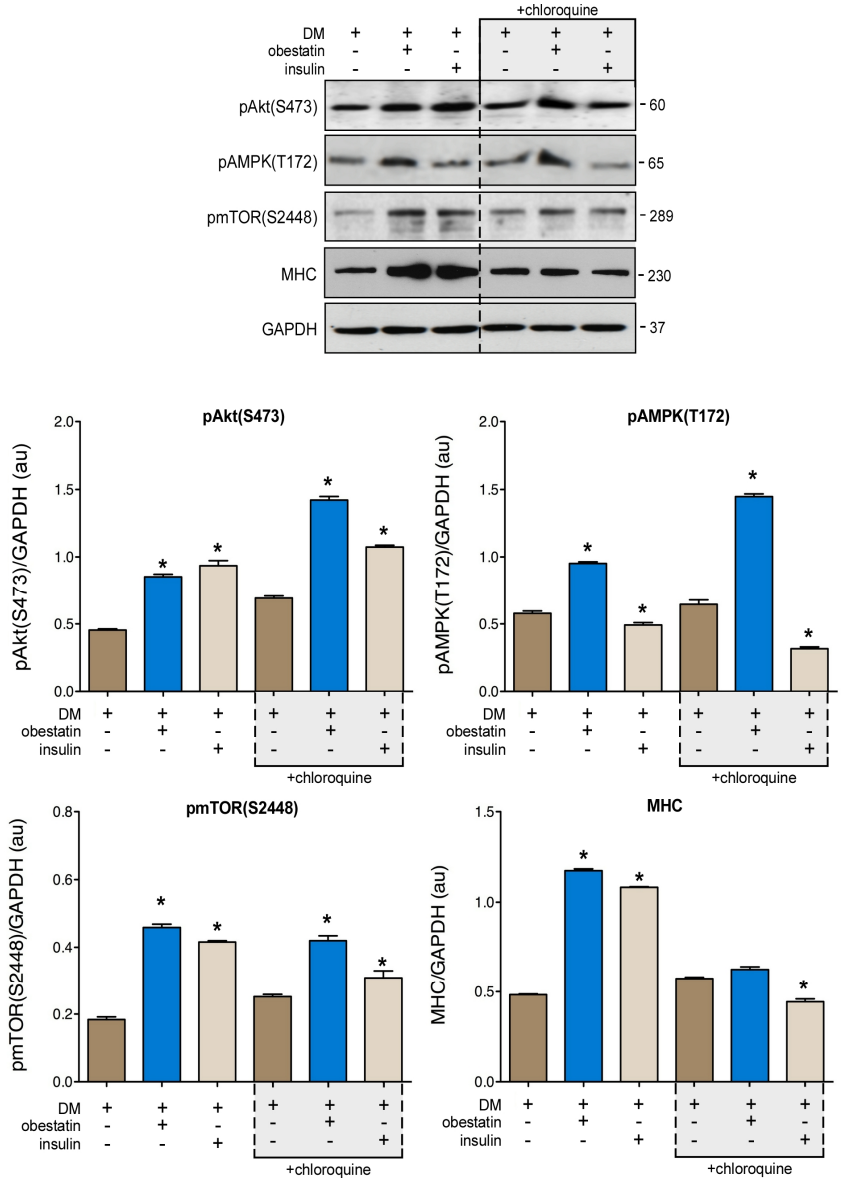


Figure 3.8. AMPK and mTOR concurrent activation through obestatin signalling on DMD cells. Immunoblot analysis of pAkt(S473), pAMPK(T172), pmTOR(S2448) and MHC on DMD myotubes under DM, DM+obestatin (10 nM, 24 h) or DM+insulin (1.72 µM, 24 h), in presence or absence of chloroquine (20 µM, 24 h). Data were expressed as arbitrary units obtained from intensity scans (mean±SEM; n=3; * $P < 0.05$ *versus* DM or DM+chloroquine values, respectively).

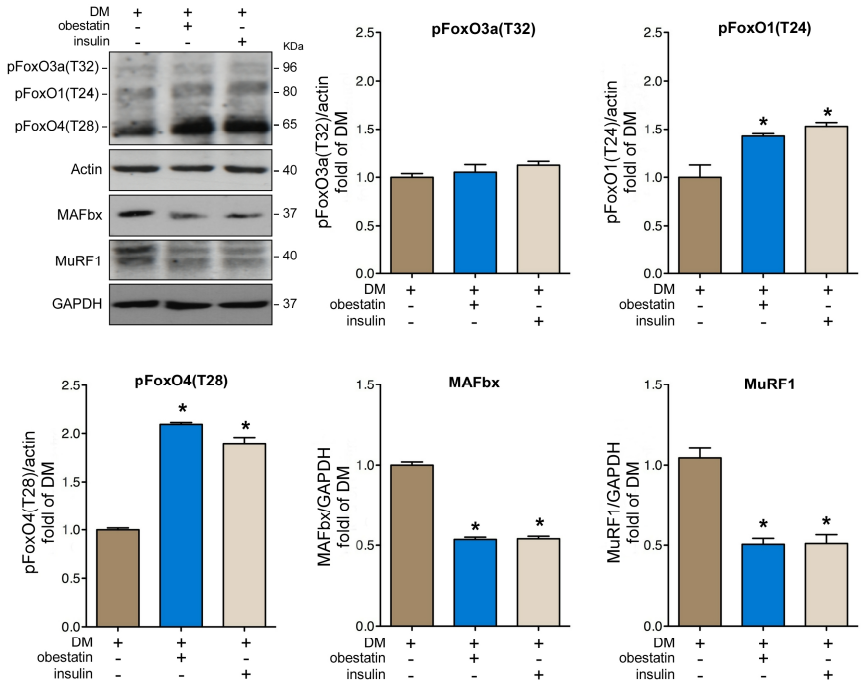


Figure 3.9. Obestatin inhibits ubiquitin E3-ligases on DMD cells. Immunoblot analysis of pFoxO3a(T32), pFoxO1(T24), pFoxO4(T28), MAFbx and MuRF1 on DMD myotubes obtained under DM, DM+obestatin (10 nM, 24 h) or DM+insulin (1.72 µM, 24 h). Protein level was expressed as fold of DM, and data were expressed as mean±SEM (n=3; * *P*< 0.05 *versus* DM values) obtained from intensity scans.

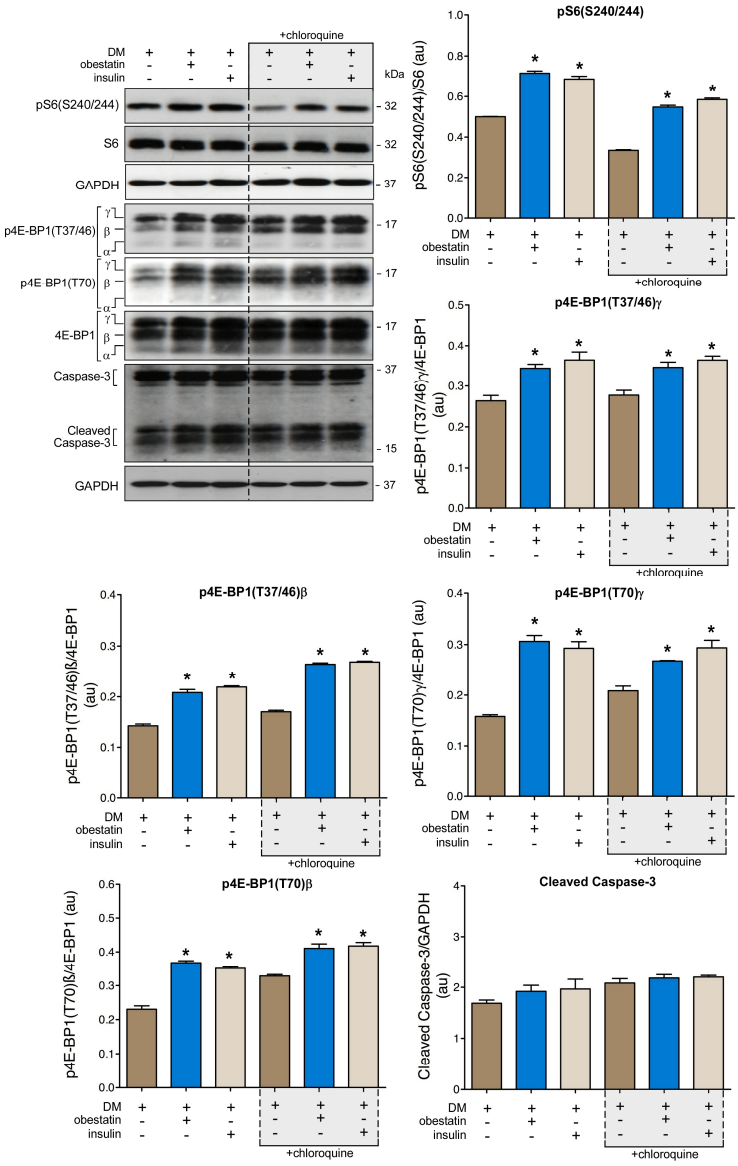


Figure 3.10. Inhibition of autophagy impairs obestatin-dependent activation of markers of protein synthesis. Immunoblot analysis of pS6(S240/244), p4E-BP1(T37/46)γ, p4E-BP1(T37/46)β, p4E-BP1(T70)γ, p4E-BP1(T70)β and cleaved caspase-3 on DMD cells under DM, DM+obestatin (10 nM, 24 h) or DM+insulin (1.72 μM, 24 h), in presence or absence of chloroquine (20 μM, 24 h). Data were expressed as arbitrary units obtained from intensity scans (n=3; mean±SEM; * *P*< 0.05 *versus* DM or DM+chloroquine values, respectively).

The finding that the obestatin/GPR39 system activates mTOR concurrently with AMPK was further validated during the differentiation process. As Figure 3.11 shows, mTOR remains active [pmTOR(S2448)] when AMPK is activated [pAMPK(T172)] by obestatin for time-tested. We further found that obestatin enhanced calmodulin-dependent protein kinase II (CaMKII) phosphorylation [pCAMKII(T286)], which has been shown to mediate AMPK phosphorylation[188,190]. Interestingly, this concurrency was observed to some extent in untreated DMD cells. Of note, CAMKII and AMPK activities were clearly reduced by insulin signalling whereas mTOR remained responsive (Figure 3.11). Thus, we explored the regulation of the autophagy-driving kinase Unc-51-like kinase-1 (ULK1) in response to obestatin signalling. AMPK activates ULK1 by phosphorylation at S317 [pULK1(S317)][191]. Indeed, pULK1(S317) was detected in untreated- and to a greater extent in obestatin-stimulated cells, and this phosphorylation was inhibited by insulin signalling (Figure 3.11). This suggests that AMPK sustains ULK1 activity in a CAMKII-dependent manner. On the other hand, mTOR in mTOR complex 1 (mTORC1) is assumed to inhibit ULK1 by phosphorylation at S758 [pULK1(S758)][191]. We found that obestatin enhanced pULK1(S758) showing that ULK1 can be phosphorylated by mTOR and AMPK at the same time.

Consistent with active autophagy in the context of active mTOR signalling, obestatin regulated the activation of the ribosomal protein S6 and 4E-BP1 hyperphosphorylation during the differentiation process (Figure 3.12). By contrast, insulin signalling was consistent with the pre-defined mTOR role for autophagy regulation (Figure 3.12). Taken together, these data are consistent with active autophagy in the context of active mTOR signalling.

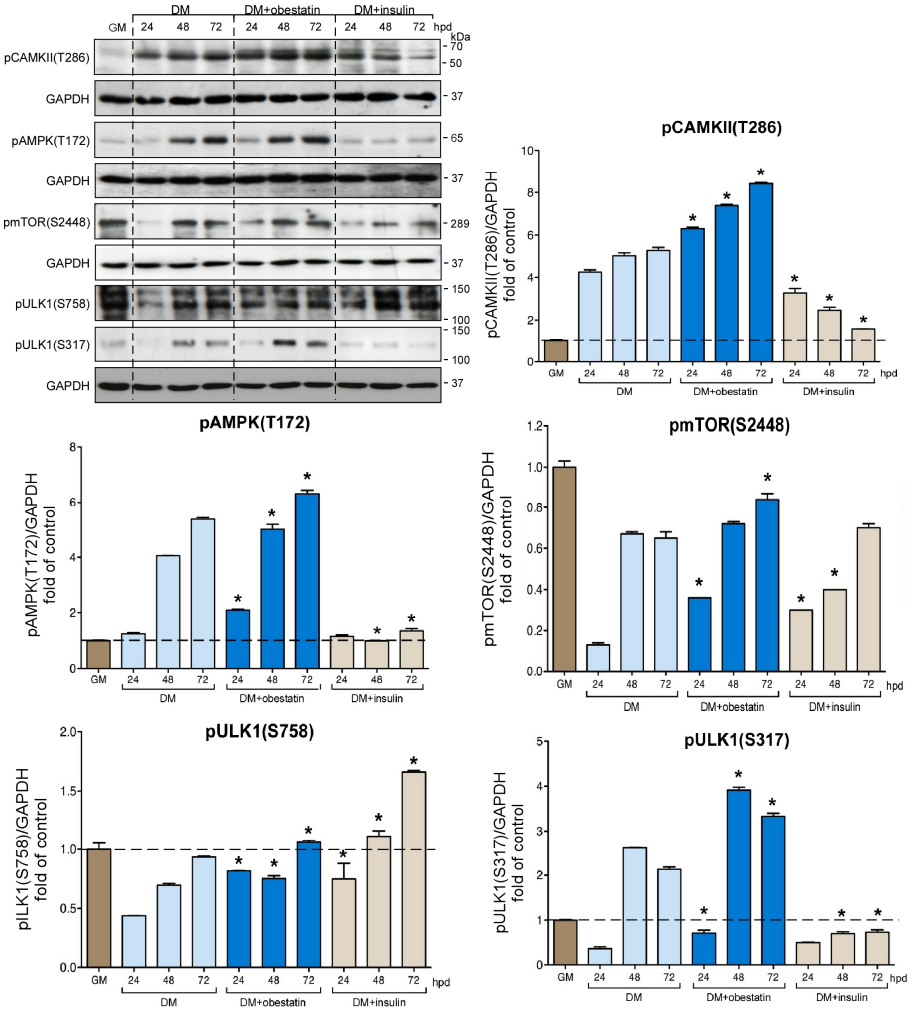


Figure 3.11. Obestatin signalling activates ULK1 on DMD cells. Immunoblot analysis of pCAMKII(T296), pAMPK(T172), pmTOR(S2448), pULK1(S758) and pULK1(S317) on differentiating DMD cells under DM, DM+obestatin (10 nM) or DM+insulin (1.72 µM). Data were expressed as mean±SEM (n=3; * $P< 0.05$ *versus* DM values) obtained from intensity scans.

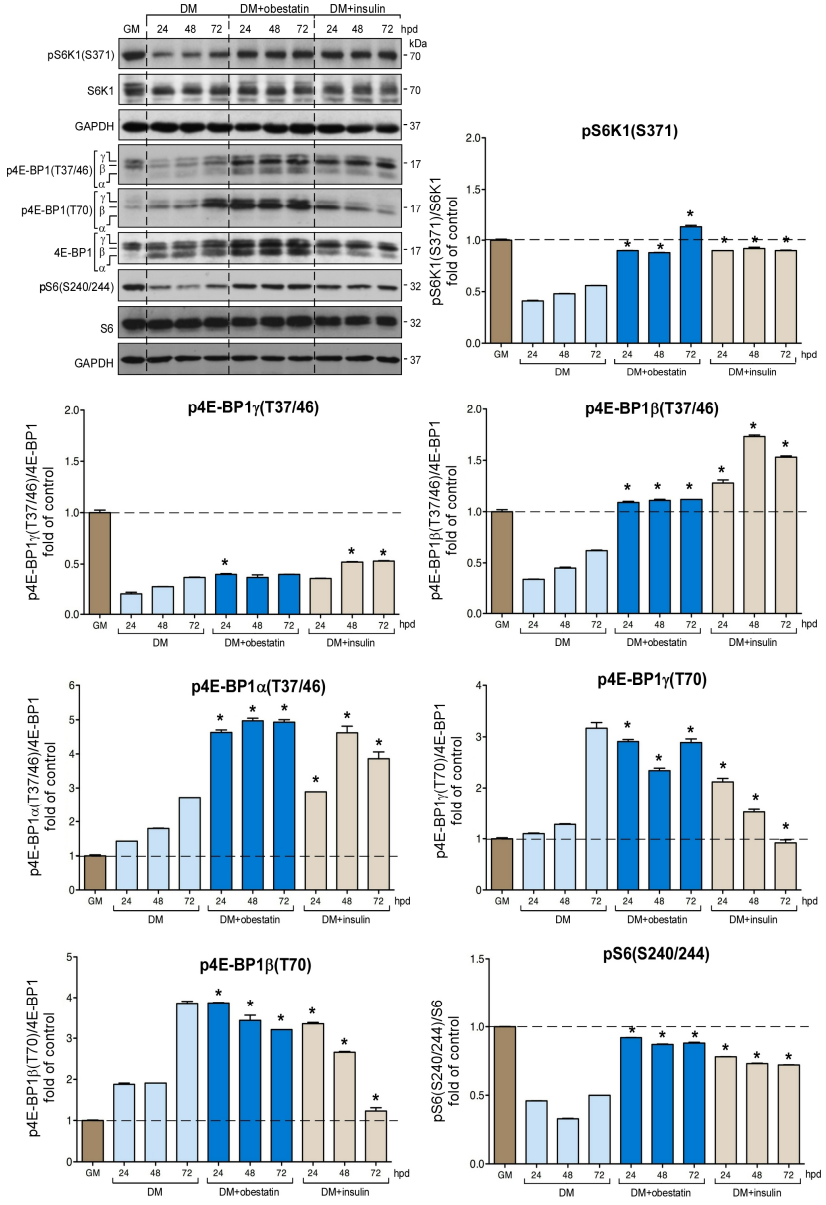


Figure 3.12. Obestatin activates Akt/mTOR signalling on DMD cells. Expression of pS6K1(S371), p4E-BP1(T37/46)γ, p4E-BP1(T37/46)β, p4E-BP1(T37/46)α, p4E-BP1(T70)γ, p4E-BP1(T70)β and pS6(S240/244) on differentiating DMD cells under DM, DM+obestatin (10 nM) or DM+insulin (1.72 µM). Protein level was expressed as fold of control. Data were expressed as mean±SEM (n=3; * *P*< 0.05 *versus* DM values) obtained from intensity scans.

As CAMKII-AMPK activation by obestatin signalling appears to sustain ULK1 activity and autophagy without altering elements of mTOR signalling, we aimed to confirm it by further experimental set-ups. We therefore performed a time-course analysis in DMD cells (72 hpd +24 h obestatin or insulin treatment). In line with our results during the differentiation process (Figure 3.11 and 3.12), we found that mTOR and AMPK were acutely activated by obestatin and sustained ULK1 activity at both the mTOR and AMPK substrate sites (S317 and S758, respectively; Figure 3.13). In contrast, insulin selectively enhanced mTOR activity and ULK1 phosphorylation at S758, the mTORC1 substrate site (Figure 3.13).

Therefore, we tested if the CAMKII inhibitor STO-609 (10 μg/mL), AMPK inhibitor Compound C (10 μM) and mTOR inhibitor Rapamycin (50 nM) modify autophagic flux. Indeed, STO-609 or Compound C decreased LC3II/LC3I ratio compared to obestatin-treated cells in the absence of inhibitors (71.8±0.9% and 52.1±1.9%, respectively; Figure 3.14). Of note, mTOR inhibitor Rapamycin also decreased LC3II/LC3I ratio (56.9±1.8%; Figure 3.14). Consistent with this inhibitory action, CAMKII inhibitor, AMPK inhibitor and mTOR inhibitor increased the expression of p62 (124.6±0.41%; 155.8±13.4%; and, 205.9±16.4%; respectively; Figure 3.14). These results suggested that the CAMKII-AMPK and mTOR signalling axis keep ULK1 activated and sustain autophagy.

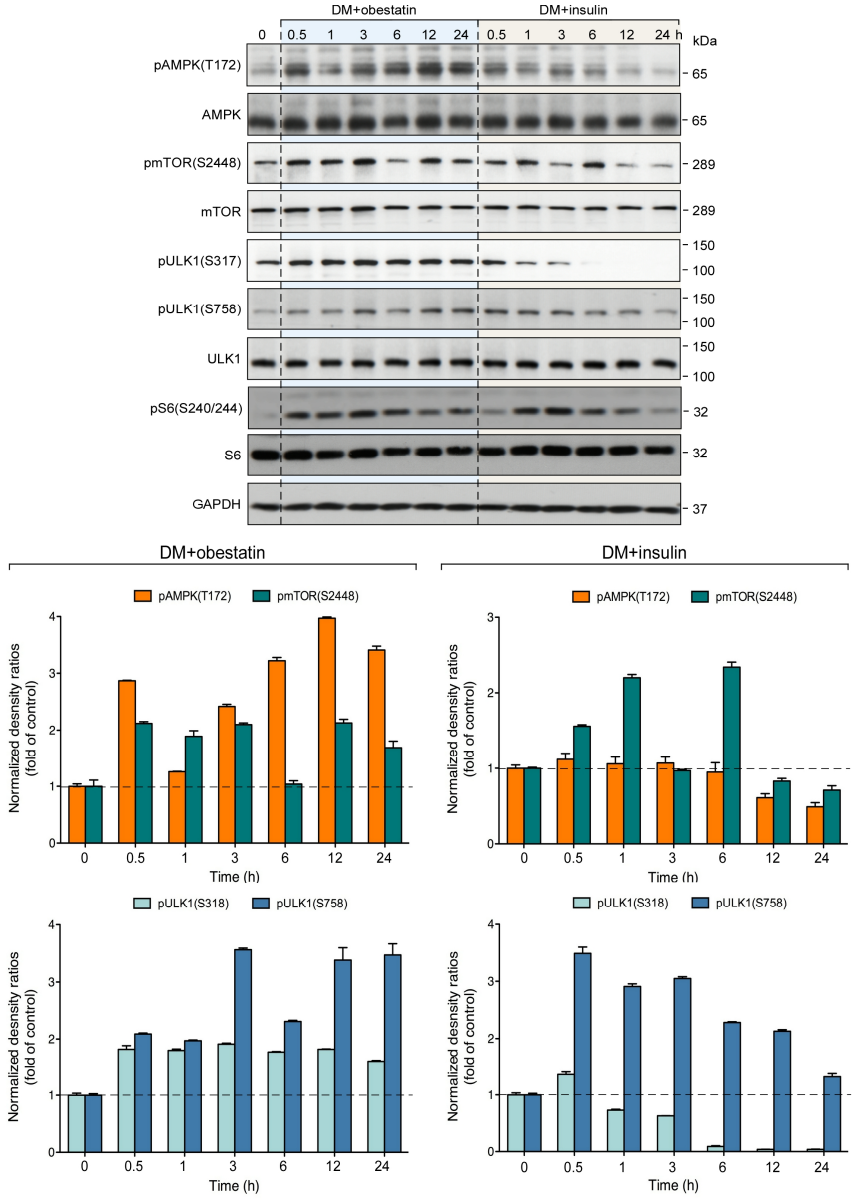


Figure 3.13. Time-course analysis of mTOR, AMPK and ULK1 on DMD cells. Immunoblot analysis of pAMPK(T172), pmTOR(S2448), pULK1(S317) and pULK1(S758) during the first 24 h post-differentiation on DMD cells under obestatin- (10 nM) or insulin- (1.72 µM) treatment. Protein level was expressed as fold of control. Data were expressed as mean±SEM (n=3; * *P*< 0.05 *versus* control values) obtained from intensity scans.

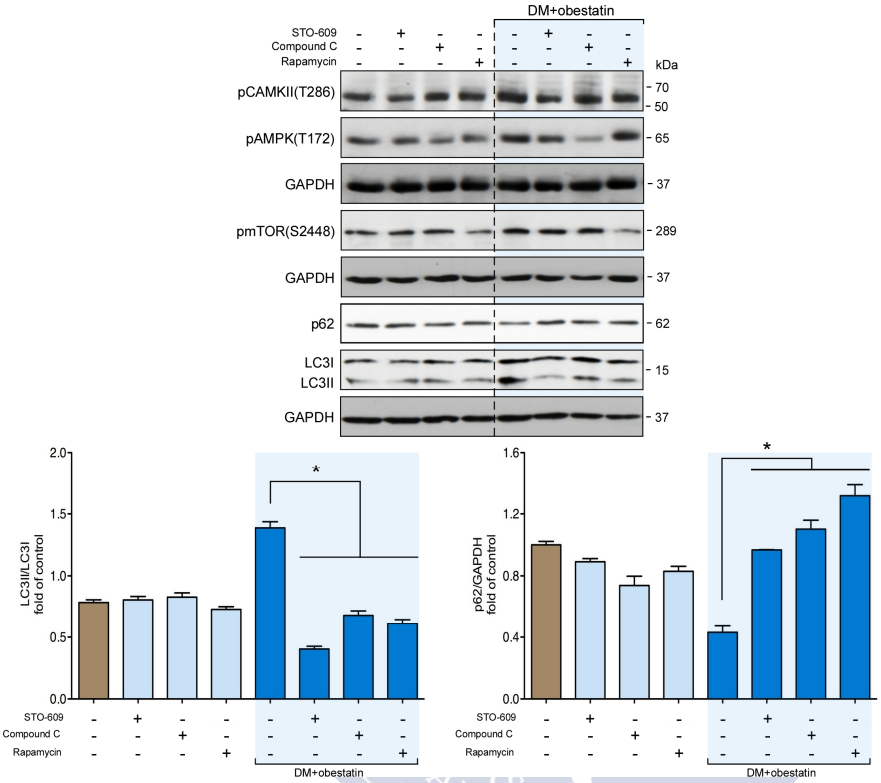


Figure 3.14. Inhibition of CAMKII, AMPK or mTOR impairs obestatin-dependent autophagy. Immunoblot analysis of pCAMKII(T286), pAMPK(T172), pmTOR(S2448), p62 and LC3I/II on DMD cells under DM or DM+obestatin (10 nM, 30 minutes) in presence or absence of STO-609 (10 µg/mL, 1 h), Compound C (10 µM, 1 h) or Rapamycin (50 nM, 1 h). Protein level was expressed as fold of DM. Data were expressed as mean±SEM (n=3; * $P < 0.05$ *versus* DM+obestatin values) obtained from intensity scans.

Obestatin signalling regulates autophagy in *mdx* mice

Finally, experimental results in human DMD model were further confirmed in 8-week-old *mdx* mice. Exogenous obestatin administration was performed via intramuscular injection into the TA muscles every 72 h during 30 days [500 nmol/kg body weight (n=5); referred as obestatin group] with sampling at 12 weeks of age, as previously described[192]. Results from this group were compared with control vehicle-treated *mdx* mice (PBS; n=5; referred as control group) under the same conditions.

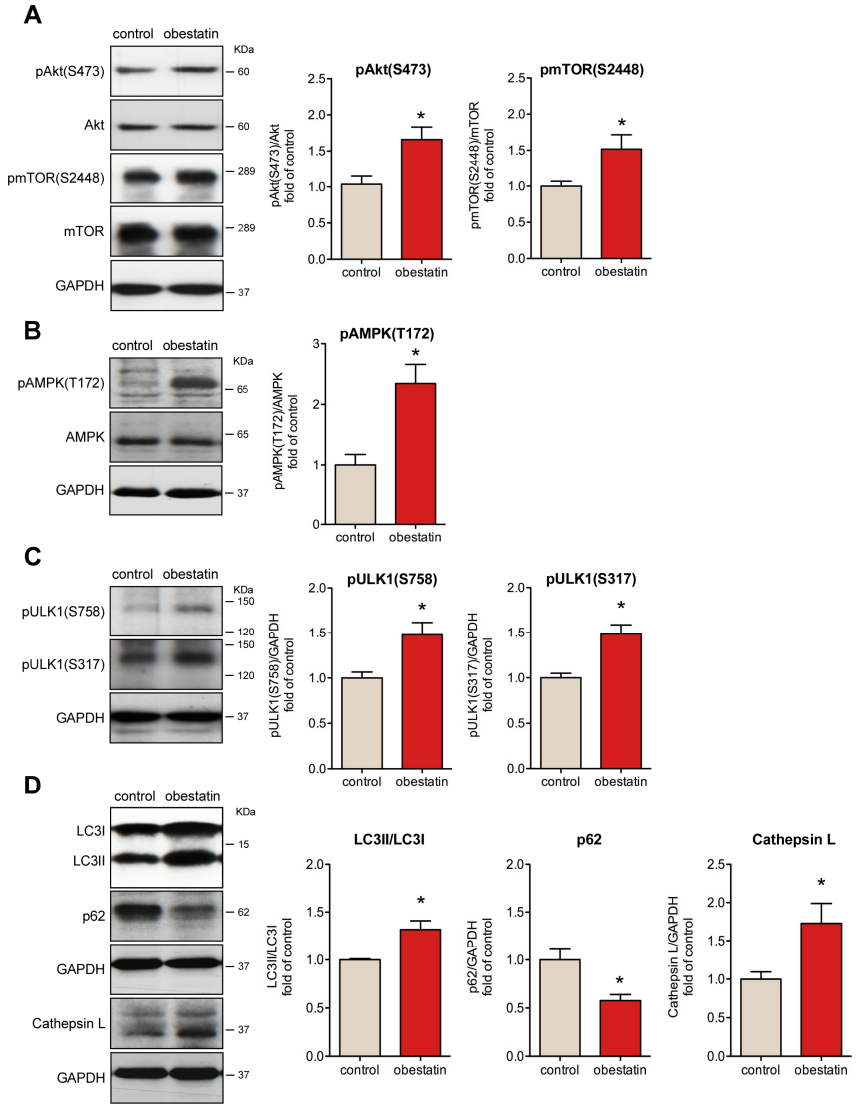


Figure 3.15. Obestatin regulates autophagy in *mdx* mice. (A) Immunoblot analysis of pAkt(S473) and pmTOR(S2448) in TA muscles of *mdx* mice after intramuscular injection of obestatin or vehicle at 30 days. (B) Expression analysis of pAMPK(T172) in obestatin- or vehicle-treated *mdx* mice at 30 days. (C) Expression analysis of pULK(S758) and pULK(S317) in obestatin- or vehicle-treated *mdx* mice at 30 days. (D) Expression analysis of LC3II, p62 and Cathepsin L in TA muscles after intramuscular injection of obestatin or vehicle at 30 days. Protein level was expressed as fold of control TA muscles. Data were expressed as mean±SEM (n=5 per group; * $P< 0.05$ *versus* control values).

As shown in Figure 3.15a, obestatin-treated mice showed an increase in pAkt(S473) (65.9±16.7%) and pmTOR(S2448) (51.6±5.4%) related to control mice. The up-regulation of Akt/mTOR signalling was concomitant with the activation of AMPK by increasing the phosphorylation at T172 (134.7±27.8%; Figure 3.15b). Consistent with this, the ULK1 activity at both the AMPK and mTOR substrate sites (S317 and S758, respectively), was increased by 48.5±9.1%, and 47.9±10.0% in obestatin-treated muscles, compared with control mice, respectively (Figure 3.15c). Of note, obestatin treatment significantly increased the autophagy marker LC3II/LC3I ratio and Cathepsin L by 32.0±1.1%, and 73.0±3.0%, while decreased p62 expression by 40.5±6.3% in obestatin-treated muscles, compared with control mice (Figure 3.15d). These results supported that under obestatin stimulation the AMPK signalling axis keeps an ULK1 fraction activated and increases basal autophagy in *mdx* mice.

USC UNIVERSIDADE DE SANTIAGO DE COMPOSTELA

DISCUSSION

USC
UNIVERSIDADE
DE SANTIAGO
DE COMPOSTELA

CHAPTER 1:

We demonstrate that obestatin/GPR39 system regulates MuSCs function. While the GPR39 receptor is identified in quiescent and activated MuSCs contributing to controlling survival and fate determination, obestatin is markedly upregulated in activated MuSCs during myogenesis. Administering obestatin significantly accelerate the processes of MuSCs activation and cell cycle entry requiring a shorter time to complete the cell division. Importantly, obestatin signalling mainly regulates the MuSC asymmetric expansion via inhibition of Notch signalling and activation of β-catenin signalling. The asymmetric localization of Par-3 in activated MuSCs is consistent with obestatin promoting asymmetric divisions. Added to these functional features, transactivation of EGFR determines the development and progression of differentiation of MuSCs linking the activated GPR39 with distinct set of effector proteins. These data emphasize the importance of the obestatin/GPR39 system in the regulation of cell fate during myogenic progression.

The obestatin/GPR39 system controls the myogenic differentiation program in an auto/paracrine manner to activate myoblast expansion during muscle regeneration[109,131]. The expression dynamics of obestatin/GPR39 system in quiescent and activated MuSCs replicates in many ways the expression pattern observed during the myoblast conversion[128]. The increase of obestatin biosynthesis by activated MuSCs, together with its weak expression in quiescent MuSCs, support the view that obestatin can enhance signalling in an autocrine fashion as a positive feedback mechanism. Remarkable, we noted that the loss of GPR39 depletes Pax7 protein and results in an up-regulation of active caspase 3 in MuSCs. Previous observations have suggested that caspase 3 protease, originally identified as the central effector of cell death pathways, controls cell fate determination independent of inducing cell death[193–198]. However, loss of GPR39 results in a significant decrease in the number of proliferating ($Pax7^+/MyoD^+$) and differentiating ($myogenin^+$) MuSCs, ruling out a permissive environment for differentiation. The reduced number of $Pax7^+$ cells with concomitant inhibition in the early markers of differentiation is

potentially due to the diminished sustainability of MuSCs associated to apoptotic programmed cell death, which in turn leads to a depletion in the pool of MuSCs. These results identify the GPR39 receptor as a part of the molecular machinery that controls MuSC fate determination by governing MuSC survival.

In our investigation, obestatin signalling induces faster kinetics of cell-cycle entry and cell division of MuSCs. The transition from quiescence to activation is linked to a set of molecular features: activation of the Akt/mTORC1/S6 signalling pathway. These cycling and molecular features are necessary and sufficient for an alert response of MuSCs - that is, the transition from a G_0 to an alerted G_{Alert} state[37,38]. Compared to G_0 MuSCs, the G_{Alert} MuSCs enter the cell cycle more quickly[37]. In this particular case, the G_0-to-G_{Alert} transition appears to be an adaptive or intermediate stage in the cell cycle progression in which obestatin signalling funnels into regulating cues to permit induction of dividing states. This mode of action fits with a sequential induction of distinct pathways required to activate quiescent cells and move them into full progression of myogenesis. Indeed, obestatin-induced myogenic determination is orchestrated by transactivation of the EGFR, as evidenced by the effect of EGFR knockdown on the MyoD protein expression in MuSCs. Consistently, obestatin-induced mitogenic action is mediated by a G-dependent mechanism while scaffolding proteins β-arrestin are essential for the activation of cell cycle exit and differentiation through the transactivation of the EGFR[128]. Upon obestatin stimulus, β-arrestins functionally interact with GPR39 leading to Src activation and signalplex formation to EGFR transactivation by matrix metalloproteinases[128]. Importantly, the obestatin-induced signalling pathways that are required to activate quiescent cells are different from those required for full progression through the cell cycle. The presence of supporting mitogenic cues associated with the obestatin/GPR39 system will dictate the level of response.

The fact the obestatin/GPR39 system drives the MuSCs entry into a pre-activation or G_{Alert} state implies a fine-tuned regulation of cell cycle activators and repressors to coordinate the different states of MuSCs. The temporal balance between proliferation and differentiation of MuSCs is

regulated by crosstalk between Notch and β-catenin signalling pathways[164]. Activation of the β-catenin signalling pathway inhibits Notch-mediated maintenance of the undifferentiated state and thus facilitates differentiation. This balance serves to assure the production of the appropriate numbers of myogenic progenitors and to precisely regulate their cell fate. Our experiments indicate that obestatin signalling impairs Notch signalling, as evidenced by a significant decrease in the translocation of the Notch intracellular domain (NICD) into the nucleus in early-activated MuSCs. Upon binding of Notch ligand to its receptor, the NICD is released and translocates into the nucleus where it interacts with recombining binding protein suppressor of hairless (Rbpj) and triggers the transcription of various genes involved in self-renewal of the MuSC pool, including those in the Hes and Hey families[199–201]. Conversely, obestatin leads to the formation of stabilized, unphosphorylated β-catenin that translocates to the nucleus during myogenic progression. Nuclear β-catenin forms a complex with the transcription factors T cell factor/lymphoid enhancer factor (TCF/LEF) and acts as a transcriptional coactivator to induce the transcriptional activity of the myogenic regulatory factors[165,202–205]. Indeed, β-catenin knockdown leads to progenitors losing their myogenic fate in response to obestatin. Thus, cell-fate determination along the myogenic lineage is controlled by a precise balance between the early, Notch, and later, β-catenin, signal transduction pathways associated with the obestatin/GPR39 system[164]. In addition to entering the cell cycle, activated MuSCs must also determine the cell fate of their daughter cells, in particular whether they self-renew or generate myogenic progenitors. When attempting to identify the division mode of MuSCs regulated by the obestatin/GPR39 system, we observe an increased proportion of asymmetric divisions. In fact, the analysis of MRF expression in proliferating MuSCs revealed segregation of different cell fate determinants into the daughter cells - that is, asymmetric expression of the determination factor Myf5 in the daughter cells. Furthermore, the fraction of obestatin-activated MuSCs with asymmetric distribution of the Par-3 is also increased. PAR complex, consisting of Par-3 and PKCλ, asymmetrically activates the p38α/β MAPK pathway in a PKCλ-dependent manner, regulating the acquisition of

distinct daughter cell fates[41,163]. Polar distribution of the Par complex orients the plane of division to produce a daughter cell committed to myogenesis and a quiescent MuSC progenitor. The increased proportion of asymmetric divisions would favour the generation of myogenic progenitors and maintenance of the stem cell pool.

On the whole, the obestatin/GPR39 system drives MuSC entry into the intermediate G_{Alert} state that prime them for a rapid transition from quiescence to activation. Once activated, obestatin orchestrates the temporal balance between Notch and β-catenin signalling to instruct the progression of MuSCs along the myogenic lineage pathway to finally establish the segregation of different polarity proteins (Par-3/PKCλ complex) and cell fate determinants that control asymmetric division. In this scenery, obestatin-mediated transactivation of the EGFR acts as a determination switch, leading to the commitment of the daughter cell into a myogenic progenitor. Thus, the obestatin/GPR39 system integrates intrinsic and extrinsic inputs to establish the character of MuSCs in the myogenic lineage. As such, deregulation of this mechanism impacts in regeneration conditions in both healthy and degenerative conditions, including ageing.

USC UNIVERSIDADE DE SANTIAGO DE COMPOSTELA

CHAPTER 2:

We have shown that obestatin ameliorates the DMD phenotype. Obestatin treatment results in a fast-to-slow fibre type switch that translates into an increase in oxidative fibres. Obestatin acts through both HDAC/MEF2 and PGC-1α mechanisms, thereby controlling the establishment of oxidative muscle fibres. Moreover, obestatin signalling regulates muscle atrophy through regulation of ubiquitin E3-ligases expression, MAFbx and MuRF1, through inactivation of FoxO4 and FoxO1. Notably, obestatin leads to a stabilization of the sarcolemma of *mdx* skeletal muscle through the expression of utrophin, α-syntrophin, β-dystroglycan, and α7β1-integrin proteins. This observation correlates with the decrease in the levels of serum CK, AST and ALT, signs that indicate a partial rescue of muscle tissue necrosis. Furthermore, treatment with obestatin reduces muscle fibrosis. All these effects provoke a substantial improvement in skeletal muscle physiological function, in terms of specific force production. These actions acquire more relevance considering the age-related loss of preproghrelin expression, and thus obestatin, in dystrophin deficient *mdx* mice.

Obestatin attenuates histopathological and biochemical features of muscular dystrophy in *mdx* mice. Rates of myofibre central nucleation, tissue fibrosis, and tissue necrosis (evaluated as IgG^+ myofibres) were reduced in *mdx* mice treated with obestatin. In addition, CK, ALT, and AST levels were significantly reduced compared to control mice, which also strongly suggest a decrease in muscle fibre damage. This improvement correlates with improved muscle function because obestatin-treated mice show a significant increase in muscle strength, as determined by generation of specific force. Because obestatin controls the fibre type determination[153], some of this gain-of-function may be linked to a conversion of fast-twitch to slow-twitch fibres, which are more resistant to degeneration. The slow and oxidative myofibre identity is governed by the balance between positive and negative signalling by MEF2 and class II HDACs, respectively[168]. Obestatin increases class II HDAC phosphorylation, thus leading to nuclear export of HDACs and allowing sustained activation of MEF2, which

promotes the establishment of slow and oxidative myofibres, i.e. MHC type I and troponin I-SS. The increase in oxidative fibre density triggered by obestatin signalling is accompanied by significant changes in known regulators of mitochondrial function, such as cytochrome C, UCP3 and CPT1. This improved mitochondrial capacity is concomitant to an increased expression of PGC-1α, a master regulator of mitochondrial gene expression involved in activation of mitochondrial biogenesis and oxidative metabolism[206]. Mechanistically, PGC-1α regulates fibre type switching through the coactivation of MEF2[177]. Furthermore, MEF2 regulates PGC-1α expression through an autoregulatory loop[171]. Therefore, MEF2 operates as a nodal point for the control of multiple downstream transcriptional regulators of the slow-fibre phenotype and PGC-1α expression. Our data show that obestatin treatment triggers an up-regulation of AchRα, a component of the NMJ gene program. This observation correlates with previous observations made with PGC-1α transgenic mice in which PGC-1α was shown to regulate the NMJ genes[173]. In addition, obestatin has an anti-atrophic effect by regulating the expression levels of the two E3-ubiquitin ligases, hallmarks of skeletal muscle atrophy, MAFbx and MuRF1. Although the exact mechanism of this effect is unknown in DMD, it is clear that obestatin inhibits the function of the pro-atrophic transcription factors FoxO1 and FoxO4 and blunts the induction of the atrogenes MAFbx and MuRF1. Interestingly, the obestatin action is not due to an effect on the FoxO3, which appears to be phosphorylated or inactivated under basal conditions. Recent data have shown that Akt/mTOR activation combined with PKD/CAMKII/AMPK inactivation by the obestatin signalling is required to inhibit FoxO-dependent atrogenes in catabolic processes provoked by glucocorticoids[155]. This is consistent with the activation of S6K1 and by eIF4E availability, through phosphorylation of 4E-BP1, key regulators of protein synthesis, which shift the balance from protein degradation to protein synthesis in obestatin-treated mice.

The absence of dystrophin leads to a decrease and a delocalization of dystrophin-associated proteins with the consequent sarcolemma instability and damage as muscle fibres detach from the laminin-rich basal lamina during contraction[61]. An alternative approach to restoring dystrophin

deficiency is to up-regulate the expression of utrophin based on the evidence for functional redundancy between these two proteins[207]. Indeed, utrophin shares a high degree of sequence identity with dystrophin and also associates with members of the dystrophin-associated protein complex[208]. Utrophin is restricted to neuromuscular and myotendinous junctions in adult muscle, but during embryonic development and in patients with DMD, it is localized at the sarcolemma when dystrophin is absent or present only at low levels. Studies in animal models have provided compelling evidence that utrophin functions in these scenarios directly to protect the muscle against dystrophic degeneration[207]. Our results indicate that obestatin signalling regulates utrophin expression. Specifically, *mdx* mice treated for 30 days with obestatin showed an increase in utrophin levels compared with control *mdx* mice, which are localized throughout the entire length of the sarcolemma. These results are consistent with the promotion of the slow oxidative myogenic program by obestatin signalling. Indeed, metabolic changes to the muscle can also influence utrophin expression[209]. Given the demonstrated role of PGC-1α in regulating utrophin transcription[176,210], we speculate that inhibition of HDAC activity through obestatin signalling results in increased MEF2 levels and stimulation of PGC1-α expression leading to utrophin up-regulation. In addition, the up-regulation of utrophin expression and its localization at the sarcolemma may stimulate the expression and correct localization of the dystrophin-glycoprotein complex, i.e. α-syntrophin and β-dystroglycan, except for NOS1, which does not show significant differences with control mice. It has been previously established that dystrophin localizes NOS1 to the sarcolemma, whereas utrophin does not[211]. The implication of this is uncertain, given that there may be compensatory pathways for the lack of NOS1[207,212]. In addition to the enhancement of structural proteins like utrophin, obestatin also regulates α7β1 integrin expression, a laminin-binding protein that contributes to the overall integrity of the sarcolemma[213]. The α7β1 integrin has structural and signalling functions that contribute to muscle development and physiology[214]. Loss of the α7 integrin in dystrophin-deficient *mdx* mice leads to a severe dystrophic phenotype[213], while transgenic overexpression of the α7β1 integrin

ameliorates disease pathology and extends the longevity of severe dystrophic models[215]. Taken together, our data suggest that the up-regulation of utrophin and α7β1 macromolecular complexes in obestatin-treated *mdx* mice protect myofibres from contraction-induced muscle injury. This action stabilizes the link between the sarcolemma and the extracellular matrix in *mdx* mice.

The convenience and cost-effectiveness of the *mdx* mouse leaves it as the predominant model for research into DMD[216]. This convenience is partly counterbalanced by the fact that the *mdx* myopathy is plainly not an exact reproduction of DMD[217]. To remain as close as possible to the human pathology, human immortalized DMD myoblasts were used to validate obestatin-signalling pathway. We report here that obestatin favours the recruitment and fusion of DMD myoblasts into myotubes, as indicated by the increased number of myonuclei in MHC^{+} cells, with increased expression of slow-MHC and hypertrophic effect. Furthermore, we show that obestatin acts to increase levels of both utrophin and α7β1-integrin complexes during the myogenic differentiation. These findings support and emphasize the role of the obestatin signalling into the myogenic program in DMD.

Although there are several promising therapeutic approaches under investigation for DMD, this pathology will require a multidisciplinary approach to address its many features. Our results illustrate how obestatin can restore to some extent muscle integrity and function in DMD. These data position obestatin as a potential DMD therapeutic candidate not only as an ameliorative treatment to slow the muscle damage but also as part of combinatorial treatment strategies[94]. In this sense, obestatin-mediated fibre restoration would allow the maintenance of vector or cell content in the decisive period between injection and/or transgene expression in the dystrophic muscles. For instance, the stability of the pre-conditioned muscle fibre could help mitigate the loss of therapeutic vectors in gene therapy and guarantee a higher therapeutic benefit in the restoration of dystrophin in the muscles of DMD patients[93,218,219]. The results presented so far provide compelling evidence for a potential way of treating DMD.

CHAPTER 3:

Obestatin signalling addresses multiple cellular pathways needed for phenotypic plasticity in DMD, including regulation of myofibre regeneration, activation of the slow oxidative myofibre program, stabilization of the sarcolemma, as well as regulation of proteasomal signalling. In this work, we demonstrate that up-regulation of the dystrophin homolog utrophin by the obestatin/GPR39 system correlates with the cooperative activation of the class II HDAC/MEF2 and calcineurin/NFATc1 pathways associated to oxidative phenotype transition. Obestatin additionally stimulates the master regulator of autophagy ULK1 through the CAMKII-AMPK signalling axis, thereby triggering the initiation of autophagic cascades. ULK1 activity and autophagy are maintained by concurrent activation of AMPK and mTOR signalling pathways. The spatial coupling of catabolic and anabolic cell machinery is required to maintain protein homoeostasis for biosynthetic processes. These findings support and emphasize the notion that by regulating complementary cellular processes, the obestatin/GPR39 system successfully mitigates the dystrophic phenotype.

Up-regulation of the dystrophin homolog utrophin, in conjunction with the utrophin-associated protein complex, compensate for the lack of dystrophin in DMD mitigating the pathology[220–222]. Previous studies in *mdx* mice provided compelling evidence that obestatin signalling regulates utrophin expression, in conjunction with the utrophin-associated protein complex[192]. Specifically, *mdx* mice treated with obestatin showed an increase in extrasynaptic utrophin expression[192]. These results were consistent with the promotion of the slow oxidative myogenic programme by obestatin signalling. In this particular case, utrophin expression is related to the crosstalk between the class II HDAC/MEF2 and calcineurin/NFATc1 pathways that converge to regulate transcriptional activation of slow fibre and utrophin gene promoters[174,175]. On the one hand, obestatin activates kinase pathways such as PKD and CAMKII that culminate with the phosphorylation of class II HDACs and their export to the cytoplasm as a complex with 14-3-3 proteins[179,223]. The nuclear export of class II HDACs

allows MEF2 transcriptional activation. On the other hand, obestatin signalling regulates the dephosphorylation of NFAT, which allows its entry into the nucleus where it acts on specific transcription factors[224]. NFAT activity is further supported by inactivation of GSK3β through obestatin-related Akt signalling that favours its entry into the nucleus[183,184]. In addition, the inhibition of FoxO-dependent ubiquitin E3-ligases MuRF1 and MAFbx might indirectly contribute to the increased calcineurin/NFAT activity based on the inhibitory role of ubiquitin E3-ligases on calcineurin[225–227]. Concomitant to HDAC/MEF2 and calcineurin/NFATc1 activity, obestatin promotes PGC-1α expression, which contributes to the functions of MEF2 and NFATc1[176,177]. Thus, the mechanisms driving utrophin expression involve multiple signalling pathways that cross-talk to coordinately regulate oxidative metabolism under the obestatin/GPR39 activity. It is well established that muscles with a greater abundance of slow and oxidative characteristics are more protected against DMD[10]. The mechanisms that create resilience to the dystrophic pathology in this fibre type appear to be related to utrophin expression along the sarcolemma. Indeed, dystrophin-utrophin double knock out (dKO) animals under AICAR administration caused the slow and oxidative phenotype transition in the absence of any functional improvements[228]. However, this point is not devoid of controversy. Transgenic *utr*$^{-/-}$*mdx* (dKO) and *mdx* mice overexpressing either PGC-1α or PGC-1β showed that up-regulation of the oxidative myogenic program improved muscle functionality without an increase in utrophin[229]. Such scenario was also described when estrogen-related receptor gamma (ERRγ) was overexpressed in *mdx* mice in which amelioration of dystrophic phenotype was described in absence of utrophin[230]. However, the greatest doubts arise from the type of transgenic approach and, most importantly, their reproducibility in a clinical setting[228,231,232]. In this context, it is important to retake data provided from mice deficient in both utrophin and dystrophin (dKO)[233,234]. These mice suffer from a severe muscular dystrophy similar to that seen in DMD. The absence of utrophin in the dKO mice results in a more severe phenotype in which fibre necrosis starts earlier compared with *mdx* mice. Reinforcing this notion, the expression of a utrophin transgene in skeletal muscle from dKO

mice mitigated dystrophic phenotype[221]. It is important to note that utrophin is part of a macromolecular complex and, as such, the expression of the other components is also necessary to reach the overall integrity of the sarcolemma. In this sense, the up-regulation of utrophin expression by obestatin signalling and its localization at the sarcolemma was concomitant to the expression and localization of the utrophin-glycoprotein complex, i.e. α-syntrophin and β-dystroglycan in *mdx* mice[192]. In addition, obestatin also regulates α7β1-integrin expression, a laminin-binding protein that contributes to the overall integrity of the sarcolemma. This action significantly prevents dystrophic phenotype as judged by histological, biochemical and physiological criteria. As activity-induced damage is one of the factors initiating muscle necrosis, the protection conferred by utrophin-associated protein complex is a fundamental advantage in this pathology. Thus, the notion that utrophin is an important component in mediating the functional benefits related to an oxidative phenotype in dystrophic muscles, represents a relevant feature in the obestatin/GPR39 system as a potential therapeutic approach to DMD.

The obestatin/GPR39 system additionally induces corrective autophagic signalling in DMD. The characteristic muscle wasting in DMD is partly attributed to defective autophagic processes and the resultant aggregation of dysfunctional and misfolded proteins[235]. Furthermore, muscles in DMD patients and murine models are overloaded by the accumulation of damaged and dysfunctional mitochondria due to deregulation in cargo-specific autophagy known as mitophagy[236]. Indeed, rectification of autophagy in DMD mitigates the dystrophic pathology[235,237]. Proautophagic signalling begins with activation of the master regulator of autophagy ULK1. Post-translational modification of ULK1, specifically phosphorylation by upstream molecules AMPK or mTOR, stimulates or suppresses the activity of ULK1, respectively[191]. mTOR, specifically mTORC1, activates anabolic processes, including protein synthesis, and inhibits catabolic processes such as autophagy, which safeguards the cell to maintain protein homeostasis[238–241]. AMPK activates catabolic processes and is typically considered to be activated by nutrient and energy shortage[242–245]. Therefore, mTORC1 and AMPK are often perceived as

antagonist signalling nodes that suppress or induce autophagy, respectively. However, the obestatin/GPR39 system adds a new signalling component by which AMPK does not inhibit mTORC1, but sustains ULK1 activity and autophagy. Consistent with this, recent studies described active autophagy in the context of active mTORC1 signalling[246–248]. How is the obestatin signal transduced to AMPK in an anabolic environment defined by the Akt/mTOR axis? Obestatin and insulin signalling pathways share common molecular components related to protein synthesis, i.e. Akt/mTOR axis. However, both systems differ on AMPK activity and autophagy response. This difference appears related to CAMKII as an AMPK activator[188,247]. Indeed, the CAMKII activation was only marginally observed in insulin-treated DMD cells. One of the main issues in this regard is why DMD cells may activate autophagy in response to the obestatin/GPR39 system. In this sense, it is important to emphasize that activation of biosynthetic pathways might require autophagy essentially due to the maintenance of protein homeostasis and on the fuel of metabolites for biosynthetic processes[189,246,249,250]. In support of this notion, inhibition of autophagy decreased MHC protein expression in both obestatin- and insulin-treated DMD cells. Future efforts will need to focus on the relative contribution of obestatin-regulated autophagy to dystrophy phenotype.

The collective evidence from studies detailing the functions of the obestatin/GPR39 system in the skeletal muscle, combined with those in DMD, strongly suggests that obestatin/GPR39 system is a mediator of skeletal muscle determination, maintenance, and plasticity in health and disease. The results point to the obestatin/GPR39 system as a practical and effective target for future DMD therapies.

CONCLUSIONS

USC
UNIVERSIDADE
DE SANTIAGO
DE COMPOSTELA

In relation to Chapter 1, "The role of obestatin/GPR39 system in the regulation of satellite cells", our conclusions are:

-Quiescent MuSCs express the receptor GPR39 while obestatin expression is highly up-regulated upon MuSC activation, suggesting that obestatin acts as an autocrine factor.

-Obestatin signalling accelerates cell cycle entry in MuSCs by inducing an intermediate-G_{Alert} state through the activation of the Akt/mTORC1/S6K1 signalling pathway.

-Obestatin signalling stimulates MuSCs asymmetric division through modulation of the dynamic interplay between Notch and Wnt/β-catenin signalling as well as the intracellular localization of the PAR polarity complex.

-Transactivation of EGFR by GPR39 acts as a determination switch, leading to the commitment of daughter cell into a myogenic progenitor.

With regard to Chapter 2, "Effect of obestatin treatment on *mdx* mice", we conclude that:

-Obestatin treatment results in a fast-to-slow fibre type switch, acting through both class II HDAC/MEF2 and PGC-1α pathways.

-Obestatin signalling regulates muscle atrophy through a mechanism involving the inactivation of FoxO1/4 and the ubiquitin E3-ligases.

-Obestatin signalling leads to stabilization of the sarcolemma through the expression of proteins of the utrophin- and α7β1-integrin- complexes to levels that preserve muscle integrity and prevent muscle necrosis.

-Obestatin treatment improves skeletal muscle physiological function, in terms of specific force production. Data position obestatin as a potential DMD therapeutic candidate.

Concerning Chapter 3, “Regulation of utrophin expression and autophagy by the obestatin/GPR39 system in DMD”, our conclusions are:

-The obestatin/GPR39 system up-regulates the dystrophin homolog utrophin by the cooperative activation of the class II HDAC/MEF2 and calcineurin/NFATc1 pathways associated with oxidative phenotype transition.

-The obestatin/GPR39 system induces corrective autophagic signalling in DMD by controlling the master regulator of autophagy ULK1 through the CAMKII-AMPK axis. ULK1 activity and autophagy are maintained by concurrent activation of AMPK and mTOR signalling pathways. The spatial coupling of catabolic and anabolic cell machinery is required to maintain protein homoeostasis for biosynthetic processes.

USC UNIVERSIDADE DE SANTIAGO DE COMPOSTELA

RESUMO

USC
UNIVERSIDADE
DE SANTIAGO
DE COMPOSTELA

O músculo esquelético é un dos tecidos máis grandes do corpo. Representa entre o 30 e o 50% do peso corporal humano adulto, e é responsable de manter a postura e a locomoción. Ademais, xoga un papel central no control do metabolismo de todo o corpo, actuando como un órgano endócrino. O músculo esquelético adulto é un tecido postmitótico estable con pouca renovación en condicións fisiolóxicas normais, pero cunha notable capacidade rexenerativa en resposta a un dano severo causado por un traumatismo intenso ou enfermidades dexenerativas musculares. En caso de lesión, o músculo esquelético sométese a un proceso altamente orquestrado que ten lugar a nivel tisular, celular e molecular, o que conduce á formación dun aparello contráctil funcional. Neste proceso xogan un papel crucial as células satélite. As células satélite son as células nai do músculo esquelético responsables do mantemento da homeostase muscular. Reciben o seu nome debido á súa posición anatómica relativa entre o sarcolema muscular e a lámina basal das miofibras, e comprenden unha poboación heteroxénea de células caracterizadas pola expresión do factor Pax7. Nos músculos adultos en repouso, as células satélite existen nun estado latente e non mitótico coñecido como quiescente. Tras una lesión muscular, as células satélite quiescentes actívanse e proliferan para dar lugar a unha poboación de células precursoras mioxénicas coñecidas como mioblastos. Despois de varias roldas de proliferación, os mioblastos saen do ciclo celular e comezan a diferenciarse e a fusionarse para formar miotubos multinucleares ou reparar as miofibras danadas existentes. Este proceso de activación e diferenciación das células satélite está regulado por unha familia de factores de transcrición chamados factores de regulación mioxénica (MRF), que consisten en Myf5, MyoD, mioxenina e MRF4. Un aspecto esencial para o mantemento da homeostase muscular é a capacidade de autorrenovación que posúen as células satélite, que permite proporcionar os proxenitores mioxénicos necesarios para a rexeneración muscular, pero tamén manter a poboación de células nai. As células satélites poden regular a autorrenovación realizando dous tipos de división celular diferentes: simétrica ou asimétrica. A través da división asimétrica, unha célula nai dá lugar a dúas células fillas funcionalmente diferentes: unha célula nai que

repón a reserva de células nai, e un proxenitor mioxénico que participa na rexeneración muscular. Pola contra, na división simétrica, unha célula nai divídese en dúas células fillas idénticas. Existen dous eventos relacionados entre si implicados no tipo de división que leva a cabo a célula satélite: a orientación do fuso mitótico e a distribución de proteínas de polaridade. En canto á orientación da división, a división simétrica prodúcese paralelamente ao eixo da miofibra, polo que ámbalas células están en contacto coa membrana plasmática e a lámina basal da miofibra. Pola contra, a división asimétrica ten lugar nunha orientación apico-basal, de maneira que a célula satélite nai ($Myf5^{-}$) permanece unida á membrana basal mentres que a célula filla comprometida ($Myf5^{+}$) mantense en contacto coa miofibra. Con respecto á distribución de proteínas de polaridade, demostrouse que a división simétrica está promovida pola activación da vía PCP, que conduce á distribución simétrica de proteínas como Vangl2 nas células fillas. Pola contra, a división asimétrica caracterízase pola segregación de diferentes determinantes de destino celular nas células fillas, destacando o papel do complexo Par3-PKCλ que se distribúe asimetricamente na célula filla comprometida. Diversos estados dexenerativos ou patolóxicos, como a distrofia muscular de Duchenne, afectan á capacidade funcional das células satélites. Por tanto, a comprensión dos mecanismos reguladores do comportamento das células satélite é indispensable para o desenvolvemento de novos enfoques terapéuticos.

A distrofia muscular de Duchenne (DMD) é un trastorno neuromuscular hereditario de tipo recesivo ligado ao cromosoma X. É a forma máis común de distrofia muscular na infancia, afectando a un de cada 5000 varóns recén nados, e caracterízase por unha debilidade muscular progresiva que desencadea en morte prematura debido a insuficiencia respiratoria e/ou cardíaca. Está causada por mutacións no xene *DMD* que resultan na ausencia de distrofina, unha proteína citoesquelética que forma parte do complexo de proteínas asociadas á distrofina (DAPC) que proporciona conexión entre o citoesqueleto da miofibra e a matriz extracelular. A distrofina proporciona estabilidade estrutural ao músculo esquelético, mantén a forza e flexibilidade e protexe

ao sarcolema de lesións inducidas pola contracción. En ausencia de distrofina, o DAPC desestabilízase e os niveis das outras proteínas do DAPC diminúen. Como consecuencia, o sarcolema vólvese máis susceptible á contracción-lesión, provocando danos na membrana que aumentan a súa permeabilidade ao calcio, o que causa disfunción celular e morte. A morte celular continua provoca unha resposta inflamatoria e un desequilibrio entre a dexeneración e a rexeneración do músculo esquelético. Estes ciclos crónicos de dexeneración e rexeneración incapacitan progresivamente ás células satélites para compensar o dano distrófico, o que conduce á patoloxía da enfermidade, caracterizada por unha diminución progresiva da función muscular debido á perda de miofibras musculares e a súa substitución por tecido conectivo e graxo. Na actualidade, non existe cura para a DMD. As estratexias de tratamento convencionais céntranse na terapia de apoio destinada a aliviar parcialmente os síntomas, e consisten no uso de corticosteroides, cirurxía, fisioterapia e manexo da cardiomiopatía e a enfermidade pulmonar. Durante os últimos anos, xurdiron diferentes enfoques terapéuticos para tratar ou compensar o defecto primario da DMD, é dicir, a ausencia de distrofina, que inclúen terapias xenéticas, celulares e farmacolóxicas. Porén, estas estratexias están limitadas debido a que en etapas avanzadas os músculos distróficos presentan unha acumulación de graxa e fibrose exacerbadas que comprometen a eficiencia das terapias ao dificultar a súa accesibilidade ao músculo. Deste xeito, existe un crecente interese no desenvolvemento de terapias combinadas, que consisten no uso dunha terapia para corrixir o defecto xenético e outra para mellorar o estado do músculo receptor, asegurando así a máxima eficacia das terapias xenéticas e celulares.

Neste contexto, o noso grupo describiu a obestatina, un péptido de 23 aminoácidos derivado do polipéptido preproghrelina, que exerce unha acción autócrina a través do receptor unido a proteínas G GPR39, regulando múltiples etapas da mioxénese: proliferación de mioblastos, saída do ciclo celular, diferenciación e recrutamento para fusionar e formar miotubos hipertróficos multinucleados. O sistema obestatina/GPR39 exerce a súa acción na mioxénese mediante a interacción coordinada entre mecanismos dependentes de proteínas G e dependentes de β-arrestinas, controlando a

especificidade, eficiencia e capacidade dos sinais para dirixir a progresión do programa mioxénico. A acción mitoxénica asociada á obestatina está determinada pola activación dependente de proteínas G que define as vías relacionadas con ERK1/2 e o eixo JunD, activando o primeiro paso de proliferación do proceso mioxénico. Por outra banda, a obestatina exerce a súa acción mioxénica a través da transactivación, dependente de β-arrestinas, de EGFR, desencadeando a saída do ciclo celular e o desenvolvemento e progresión da diferenciación a través dunha xerarquía de cinases determinada polos eixos Akt, CaMKII, c-Jun, e p38. A nivel funcional, a inxección intramuscular de obestatina ou a súa sobreexpresión nun modelo *in vivo* de dano muscular agudo mellora de maneira significativa a rexeneración e funcionalidade muscular sen un efecto significativo sobre a deposición de coláxeno. Ademais desta acción, a obestatina participa na especificación da identidade das fibras musculares ao inducir a remodelación do músculo esquelético cara un fenotipo oxidativo máis resistente ao dano. Estudos recentes demostran a acción do sistema obestatina/GPR39 na activación da expansión dos mioblastos humanos. Por outra banda, o sistema obestatina/GPR39 é capaz de contrarrestar as alteracións na proteostase (por exemplo, as asociadas á atrofia de miotubos inducida por glucocorticoides) e de restaurar unha homeostase basal eficaz. Na terapia de transplante celular (por exemplo, a terapia baseada no xenotrasplante de mioblastos humanos primarios en ratos inmunodeficientes), a obestatina non só mellora a eficacia do transplante, senón que tamén facilita unha distribución uniforme dos mioblastos dentro do músculo hóspede. Estas propiedades fan da obestatina un candidato terapéutico prometedor para o tratamento de enfermidades relacionadas coa rexeneración muscular. En base ao exposto, os obxectivos deste traballo son: (i) determinar o papel do sistema obestatina/GPR39 na regulación das células satélite; e (ii) investigar o potencial terapéutico do sistema obestatina/GPR39 para o tratamento local dos músculos distróficos usando o modelo de rato deficiente en distrofina *mdx* e modelos *in vitro* de cultivo celular de células musculares esqueléticas DMD humanas.

Os resultados deste traballo demostran que o sistema

obestatina/GPR39 participa na regulación das células satélite. Observamos que o receptor GPR39 exprésase tanto en células satélite quiescentes como en activadas, contribuíndo a controlar a supervivencia e a determinación do destino celular, mentres que a obestatina sobreexprésase marcadamente en células satélite activadas durante a mioxénese. O aumento da biosíntese da obestatina en células satélite activadas, xunto coa súa débil expresión en células satélite quiescentes, apoian a hipótese de que a obestatina pode incrementar a sinalización de maneira autócrina actuando como un mecanismo de retroalimentación positiva. Ademais, observamos que a perda de GPR39 provoca unha perda de Pax7 e un aumento da expresión de caspasa activa 3 en células satélite. Este efecto está acompañado dunha diminución significativa do número de células satélite proliferantes ($Pax7^+/MyoD^+$) e diferenciantes ($mioxenina^+$), o que descarta un ambiente permisivo para a diferenciación. O reducido número de células $Pax7^+$ xunto coa inhibición concomitante dos marcadores de diferenciación temperáns débese potencialmente á diminución da viabilidade das células satélite debido á morte celular programada por apoptose, o que á súa vez conduce a un esgotamento das células satélite. Estes resultados identifican o receptor GPR39 como parte da maquinaria molecular que controla a determinación do destino celular das células satélite regulando a súa supervivencia. Por outra banda, vimos que a sinalización da obestatina induce cinéticas máis rápidas de entrada no ciclo celular e de división celular das células satélite. A transición da quiescencia á activación está ligada á activación da vía de sinalización Akt/mTORC1/S6, responsable da transición dun estado G_0 a un estado G_{Alert} no que as células entran máis rapidamente no ciclo celular. Neste caso en particular, a transición de G_0 a G_{Alert} parece ser unha etapa intermedia na progresión do ciclo celular na cal a sinalización da obestatina canalízase cara a sinais de regulación que permiten a indución da división celular. O feito de que o sistema obestatina/GPR39 impulse a entrada das células satélite nun estado de pre-activación ou G_{Alert} implica unha regulación precisa dos activadores e represores do ciclo celular para coordinar os diferentes estados das células satélite. Os nosos experimentos indican que a sinalización de obestatina provoca unha diminución significativa na translocación ao núcleo do

dominio intracelular de Notch (NICD) en células satélite activadas en fase temperá. A unión de Notch ao seu receptor libera NICD, que se transloca ao núcleo onde desencadea a transcrición de varios xenes involucrados na autorrenovación do nicho de células satélite. Pola contra, a obestatina conduce á estabilización da forma non fosforilada de β-catenina, que se transloca ao núcleo para inducir a actividade transcricional de factores reguladores da mioxénese. De feito, o silenciado de β-catenina provoca a perda do destino mioxénico dos proxenitores en resposta á obestatina. Así, a determinación do destino celular ao longo da liñaxe mioxénica está controlada por un equilibrio preciso entre as vías de sinalización de, primeiro, Notch, e despois, β-catenina, asociadas ao sistema obestatina/GPR39. A continuación, estudiamos o efecto do sistema obestatina/GPR39 na determinación do destino celular das células satélite, observando un aumento na proporción de divisións asimétricas. De feito, a análise da expresión dos MRF nas células satélite proliferantes revelou a expresión asimétrica do factor de determinación Myf5 nas células fillas. Ademais, a fracción de células satélite activadas pola obestatina con distribución asimétrica de Par-3 tamén se incrementa. O complexo PAR, formado por Par-3 e PKCλ, activa de forma asimétrica a vía MAPK p38α/β, regulando a adquisición de distintos destinos das células fillas. A distribución polar do complexo Par orienta o plano de división para producir unha célula filla comprometida coa mioxénese e una célula satélite quiescente. O aumento da proporción de divisións asimétricas favorecería a xeración de proxenitores mioxénicos e o mantemento do nicho de células satélite. Ademais destas características funcionais, vimos que a transactivación de EGFR actúa como un interruptor de determinación, conducindo á transformación da célula filla comprometida nun proxenitor mioxénico. En resumo, o sistema obestatina/GPR39 integra sinais intrínsecos e extrínsecos para establecer o carácter das células satélite na liñaxe mioxénica. A alteración deste mecanismo pode repercutir na rexeneración muscular, tanto en condicións fisiolóxicas como dexenerativas.

Unha vez elucidado o papel do sistema obestatina/GPR39 na regulación das células satélite, estudiamos o potencial terapéutico da

obestatina en DMD, avaliando o efecto do tratamento local con obestatina en ratos *mdx* deficientes para distrofina. Os resultados obtidos demostran que o tratamento con obestatina atenúa as características histopatolóxicas e bioquímicas da distrofia muscular en ratos *mdx*. Deste xeito, observamos una redución na porcentaxe de núcleos centralizados e na fibrose e necrose tisular (avaliada como miofibras IgG^+) en ratos *mdx* tratados con obestatina. Ademais, tamén se reduciron os niveis de creatina cinase, alanina aminotransferase e aspartato aminotransferase en comparación cos ratos control, o que suxire una forte diminución do dano da fibra muscular. Isto ten correlación coa mellora da función muscular que evidencia o aumento significativo na forza muscular nos ratos *mdx* tratados con obestatina. Debido a que a obestatina controla a determinación do tipo de fibra, parte desta ganancia de función pode estar relacionada cunha conversión de fibras de tipo rápido a fibras de tipo lento, que son máis resistentes á dexeneración. Neste sentido, observamos como o tratamento con obestatina aumenta a fosforilación das HDAC de clase II, o que conduce á exportación nuclear de HDAC e permite a activación de MEF2, promovendo o establecemento de miofibras lentas e oxidativas, é dicir, MHC tipo I e troponina I-SS. O aumento de fibras de tipo oxidativo provocado pola sinalización da obestatina vai acompañado de cambios significativos en proteínas reguladoras da función mitocondrial como citocromo C, UCP3, CPT1 e PGC-1α. Consistente co aumento da expresión de PGC1-α, a obestatina tamén aumenta os niveis de AchRα, un compoñente do programa de xenes das unións neuromusculares. Por outra banda, a obestatina exerce un efecto anti-atrófico ao regular os niveis de expresión das E3-ubiquitina ligases características da atrofia muscular esquelética, MAFbx e MuRF1. Aínda que se descoñece o mecanismo exacto deste efecto na DMD, a obestatina inhibe a función dos factores de transcrición pro-atróficos FoxO1 e FoxO4 e reduce a indución dos atroxenes MAFbx e MuRF1. Isto é consistente coa activación de S6K1 e a dispoñibilidade de eIF4E a través da fosforilación de 4E-BP1, reguladores clave da síntese de proteínas, cambiando o balance da degradación á síntese de proteínas en ratos tratados con obestatina. Un enfoque alternativo para restaurar a deficiencia de distrofina é aumentar a expresión da utrofina baseándose na

redundancia funcional evidenciada entre estas dúas proteínas. Os nosos resultados indican que a sinalización da obestatina regula a expresión da utrofina. De feito, os ratos *mdx* tratados con obestatina mostraron un aumento nos niveis de utrofina en comparación cos ratos *mdx* control, atopándose localizada ao longo de todo o sarcolema. Ademais, a obestatina estimula a expresión e correcta localización de proteínas do DAPC, como α-sintrofina e β-distroglicano, e do complexo αβ-integrina, unhas proteínas de unión á laminina que contribúen á integridade xeral do sarcolema. Estes datos suxiren que o tratamento con obestatina protexe as miofibras de lesións musculares inducidas pola contracción.

Numerosos estudos revelan a importancia da sobreexpresión de utrofina para mitigar a patoloxía da DMD. Por tanto, decidimos estudar a continuación o papel do sistema obestatina/GPR39 na regulación da expresión de utrofina. Para isto, empregamos un modelo *in vitro* de células humanas DMD, como único modelo dispoñible para avaliar a sinalización nun contexto humano. A expresión da utrofina está relacionada co entrecruzamento entre as vías de sinalización HDACII/MEF2 e calcineurina/NFATc1 que converxen para regular a activación transcricional de xenes promotores de fibras lentas e utrofina. Por unha banda, a obestatina activa vías cinases como PKD e CAMKII que culminan coa fosforilación dos HDACs de clase II e a activación transcricional de MEF2. Doutra banda, a sinalización da obestatina regula a desfosforilación de NFAT, permitindo a súa translocación ao núcleo onde actúa sobre factores de transcrición específicos. A actividade de NFAT apóiase na inactivación de GSK3β a través da sinalización obestatina-dependente de Akt, o que favorece a súa entrada no núcleo. Ademais, a inhibición dependente de FoxO das E3-ubiquitina ligases MuRF1 e MAFbx podería contribuír indirectamente ao aumento da actividade da vía calcineurina/NFAT. Concomitante coa actividade das vías HDAC/MEF2 e calcineurina/NFATc1, a obestatina promove a expresión de PGC-1α, que contribúe ás funcións de MEF2 e NFATc1. Por tanto, os mecanismos que impulsan a expresión da utrofina involucran múltiples vías de sinalización que se entrecruzan para regular de maneira coordinada o metabolismo oxidativo baixo a actividade do sistema obestatina/GPR39. O feito de que a utrofina sexa un

compoñente importante na mediación dos beneficios funcionais asociados cun fenotipo oxidativo nos músculos distróficos representa unha característica relevante do sistema obestatina/GPR39 como potencial enfoque terapéutico para a DMD.

Os experimentos levados a cabo en células DMD revelan que o sistema obestatina/GPR39 tamén induce autofaxia en condición distróficas. O desgaste muscular característico da DMD atribúese en parte a procesos autofáxicos defectuosos e á resultante agregación de proteínas non funcionais. De feito, diversos estudos demostran que a rectificación da autofaxia mitiga a patoloxía distrófica. A sinalización proautofáxica comeza coa activación do regulador mestre da autofaxia, ULK1. A modificación post-traducional de ULK1, especificamente a fosforilación polas moléculas AMPK ou mTOR, estimula ou suprime a actividade de ULK1, respectivamente. mTOR, en concreto mTORC1, activa procesos anabólicos, incluíndo a síntese de proteínas, e inhibe procesos catabólicos como a autofaxia, que protexe á célula mantendo a homeostase proteica. AMPK activa os procesos catabólicos e xeralmente actívase en condición de escaseza de nutrientes e enerxía. Por tanto, mTORC1 e AMPK son considerados a miúdo como nodos de sinalización antagonistas que suprimen ou inducen a autofaxia, respectivamente. Neste sentido, os nosos resultados demostran que o sistema obestatina/GPR39 engade un novo compoñente de sinalización polo cal AMPK non inhibe mTORC1, senón que mantén a actividade de ULK1 e a autofaxia. Deste xeito, a obestatina estimula ULK1 a través do eixo de sinalización CAMKII-AMPK, desencadeando así o inicio de sinais autofáxicas. A actividade de ULK1 e a autofaxia mantéñense mediante a activación concorrente das vías de sinalización AMPK e mTOR. Ademais, os datos obtidos suxiren que a activación das vías anabólicas requiren do proceso de autofaxia para o mantemento da homeostase proteica e como combustible de metabolitos para os procesos biosintéticos. Estes achados apoian e salientan o feito de que o sistema obestatina/GPR39 mitiga o fenotipo distrófico mediante o regulamento de procesos celulares complementarios. En conxunto, os nosos resultados ilustran como a obestatina pode restaurar parcialmente a integridade e función muscular na DMD, postulando á obestatina como un

potencial candidato terapéutico para a DMD, non só como un tratamento para diminuír o dano muscular, senón tamén como parte de estratexias de terapias combinatorias. Neste sentido, a restauración da fibra muscular mediada pola obestatina permitiría mitigar a perda de vectores terapéuticos na terapia xénica e garantir un maior beneficio terapéutico na restauración da distrofina nos músculos dos pacientes con DMD. Finalmente, a evidencia colectiva dos estudos que detallan as funcións do sistema obestatina/GPR39 no músculo esquelético e na DMD suxiren que este sistema é un mediador da determinación, mantemento e plasticidade do músculo esquelético, tanto en condicións fisiolóxicas como patolóxicas.

USC UNIVERSIDADE DE SANTIAGO DE COMPOSTELA

AGRADECEMENTOS

USC
UNIVERSIDADE
DE SANTIAGO
DE COMPOSTELA

Chegou o final desta etapa, sendo o momento de agradecer a tódalas persoas que formaron parte dela e que fixeron posible este traballo.

Primeiro, agradecer aos meus directores de Tese, o Dr. Jesús Pérez Camiña, o Dr. José Luis Relova Quinteiro e o Dr. Felipe Casanueva Freijo, a oportunidade que me brindaron para levar a cabo este traballo. A Felipe, polo seu respaldo. A José Luis, pola súa continua disposición e inestimable axuda. A Jesús, por permitirme formar parte do seu equipo, pola guía e dedicación durante estes anos que fixeron posible esta Tese e, en especial, pola cordialidade e comprensión das situacións persoais.

A Yola, pola súa axuda, disposición e preocupación máis aló do profesional.

A toda a xente do IDIS, CIMUS e animalario que me botou amablemente unha man sempre que o precisei.

Aos meus compañeiros do labo 4, a xente coa que compartín tantos momentos e experiencias nestes anos e que me axudou tanto sempre: Boli, Saúl, Tania, Carlos… A Lara e a Bego, por tódalas conversas, por todo o alento, por facer moito máis fácil e levadía esta etapa.

Ás miñas amigas, polo apoio e por tódolos bos momentos para repoñer forzas. A Nere, por animarme a emprender este camiño, e por percorrelo comigo facendo curtas as distancias.

Á miña irmá Vero, por todo o vivido xuntas, por todo o cariño e por estar sempre aí para animarme e sacarme un sorriso.

Aos meus pais, a quen lles debo todo o que teño e todo o que son. Por estar sempre e para todo. Por todo o traballo, esforzo e amor e apoio incondicionais que me fixeron chegar até aquí.

A Gus, o meu piar fundamental nesta etapa que comezamos xuntos. Por ser o meu compañeiro de equipo, dentro e fóra do laboratorio. Por acompañarme nesta viaxe crendo en min, apoiándome e ensinándome tanto de todo, sempre e incondicionalmente.

USC
UNIVERSIDADE
DE SANTIAGO
DE COMPOSTELA

BIBLIOGRAPHY

USC
UNIVERSIDADE
DE SANTIAGO
DE COMPOSTELA

1. Iizuka K, Machida T, Hirafuji M. Skeletal muscle is an endocrine organ. *J Pharmacol Sci*. 2014;125(2):125-131.
2. Yin H, Price F, Rudnicki MA. Satellite cells and the muscle stem cell niche. *Physiol Rev*. 2013;93(1):23-67.
3. Betts JG, Desaix P, Johnson JE, et al. Anatomy & Physiology. In: Open Textbooks. OpenStax College, Rice University; 2013.
4. Bassel-Duby R, Olson EN. Signaling pathways in skeletal muscle remodeling. *Annu Rev Biochem*. 2006;75(1):19-37.
5. Frontera WR, Ochala J. Skeletal muscle: a brief review of structure and function. *Calcif Tissue Int*. 2015;96(3):183-195.
6. Pette D, Staron RS. Myosin isoforms, muscle fiber types, and transitions. *Microsc Res Tech*. 2000;50(6):500-509.
7. Schiaffino S, Reggiani C. Fiber types in mammalian skeletal muscles. *Physiol Rev*. 2011;91(4):1447-1531.
8. Buller AJ, Eccles JC, Eccles RM. Interactions between motoneurones and muscles in respect of the characteristic speeds of their responses. *J Physiol*. 1960;150(2):417-439.
9. Zierath JR, Hawley JA. Skeletal muscle fiber type: Influence on contractile and metabolic properties. *PLoS Biol*. 2004;2(10).
10. Webster C , Silberstein L , Hays AP , Blau HM. Fast muscle fibers are preferentially affected in Duchenne muscular dystrophy. *Cell*. 1988;52(4):503-513.
11. Ljubicic V, Burt M, Jasmin BJ. The therapeutic potential of skeletal muscle plasticity in Duchenne muscular dystrophy: phenotypic modifiers as pharmacologic targets. *FASEB J*. 2014;28(2):548-568.
12. Schmalbruch H, Lewis DM. Dynamics of nuclei of muscle fibers and connective tissue cells in normal and denervated rat muscles. *Muscle Nerve*. 2000;23(4):617-626.
13. Chargé SB, Rudnicki MA. Cellular and molecular regulation of muscle regeneration. *Physiol Rev.* 2004;84(1):209-238.
14. Karalaki M, Fili S, Philippou A, Koutsilieris M. Muscle regeneration: cellular and molecular events. *In Vivo*. 2009;23(5):779-796.
15. Orimo S, Hiyamuta E, Arahata K, Sugita H. Analysis of inflammatory cells and complement C3 in bupivacaine-induced myonecrosis. *Muscle Nerve*. 1991;14(6):515-520.
16. Chazaud B, Brigitte M, Yacoub-Youssef H, et al. Dual and beneficial roles of

macrophages during skeletal muscle regeneration. *Exerc Sport Sci Rev*. 2009;37(1):18-22.

17. Merly F, Lescaudron L, Rouaud T, Crossin F, Gardahaut MF. Macrophages enhance muscle satellite cell proliferation and delay their differentiation. *Muscle Nerve*. 1999;22(6):724-732.
18. Sambasivan R, Yao R, Kissenpfennig A, et al. Pax7-expressing satellite cells are indispensable for adult skeletal muscle regeneration. *Development*. 2011;138(19):4333-4333.
19. Dumont NA, Bentzinger CF, Sincennes M-C, Rudnicki MA. Satellite Cells and Skeletal Muscle Regeneration. *Compr Physiol*. 2015;5(3):1027-1059.
20. Mauro A. Satellite cell of skeletal muscle fibers. *J Biophys Biochem Cytol*. 1961;9:493-495.
21. Yin H, Price F, Rudnicki M a. Satellite cells and the muscle stem cell niche. *Physiol Rev*. 2013;93(1):23-67.
22. Seale P, Sabourin LA, Girgis-Gabardo A, Mansouri A, Gruss P, Rudnicki MA. Pax7 is required for the specification of myogenic satellite cells. *Cell*. 2000;102(6):777-786..
23. Seale P, Ishibashi J, Scimè A, Rudnicki MA. Pax7 is necessary and sufficient for the myogenic specification of CD45+:Sca1+ stem cells from injured muscle. *PLoS Biol*. 2004;2(5):E130.
24. Relaix F, Rocancourt D, Mansouri A, Buckingham M. A Pax3/Pax7-dependent population of skeletal muscle progenitor cells. *Nature*. 2005;435(7044):948-953.
25. Kassar-Duchossoy L, Giacone E, Gayraud-Morel B, Jory A, Gomès D, Tajbakhsh S. Pax3/Pax7 mark a novel population of primitive myogenic cells during development. *Genes Dev*. 2005;19(12):1426-1431.
26. Zammit PS. All muscle satellite cells are equal, but are some more equal than others? *J Cell Sci*. 2008;121(Pt 18):2975-2982.
27. Relaix F, Montarras D, Zaffran S, et al. Pax3 and Pax7 have distinct and overlapping functions in adult muscle progenitor cells. *J Cell Biol*. 2006;172(1):91-102.
28. Beauchamp JR, Heslop L, Yu DSW, et al. Expression of CD34 and Myf5 defines the majority of quiescent adult skeletal muscle satellite cells. *J Cell Biol*. 2000;151(6):1221-1234.
29. Schultz E. Satellite cell proliferative compartments in growing skeletal muscles. *Dev Biol*. 1996;175(1):84-94.
30. Kuang S, Kuroda K, Le Grand F, Rudnicki MA. Asymmetric self-renewal and

commitment of satellite stem cells in muscle. *Cell*. 2007;129(5):999-1010.

31. Collins CA, Olsen I, Zammit PS, et al. Stem cell function, self-renewal, and behavioral heterogeneity of cells from the adult muscle satellite cell niche. *Cell*. 2005;122(2):289-301.
32. Fukada S, Ma Y, Ohtani T, Watanabe Y, Murakami S, Yamaguchi M. Isolation, characterization, and molecular regulation of muscle stem cells. *Front Physiol*. 2013;4(November):317.
33. Almada AE, Wagers AJ. Molecular circuitry of stem cell fate in skeletal muscle regeneration, ageing and disease. *Nat Rev Mol Cell Biol*. 2016;17(5):267-279.
34. Dumont NA, Wang YX, Rudnicki MA. Intrinsic and extrinsic mechanisms regulating satellite cell function. *Development*. 2015;142(9):1572-1581.
35. Zammit PS, Golding JP, Nagata Y, Hudon V, Partridge TA, Beauchamp JR. Muscle satellite cells adopt divergent fates: a mechanism for self-renewal? *J Cell Biol*. 2004;166(3):347-357.
36. Wang YX, Dumont NA, Rudnicki MA. Muscle stem cells at a glance. *J Cell Sci*. 2014;127(Pt 21):4543-4548.
37. Rodgers JT, King KY, Brett JO, et al. mTORC1 controls the adaptive transition of quiescent stem cells from G0 to G(Alert). *Nature*. 2014;510(7505):393-396.
38. Rodgers JT, Schroeder MD, Ma C, Rando TA. HGFA Is an Injury-Regulated Systemic Factor that Induces the Transition of Stem Cells into GAlert. *Cell Rep*. 2017;19(3):479-486.
39. Motohashi N, Asakura A. Muscle satellite cell heterogeneity and self-renewal. *Front cell Dev Biol*. 2014;2(January):1.
40. Le Grand F, Jones AE, Seale V, Scimè A, Rudnicki MA. Wnt7a activates the planar cell polarity pathway to drive the symmetric expansion of satellite stem cells. *Cell Stem Cell*. 2009;4(6):535-547.
41. Troy A, Cadwallader AB, Fedorov Y, Tyner K, Tanaka KK, Olwin BB. Coordination of satellite cell activation and self-renewal by Par-complex-dependent asymmetric activation of p38α/β MAPK. *Cell Stem Cell*. 2012;11(4):541-553.
42. Kuang S, Rudnicki M a. The emerging biology of satellite cells and their therapeutic potential. *Trends Mol Med*. 2008;14(2):82-91.
43. Bentzinger CF, Von Maltzahn J, Rudnicki MA. Extrinsic regulation of satellite cell specification. *Stem Cell Res Ther*. 2010;1(3):11-15.
44. Lee S-J. Regulation of muscle mass by myostatin. *Annu Rev Cell Dev Biol*. 2004;20(1):61-86.

45. Haidet AM, Rizo L, Handy C, et al. Long-term enhancement of skeletal muscle mass and strength by single gene administration of myostatin inhibitors. *Proc Natl Acad Sci U S A*. 2008;105(11):4318-4322.

46. Miller KJ, Thaloor D, Matteson S, Pavlath GK. Hepatocyte growth factor affects satellite cell activation and differentiation in regenerating skeletal muscle. *Am J Physiol Cell Physiol*. 2000;278(1):C174-81.

47. Floss T, Arnold HH, Braun T. A role for FGF-6 in skeletal muscle regeneration. *Genes Dev*. 1997;11(16):2040-2051.

48. Schiaffino S, Mammucari C. Regulation of skeletal muscle growth by the IGF1-Akt/PKB pathway: insights from genetic models. *Skelet Muscle*. 2011;1(1):4.

49. von Maltzahn J, Bentzinger CF, Rudnicki MA. Wnt7a-Fzd7 signalling directly activates the Akt/mTOR anabolic growth pathway in skeletal muscle. *Nat Cell Biol*. 2011;14(2):186-191.

50. Birnkrant DJ, Bushby K, Bann CM, et al. Diagnosis and management of Duchenne muscular dystrophy, part 1: diagnosis, and neuromuscular, rehabilitation, endocrine, and gastrointestinal and nutritional management. *Lancet Neurol*. 2018;17(3):251-267.

51. Blake DJ, Weir A, Newey SE, Davies KE. Function and genetics of dystrophin and dystrophin-related proteins in muscle. *Physiol Rev*. 2002;82(2):291-329.

52. Mendell JR, Shilling C, Leslie ND, et al. Evidence-based path to newborn screening for Duchenne muscular dystrophy. *Ann Neurol*. 2012;71(3):304-313.

53. Hoogerwaard EM, van der Wouw P a, Wilde a a, et al. Cardiac involvement in carriers of Duchenne and Becker muscular dystrophy. *Neuromuscul Disord*. 1999;9(5):347-351.

54. Hoogerwaard EM, Bakker E, Ippel PF, et al. Signs and symptoms of Duchenne muscular dystrophy and Becker muscular dystrophy among carriers in The Netherlands: a cohort study. *Lancet*. 1999;353(9170):2116-2119.

55. Messina S, Vita GL. Clinical management of Duchenne muscular dystrophy: the state of the art. *Neurol Sci*. September 2018.

56. Koenig M, Hoffman EP, Bertelson CJ, Monaco AP, Feener C, Kunkel LM. Complete cloning of the Duchenne muscular dystrophy (DMD) cDNA and preliminary genomic organization of the DMD gene in normal and affected individuals. *Cell*. 1987;50(3):509-517.

57. Bladen CL, Salgado D, Monges S, et al. The TREAT-NMD DMD Global Database: analysis of more than 7,000 Duchenne muscular dystrophy mutations. *Hum Mutat*. 2015;36(4):395-402.

58. Hoffman EP, Brown RH, Kunkel LM. Dystrophin: the protein product of the

Duchenne muscular dystrophy locus. *Cell*. 1987;51(6):919-928.

59. Koenig M, Monaco AP, Kunkel LM. The complete sequence of dystrophin predicts a rod-shaped cytoskeletal protein. *Cell*. 1988;53(2):219-228.
60. Constantin B. Dystrophin complex functions as a scaffold for signalling proteins. *Biochim Biophys Acta*. 2014;1838(2):635-642.
61. Petrof BJ, Shrager JB, Stedman HH, Kelly AM, Sweeney HL. Dystrophin protects the sarcolemma from stresses developed during muscle contraction. *Proc Natl Acad Sci U S A*. 1993;90(8):3710-3714.
62. Wallace GQ, McNally EM. Mechanisms of muscle degeneration, regeneration, and repair in the muscular dystrophies. *Annu Rev Physiol*. 2009;71:37-57.
63. Rahimov F, Kunkel LM. The cell biology of disease: cellular and molecular mechanisms underlying muscular dystrophy. *J Cell Biol*. 2013;201(4):499-510.
64. Guiraud S, Aartsma-Rus A, Vieira NM, Davies KE, van Ommen G-JB, Kunkel LM. The Pathogenesis and Therapy of Muscular Dystrophies. *Annu Rev Genomics Hum Genet*. 2015;16(1):281-308.
65. Yucel N, Chang AC, Day JW, Rosenthal N, Blau HM. Humanizing the mdx mouse model of DMD: the long and the short of it. *NPJ Regen Med*. 2018;3(1):4.
66. Flanigan KM. Duchenne and Becker muscular dystrophies. *Neurol Clin*. 2014;32(3):671-88, viii.
67. Yiu EM, Kornberg AJ. Duchenne muscular dystrophy. *J Paediatr Child Health*. 2015;51(8):759-764.
68. Birnkrant DJ, Bushby K, Bann CM, et al. Diagnosis and management of Duchenne muscular dystrophy, part 2: respiratory, cardiac, bone health, and orthopaedic management. *Lancet Neurol*. 2018;17(4):347-361.
69. Eagle M, Bourke J, Bullock R, et al. Managing Duchenne muscular dystrophy--the additive effect of spinal surgery and home nocturnal ventilation in improving survival. *Neuromuscul Disord*. 2007;17(6):470-475.
70. Ciafaloni E, Fox DJ, Pandya S, et al. Delayed diagnosis in duchenne muscular dystrophy: data from the Muscular Dystrophy Surveillance, Tracking, and Research Network (MD STARnet). *J Pediatr*. 2009;155(3):380-385.
71. Veropalumbo C, Del Giudice E, Esposito G, Maddaluno S, Ruggiero L, Vajro P. Aminotransferases and muscular diseases: a disregarded lesson. Case reports and review of the literature. *J Paediatr Child Health*. 2012;48(10):886-890.
72. McDonald CM, Henricson EK, Abresch RT, et al. Long-term effects of glucocorticoids on function, quality of life, and survival in patients with Duchenne muscular dystrophy: a prospective cohort study. *Lancet*.

2018;391(10119):451-461.

73. Finsterer J. Cardiopulmonary support in duchenne muscular dystrophy. *Lung*. 2006;184(4):205-215.
74. Guiraud S, Chen H, Burns DT, Davies KE. Advances in genetic therapeutic strategies for Duchenne muscular dystrophy. *Exp Physiol*. 2015;100(12):1458-1467.
75. Rodrigues M, Echigoya Y, Fukada S, Yokota T. Current Translational Research and Murine Models For Duchenne Muscular Dystrophy. *J Neuromuscul Dis*. 2016;3(1):29-48.
76. Mah JK. Current and emerging treatment strategies for Duchenne muscular dystrophy. *Neuropsychiatr Dis Treat*. 2016;12:1795-1807.
77. Salmaninejad A, Valilou SF, Bayat H, et al. Duchenne muscular dystrophy: an updated review of common available therapies. *Int J Neurosci*. 2018;7454:1-11.
78. Okada T, Takeda S. Current Challenges and Future Directions in Recombinant AAV-Mediated Gene Therapy of Duchenne Muscular Dystrophy. *Pharmaceuticals*. 2013;6(7):813-836.
79. Goyenvalle A, Davies KE. Challenges to oligonucleotides-based therapeutics for Duchenne muscular dystrophy. *Skelet Muscle*. 2011;1(1):8.
80. Nakamura A, Takeda S. Exon-skipping therapy for Duchenne muscular dystrophy. *Neuropathology*. 2009;29(4):494-501.
81. Aslesh T, Maruyama R, Yokota T. Skipping Multiple Exons to Treat DMD-Promises and Challenges. *Biomedicines*. 2018;6(1):1.
82. Finkel RS. Read-through strategies for suppression of nonsense mutations in Duchenne/ Becker muscular dystrophy: aminoglycosides and ataluren (PTC124). *J Child Neurol*. 2010;25(9):1158-1164.
83. Long C, McAnally JR, Shelton JM, Mireault AA, Bassel-Duby R, Olson EN. Prevention of muscular dystrophy in mice by CRISPR/Cas9-mediated editing of germline DNA. *Science*. 2014;345(6201):1184-1188.
84. Amoasii L, Hildyard JCW, Li H, et al. Gene editing restores dystrophin expression in a canine model of Duchenne muscular dystrophy. *Science*. 2018;362(6410):86-91.
85. Wang J-Z, Wu P, Shi Z-M, Xu Y-L, Liu Z-J. The AAV-mediated and RNA-guided CRISPR/Cas9 system for gene therapy of DMD and BMD. *Brain Dev*. 2017;39(7):547-556.
86. Mamchaoui K, Trollet C, Bigot A, et al. Immortalized pathological human myoblasts: towards a universal tool for the study of neuromuscular disorders.

Skelet Muscle. 2011;1(1):34.

87. Negroni E, Vallese D, Vilquin J-T, Butler-Browne G, Mouly V, Trollet C. Current advances in cell therapy strategies for muscular dystrophies. *Expert Opin Biol Ther*. 2011;11(2):157-176.
88. Love DR, Hill DF, Dickson G, et al. An autosomal transcript in skeletal muscle with homology to dystrophin. *Nature*. 1989;339(6219):55-58.
89. Tinsley JM, Blake DJ, Roche A, et al. Primary structure of dystrophin-related protein. *Nature*. 1992;360(6404):591-593.
90. Fairclough RJ, Bareja A, Davies KE. Progress in therapy for Duchenne muscular dystrophy. *Exp Physiol*. 2011;96(11):1101-1113.
91. Guiraud S, Davies KE. Pharmacological advances for treatment in Duchenne muscular dystrophy. *Curr Opin Pharmacol*. 2017;34:36-48.
92. Guiraud S, Squire SE, Edwards B, et al. Second-generation compound for the modulation of utrophin in the therapy of DMD. *Hum Mol Genet*. 2015;24(15):4212-4224.
93. Le Hir M, Goyenvalle A, Peccate C, et al. AAV genome loss from dystrophic mouse muscles during AAV-U7 snRNA-mediated exon-skipping therapy. *Mol Ther*. 2013;21(8):1551-1558.
94. Cordova G, Negroni E, Cabello-Verrugio C, Mouly V, Trollet C. Combined Therapies for Duchenne Muscular Dystrophy to Optimize Treatment Efficacy. *Front Genet*. 2018;9(APR):114.
95. Mozzetta C, Minetti G, Puri PL. Regenerative pharmacology in the treatment of genetic diseases: the paradigm of muscular dystrophy. *Int J Biochem Cell Biol*. 2009;41(4):701-710.
96. Abmayr S, Gregorevic P, Allen JM, Chamberlain JS. Phenotypic improvement of dystrophic muscles by rAAV/microdystrophin vectors is augmented by Igf1 codelivery. *Mol Ther*. 2005;12(3):441-450.
97. Dumonceaux J, Marie S, Beley C, et al. Combination of myostatin pathway interference and dystrophin rescue enhances tetanic and specific force in dystrophic mdx mice. *Mol Ther*. 2010;18(5):881-887.
98. Morales MG, Gutierrez J, Cabello-Verrugio C, et al. Reducing CTGF/CCN2 slows down mdx muscle dystrophy and improves cell therapy. *Hum Mol Genet*. 2013;22(24):4938-4951.
99. Peterson JM, Kline W, Canan BD, et al. Peptide-based inhibition of NF-κB rescues diaphragm muscle contractile dysfunction in a murine model of Duchenne muscular dystrophy. *Mol Med*. 2011;17(5-6):508-515.
100. Zhang J V., Ren P-G, Avsian-Kretchmer O, et al. Obestatin, a peptide encoded

by the ghrelin gene, opposes ghrelin's effects on food intake. *Science*. 2005;310(5750):996-999.

101. Gualillo O, Lago F, Casanueva FF, Dieguez C. One ancestor, several peptides post-translational modifications of preproghrelin generate several peptides with antithetical effects. *Mol Cell Endocrinol*. 2006;256(1-2):1-8.

102. Soares J-B, Leite-Moreira AF. Ghrelin, des-acyl ghrelin and obestatin: three pieces of the same puzzle. *Peptides*. 2008;29(7):1255-1270.

103. Alén BO, Nieto L, Gurriarán-Rodríguez U, et al. The NMR structure of human obestatin in membrane-like environments: insights into the structure-bioactivity relationship of obestatin. *PLoS One*. 2012;7(10):e45434.

104. Dun SL, Brailoiu GC, Brailoiu E, Yang J, Chang JK, Dun NJ. Distribution and biological activity of obestatin in the rat. *J Endocrinol*. 2006;191(2):481-489.

105. Granata R, Baragli A, Settanni F, Scarlatti F, Ghigo E. Unraveling the role of the ghrelin gene peptides in the endocrine pancreas. *J Mol Endocrinol*. 2010;45(3):107-118.

106. Granata R, Settanni F, Gallo D, et al. Obestatin promotes survival of pancreatic beta-cells and human islets and induces expression of genes involved in the regulation of beta-cell mass and function. *Diabetes*. 2008;57(4):967-979.

107. Volante M, Rosas R, Ceppi P, et al. Obestatin in human neuroendocrine tissues and tumours: expression and effect on tumour growth. *J Pathol*. 2009;218(4):458-466.

108. Zhao C-M, Furnes MW, Stenström B, Kulseng B, Chen D. Characterization of obestatin- and ghrelin-producing cells in the gastrointestinal tract and pancreas of rats: an immunohistochemical and electron-microscopic study. *Cell Tissue Res*. 2008;331(3):575-587.

109. Gurriarán-Rodríguez U, Santos-Zas I, Al-Massadi O, et al. The obestatin/GPR39 system is up-regulated by muscle injury and functions as an autocrine regenerative system. *J Biol Chem*. 2012;287(45):38379-38389.

110. Moretti E, Vindigni C, Tripodi SA, et al. Immunolocalisation of ghrelin and obestatin in human testis, seminal vesicles, prostate and spermatozoa. *Andrologia*. 2014;46(9):979-985.

111. McKee KK, Tan CP, Palyha OC, et al. Cloning and characterization of two human G protein-coupled receptor genes (GPR38 and GPR39) related to the growth hormone secretagogue and neurotensin receptors. *Genomics*. 1997;46(3):426-434.

112. Egerod KL, Holst B, Petersen PS, et al. GPR39 splice variants versus antisense gene LYPD1: expression and regulation in gastrointestinal tract, endocrine

pancreas, liver, and white adipose tissue. *Mol Endocrinol*. 2007;21(7):1685-1698.

113. Holst B, Holliday ND, Bach A, Elling CE, Cox HM, Schwartz TW. Common structural basis for constitutive activity of the ghrelin receptor family. *J Biol Chem*. 2004;279(51):53806-53817.

114. Dong XY, He JM, Tang SQ, Li HY, Jiang QY, Zou XT. Is GPR39 the natural receptor of obestatin? *Peptides*. 2009;30(2):431-438.

115. Gurriarán-Rodríguez U, Al-Massadi O, Roca-Rivada A, et al. Obestatin as a regulator of adipocyte metabolism and adipogenesis. *J Cell Mol Med*. 2011;15(9):1927-1940.

116. Chartrel N, Alvear-Perez R, Leprince J, et al. Comment on "Obestatin, a peptide encoded by the ghrelin gene, opposes ghrelin's effects on food intake". *Science*. 2007;315(5813):766; author reply 766.

117. Lauwers E, Landuyt B, Arckens L, Schoofs L, Luyten W. Obestatin does not activate orphan G protein-coupled receptor GPR39. *Biochem Biophys Res Commun*. 2006;351(1):21-25.

118. Tremblay F, Perreault M, Klaman LD, Tobin JF, Smith E, Gimeno RE. Normal food intake and body weight in mice lacking the G protein-coupled receptor GPR39. *Endocrinology*. 2007;148(2):501-506.

119. Zhang J V., Klein C, Ren P-G, et al. Response to Comment on "Obestatin, a Peptide Encoded by the Ghrelin Gene, Opposes Ghrelin's Effects on Food Intake." *Science*. 2007;315(5813):766d-766d.

120. De Spiegeleer B, Vergote V, Pezeshki A, Peremans K, Burvenich C. Impurity profiling quality control testing of synthetic peptides using liquid chromatography-photodiode array-fluorescence and liquid chromatography-electrospray ionization-mass spectrometry: the obestatin case. *Anal Biochem*. 2008;376(2):229-234.

121. Zhang J V., Jahr H, Luo C-W, et al. Obestatin induction of early-response gene expression in gastrointestinal and adipose tissues and the mediatory role of G protein-coupled receptor, GPR39. *Mol Endocrinol*. 2008;22(6):1464-1475.

122. Unniappan S, Speck M, Kieffer TJ. Metabolic effects of chronic obestatin infusion in rats. *Peptides*. 2008;29(8):1354-1361.

123. Holst B, Egerod KL, Schild E, et al. GPR39 signaling is stimulated by zinc ions but not by obestatin. *Endocrinology*. 2007;148(1):13-20.

124. Besser L, Chorin E, Sekler I, et al. Synaptically released zinc triggers metabotropic signaling via a zinc-sensing receptor in the hippocampus. *J Neurosci*. 2009;29(9):2890-2901.

125. Tremblay F, Richard A-MT, Will S, et al. Disruption of G protein-coupled receptor 39 impairs insulin secretion in vivo. *Endocrinology*. 2009;150(6):2586-2595.

126. Pacheco-Pantoja EL, Ranganath LR, Gallagher JA, Wilson PJ, Fraser WD. Receptors and effects of gut hormones in three osteoblastic cell lines. *BMC Physiol*. 2011;11(1):12.

127. Fontenot E, DeVente JE, Seidel ER. Obestatin and ghrelin in obese and in pregnant women. *Peptides*. 2007;28(10):1937-1944.

128. Santos-Zas I, Gurriarán-Rodríguez U, Cid-Díaz T, et al. β-Arrestin scaffolds and signaling elements essential for the obestatin/GPR39 system that determine the myogenic program in human myoblast cells. *Cell Mol Life Sci*. 2016;73(3):617-635.

129. Alén BO, Leal-lópez S, Alén MO, et al. The role of the obestatin / GPR39 system in human gastric adenocarcinomas. *Oncotarget*. 2015;7(5):5957-5971.

130. Camiña JP, Campos JF, Caminos JE, Dieguez C, Casanueva FF. Obestatin-mediated proliferation of human retinal pigment epithelial cells: regulatory mechanisms. *J Cell Physiol*. 2007;211(1):1-9.

131. Gurriarán-Rodríguez U, Santos-Zas I, González-Sánchez J, et al. Action of obestatin in skeletal muscle repair: stem cell expansion, muscle growth, and microenvironment remodeling. *Mol Ther*. 2015;23(6):1003-1021.

132. Green BD, Irwin N, Flatt PR. Direct and indirect effects of obestatin peptides on food intake and the regulation of glucose homeostasis and insulin secretion in mice. *Peptides*. 2007;28(5):981-987.

133. Gourcerol G, Million M, Adelson DW, et al. Lack of interaction between peripheral injection of CCK and obestatin in the regulation of gastric satiety signaling in rodents. *Peptides*. 2006;27(11):2811-2819.

134. Seoane LM, Al-Massadi O, Pazos Y, Pagotto U, Casanueva FF. Central obestatin administration does not modify either spontaneous or ghrelin-induced food intake in rats. *J Endocrinol Invest*. 2006;29(8):RC13-5.

135. Nogueiras R, Pfluger P, Tovar S, et al. Effects of obestatin on energy balance and growth hormone secretion in rodents. *Endocrinology*. 2007;148(1):21-26.

136. Yamamoto D, Ikeshita N, Daito R, et al. Neither intravenous nor intracerebroventricular administration of obestatin affects the secretion of GH, PRL, TSH and ACTH in rats. *Regul Pept*. 2007;138(2-3):141-144.

137. Zizzari P, Longchamps R, Epelbaum J, Bluet-Pajot MT. Obestatin partially affects ghrelin stimulation of food intake and growth hormone secretion in rodents. *Endocrinology*. 2007;148(4):1648-1653.

138. Pazos Y, Alvarez CJP, Camiña JP, Casanueva FF. Stimulation of extracellular signal-regulated kinases and proliferation in the human gastric cancer cells KATO-III by obestatin. *Growth Factors*. 2007;25(6):373-381.

139. Granata R, Gallo D, Luque RM, et al. Obestatin regulates adipocyte function and protects against diet-induced insulin resistance and inflammation. *FASEB J*. 2012;26(8):3393-3411.

140. Aragno M, Mastrocola R, Ghé C, et al. Obestatin induced recovery of myocardial dysfunction in type 1 diabetic rats: underlying mechanisms. *Cardiovasc Diabetol*. 2012;11(1):129.

141. Ceranowicz P, Warzecha Z, Dembinski A, et al. Pretreatment with obestatin inhibits the development of cerulein-induced pancreatitis. *J Physiol Pharmacol*. 2009;60(3):95-101.

142. Trovato L, Gallo D, Settanni F, Gesmundo I, Ghigo E, Granata R. Obestatin: is it really doing something? *Front Horm Res*. 2014;42:175-185.

143. Green BD, Grieve DJ. Biochemical properties and biological actions of obestatin and its relevence in type 2 diabetes. *Peptides*. 2018;100:249-259.

144. Gurriarán-Rodríguez U, Al-Massadi O, Crujeiras AB, et al. Preproghrelin expression is a key target for insulin action on adipogenesis. *J Endocrinol*. 2011;210(2):1-7.

145. Baragli A, Baragli L, Grande C, et al. Obestatin enhances in vitro generation of pancreatic islets through regulation of developmental pathways. *PLoS One*. 2013;8(5):e64374.

146.Alloatti G, Arnoletti E, Bassino E, et al. Obestatin affords cardioprotection to the ischemic-reperfused isolated rat heart and inhibits apoptosis in cultures of similarly stressed cardiomyocytes. *Am J Physiol Heart Circ Physiol*. 2010;299(2):H470-81.

147. Penna C, Tullio F, Femminò S, et al. Obestatin regulates cardiovascular function and promotes cardioprotection through the nitric oxide pathway. *J Cell Mol Med*. 2017;21(12):3670-3678.

148. Li H-Q, Wu Y-B, Yin C-S, Chen L, Zhang Q, Hu L-Q. Obestatin attenuated doxorubicin-induced cardiomyopathy via enhancing long noncoding Mhrt RNA expression. *Biomed Pharmacother*. 2016;81:474-481.

149. Li Z-F, Guo Z-F, Cao J, et al. Plasma ghrelin and obestatin levels are increased in spontaneously hypertensive rats. *Peptides*. 2010;31(2):297-300.

150. Samson WK, White MM, Price C, Ferguson A V. Obestatin acts in brain to inhibit thirst. *Am J Physiol Regul Integr Comp Physiol*. 2007;292(1):R637-43.

151. Carlini VP, Schiöth HB, Debarioglio SR. Obestatin improves memory

performance and causes anxiolytic effects in rats. *Biochem Biophys Res Commun*. 2007;352(4):907-912.

152. Szentirmai E, Krueger JM. Obestatin alters sleep in rats. *Neurosci Lett*. 2006;404(1-2):222-226.

153. Santos-Zas I, Cid-Díaz T, González-Sánchez J, et al. Obestatin controls skeletal muscle fiber-type determination. *Sci Rep*. 2017;7(1):2137.

154. Santos-Zas I, Negroni E, Mamchaoui K, et al. Obestatin Increases the Regenerative Capacity of Human Myoblasts Transplanted Intramuscularly in an Immunodeficient Mouse Model. *Mol Ther*. 2017;25(10):2345-2359.

155. Cid-Díaz T, Santos-Zas I, González-Sánchez J, et al. Obestatin controls the ubiquitin-proteasome and autophagy-lysosome systems in glucocorticoid-induced muscle cell atrophy. *J Cachexia Sarcopenia Muscle*. 2017;8(6):974-990.

156. Bentzinger CF, Wang YX, Rudnicki MA, Bentzinger CF, Wang YX, Rudnicki MA. Building Muscle : Molecular Regulation of Myogenesis. *Cold Spring Harb Perspect Biol*. 2012:1-16.

157. Leloup L, Daury L, Mazères G, Cottin P, Brustis J-J. Involvement of the ERK/MAP kinase signalling pathway in milli-calpain activation and myogenic cell migration. *Int J Biochem Cell Biol*. 2007;39(6):1177-1189.

158. Winter B, Arnold HH. Activated raf kinase inhibits muscle cell differentiation through a MEF2-dependent mechanism. *J Cell Sci*. 2000;113 Pt 23:4211-4220.

159. Gredinger E, Gerber AN, Tamir Y, Tapscott SJ, Bengal E. Mitogen-activated protein kinase pathway is involved in the differentiation of muscle cells. *J Biol Chem*. 1998;273(17):10436-10444.

160. Wu Z, Woodring PJ, Bhakta KS, et al. p38 and extracellular signal-regulated kinases regulate the myogenic program at multiple steps. *Mol Cell Biol*. 2000;20(11):3951-3964.

161. Pasut A, Jones AE, Rudnicki MA. Isolation and culture of individual myofibers and their satellite cells from adult skeletal muscle. *J Vis Exp*. 2013;(73):e50074.

162. Livak KJ, Schmittgen TD. Analysis of relative gene expression data using real-time quantitative PCR and the 2(-Delta Delta C(T)) Method. *Methods*. 2001;25(4):402-408.

163. Suzuki A, Ohno S. The PAR-aPKC system: lessons in polarity. *J Cell Sci*. 2006;119(Pt 6):979-987.

164. Brack AS, Conboy IM, Conboy MJ, Shen J, Rando TA. A temporal switch from notch to Wnt signaling in muscle stem cells is necessary for normal adult

myogenesis. *Cell Stem Cell*. 2008;2(1):50-59.

165. Rudolf A, Schirwis E, Giordani L, et al. β-Catenin Activation in Muscle Progenitor Cells Regulates Tissue Repair. *Cell Rep*. 2016;15(6):1277-1290.

166. Conboy IM, Rando TA. The regulation of Notch signaling controls satellite cell activation and cell fate determination in postnatal myogenesis. *Dev Cell*. 2002;3(3):397-409.

167. Ciciliot S, Rossi AC, Dyar KA, Blaauw B, Schiaffino S. Muscle type and fiber type specificity in muscle wasting. *Int J Biochem Cell Biol*. 2013;45(10):2191-2199.

168. Potthoff MJ, Wu H, Arnold MA, et al. Histone deacetylase degradation and MEF2 activation promote the formation of slow-twitch myofibers. *J Clin Invest*. 2007;117(9):2459-2467.

169. McKinsey TA, Zhang CL, Lu J, Olson EN. Signal-dependent nuclear export of a histone deacetylase regulates muscle differentiation. *Nature*. 2000;408(6808):106-111.

170. McKinsey TA, Zhang CL, Olson EN. Signaling chromatin to make muscle. *Curr Opin Cell Biol*. 2002;14(6):763-772.

171. Potthoff MJ, Olson EN. MEF2: a central regulator of diverse developmental programs. *Development*. 2007;134(23):4131-4140.

172. Glass DJ. Signaling pathways perturbing muscle mass. *Curr Opin Clin Nutr Metab Care*. 2010;13(3):225-229.

173. Handschin C, Kobayashi YM, Chin S, Seale P, Campbell KP, Spiegelman BM. PGC-1alpha regulates the neuromuscular junction program and ameliorates Duchenne muscular dystrophy. *Genes Dev*. 2007;21(7):770-783.

174. Chakkalakal J V, Stocksley MA, Harrison M-A, et al. Expression of utrophin A mRNA correlates with the oxidative capacity of skeletal muscle fiber types and is regulated by calcineurin/NFAT signaling. *Proc Natl Acad Sci U S A*. 2003;100(13):7791-7796.

175. Chakkalakal J V., Harrison M-A, Carbonetto S, Chin E, Michel RN, Jasmin BJ. Stimulation of calcineurin signaling attenuates the dystrophic pathology in mdx mice. *Hum Mol Genet*. 2004;13(4):379-388.

176. Angus LM, Chakkalakal J V, Méjat A, et al. Calcineurin-NFAT signaling, together with GABP and peroxisome PGC-1{alpha}, drives utrophin gene expression at the neuromuscular junction. *Am J Physiol Cell Physiol*. 2005;289(4):C908-17.

177. Lin J, Wu H, Tarr PT, et al. Transcriptional co-activator PGC-1 alpha drives the formation of slow-twitch muscle fibres. *Nature*. 2002;418(6899):797-801.

178. Wu H, Kanatous SB, Thurmond FA, et al. Regulation of mitochondrial biogenesis in skeletal muscle by CaMK. *Science*. 2002;296(5566):349-352.

179. Kim M-S, Fielitz J, McAnally J, et al. Protein kinase D1 stimulates MEF2 activity in skeletal muscle and enhances muscle performance. *Mol Cell Biol*. 2008;28(11):3600-3609.

180. McKinsey TA, Zhang CL, Olson EN. MEF2: a calcium-dependent regulator of cell division, differentiation and death. *Trends Biochem Sci*. 2002;27(1):40-47.

181. Youn HD, Chatila T a, Liu JO. Integration of calcineurin and MEF2 signals by the coactivator p300 during T-cell apoptosis. *EMBO J*. 2000;19(16):4323-4331.

182. McKinsey TA, Olson EN. Toward transcriptional therapies for the failing heart: chemical screens to modulate genes. *J Clin Invest*. 2005;115(3):538-546.

183. Beals CR, Sheridan CM, Turck CW, Gardner P, Crabtree GR. Nuclear export of NF-ATc enhanced by glycogen synthase kinase-3. *Science*. 1997;275(5308):1930-1934.

184. Neal JW, Clipstone NA. Glycogen Synthase Kinase-3 Inhibits the DNA Binding Activity of NFATc. *J Biol Chem*. 2001;276(5):3666-3673.

185. De Palma C, Morisi F, Cheli S, et al. Autophagy as a new therapeutic target in Duchenne muscular dystrophy. *Cell Death Dis*. 2012;3(11):e418.

186. Klionsky DJ, Abdelmohsen K, Abe A, et al. Guidelines for the use and interpretation of assays for monitoring autophagy (3rd edition). *Autophagy*. 2016;12(1):1-222.

187. Neel BA, Lin Y, Pessin JE. Skeletal muscle autophagy: a new metabolic regulator. *Trends Endocrinol Metab*. 2013;24(12):635-643.

188. Hindupur SK, González A, Hall MN. The opposing actions of target of rapamycin and AMP-activated protein kinase in cell growth control. *Cold Spring Harb Perspect Biol*. 2015;7(8):a019141.

189. Kaur J, Debnath J. Autophagy at the crossroads of catabolism and anabolism. *Nat Rev Mol Cell Biol*. 2015;16(8):461-472.

190. Kim JH, Lee JO, Lee SK, et al. The glutamate agonist homocysteine sulfinic acid stimulates glucose uptake through the calcium-dependent AMPK-p38 MAPK-protein kinase C zeta pathway in skeletal muscle cells. *J Biol Chem*. 2011;286(9):7567-7576.

191. Kim J, Kundu M, Viollet B, Guan K-L. AMPK and mTOR regulate autophagy through direct phosphorylation of Ulk1. *Nat Cell Biol*. 2011;13(2):132-141.

192. González-Sánchez J, Sánchez-Temprano A, Cid-Díaz T, et al. Improvement of Duchenne muscular dystrophy phenotype following obestatin treatment. *J Cachexia Sarcopenia Muscle*. September 2018.

193. Abdul-Ghani M, Megeney LA. Rehabilitation of a contract killer: caspase-3 directs stem cell differentiation. *Cell Stem Cell*. 2008;2(6):515-516.

194. Fujita J, Crane AM, Souza MK, et al. Caspase activity mediates the differentiation of embryonic stem cells. *Cell Stem Cell*. 2008;2(6):595-601.

195. Larsen BD, Rampalli S, Burns LE, Brunette S, Dilworth FJ, Megeney LA. Caspase 3/caspase-activated DNase promote cell differentiation by inducing DNA strand breaks. *Proc Natl Acad Sci U S A*. 2010;107(9):4230-4235.

196. Olguín HC. Regulation of Pax7 protein levels by caspase-3 and proteasome activity in differentiating myoblasts. *Biol Res*. 2011;44(4):323-327.

197. Dick SA, Chang NC, Dumont NA, et al. Caspase 3 cleavage of Pax7 inhibits self-renewal of satellite cells. *Proc Natl Acad Sci U S A*. 2015;112(38):E5246-52.

198. González N, Moresco JJ, Cabezas F, et al. Ck2-Dependent Phosphorylation Is Required to Maintain Pax7 Protein Levels in Proliferating Muscle Progenitors. *PLoS One*. 2016;11(5):e0154919.

199. Bjornson CRR, Cheung TH, Liu L, Tripathi P V, Steeper KM, Rando TA. Notch signaling is necessary to maintain quiescence in adult muscle stem cells. *Stem Cells*. 2012;30(2):232-242.

200. Fukada S, Yamaguchi M, Kokubo H, et al. Hesr1 and Hesr3 are essential to generate undifferentiated quiescent satellite cells and to maintain satellite cell numbers. *Development*. 2011;138(21):4609-4619.

201. Mourikis P, Gopalakrishnan S, Sambasivan R, Tajbakhsh S. Cell-autonomous Notch activity maintains the temporal specification potential of skeletal muscle stem cells. *Development*. 2012;139(24):4536-4548.

202. DasGupta R, Fuchs E. Multiple roles for activated LEF/TCF transcription complexes during hair follicle development and differentiation. *Development*. 1999;126(20):4557-4568.

203. Jho E, Zhang T, Domon C, Joo C, Freund J, Costantini F. Wnt/beta-catenin/Tcf signaling induces the transcription of Axin2, a negative regulator of the signaling pathway. *Mol Cell Biol*. 2002;22(4):1172-1183.

204. Pan W, Jia Y, Wang J, et al. Beta-catenin regulates myogenesis by relieving I-mfa-mediated suppression of myogenic regulatory factors in P19 cells. *Proc Natl Acad Sci U S A*. 2005;102(48):17378-17383.

205. Pan W, Jia Y, Huang T, et al. Beta-catenin relieves I-mfa-mediated suppression of LEF-1 in mammalian cells. *J Cell Sci*. 2006;119(Pt 23):4850-4856.

206. Correia JC, Ferreira DMS, Ruas JL. Intercellular: local and systemic actions of skeletal muscle PGC-1s. *Trends Endocrinol Metab*. 2015;26(6):305-314.

207. Fairclough RJ, Wood MJ, Davies KE. Therapy for Duchenne muscular dystrophy: renewed optimism from genetic approaches. *Nat Rev Genet*. 2013;14(6):373-378.

208. Miura P, Jasmin BJ. Utrophin upregulation for treating Duchenne or Becker muscular dystrophy: how close are we? *Trends Mol Med*. 2006;12(3):122-129.

209. Miura P, Andrews M, Holcik M, Jasmin BJ. IRES-mediated translation of utrophin A is enhanced by glucocorticoid treatment in skeletal muscle cells. *PLoS One*. 2008;3(6):e2309.

210. Hollinger K, Gardan-Salmon D, Santana C, Rice D, Snella E, Selsby JT. Rescue of dystrophic skeletal muscle by PGC-1α involves restored expression of dystrophin-associated protein complex components and satellite cell signaling. *Am J Physiol Regul Integr Comp Physiol*. 2013;305(1):R13-23.

211. Li D, Bareja A, Judge L, et al. Sarcolemmal nNOS anchoring reveals a qualitative difference between dystrophin and utrophin. *J Cell Sci*. 2010;123(Pt 12):2008-2013.

212. van den Bergen JC, Wokke BHA, Hulsker MA, Verschuuren JJGM, Aartsma-Rus AM. Studying the role of dystrophin-associated proteins in influencing Becker muscular dystrophy disease severity. *Neuromuscul Disord*. 2015;25(3):231-237.

213. Rooney JE, Welser J V, Dechert MA, Flintoff-Dye NL, Kaufman SJ, Burkin DJ. Severe muscular dystrophy in mice that lack dystrophin and alpha7 integrin. *J Cell Sci*. 2006;119(Pt 11):2185-2195.

214. Song WK, Wang W, Sato H, Bielser DA, Kaufman SJ. Expression of alpha 7 integrin cytoplasmic domains during skeletal muscle development: alternate forms, conformational change, and homologies with serine/threonine kinases and tyrosine phosphatases. *J Cell Sci*. 1993;106(Pt4):1139-1152.

215. Burkin DJ, Wallace GQ, Nicol KJ, Kaufman DJ, Kaufman SJ. Enhanced expression of the alpha 7 beta 1 integrin reduces muscular dystrophy and restores viability in dystrophic mice. *J Cell Biol*. 2001;152(6):1207-1218.

216. Partridge TA. The mdx mouse model as a surrogate for Duchenne muscular dystrophy. *FEBS J*. 2013;280(17):4177-4186.

217. McGreevy JW, Hakim CH, McIntosh MA, Duan D. Animal models of Duchenne muscular dystrophy: from basic mechanisms to gene therapy. *Dis Model Mech*. 2015;8(3):195-213.

218. Peccate C, Mollard A, Le Hir M, et al. Antisense pre-treatment increases gene therapy efficacy in dystrophic muscles. *Hum Mol Genet*. 2016;25(16):3555-3563.

219. Godfrey C, Desviat LR, Smedsrød B, et al. Delivery is key: lessons learnt from developing splice-switching antisense therapies. *EMBO Mol Med*. 2017;9(5):545-557.

220. Ljubicic V, Jasmin BJ. AMP-activated protein kinase at the nexus of therapeutic skeletal muscle plasticity in Duchenne muscular dystrophy. *Trends Mol Med*. 2013;19(10):614-624.

221. Rafael JA, Tinsley JM, Potter AC, Deconinck AE, Davies KE. Skeletal muscle-specific expression of a utrophin transgene rescues utrophin-dystrophin deficient mice. *Nat Genet*. 1998;19(1):79-82.

222. Gramolini AO, Bélanger G, Thompson JM, Chakkalakal J V, Jasmin BJ. Increased expression of utrophin in a slow vs. a fast muscle involves posttranscriptional events. *Am J Physiol Cell Physiol*. 2001;281(4):C1300-9.

223. Liu Y, Randall WR, Schneider MF. Activity-dependent and -independent nuclear fluxes of HDAC4 mediated by different kinases in adult skeletal muscle. *J Cell Biol*. 2005;168(6):887-897.

224. Shen T, Cseresnyés Z, Liu Y, Randall WR, Schneider MF. Regulation of the nuclear export of the transcription factor NFATc1 by protein kinases after slow fibre type electrical stimulation of adult mouse skeletal muscle fibres. *J Physiol*. 2007;579(Pt 2):535-551.

225. Li H-H, Kedar V, Zhang C, et al. Atrogin-1/muscle atrophy F-box inhibits calcineurin-dependent cardiac hypertrophy by participating in an SCF ubiquitin ligase complex. *J Clin Invest*. 2004;114(8):1058-1071.

226. Ni YG, Berenji K, Wang N, et al. Foxo Transcription Factors Blunt Cardiac Hypertrophy by Inhibiting Calcineurin Signaling. *Circulation*. 2006;114(11):1159-1168.

227. Lara-Pezzi E, Winn N, Paul A, et al. A naturally occurring calcineurin variant inhibits FoxO activity and enhances skeletal muscle regeneration. *J Cell Biol*. 2007;179(6):1205-1218.

228. Al-Rewashdy H, Ljubicic V, Lin W, Renaud J-M, Jasmin BJ. Utrophin A is essential in mediating the functional adaptations of mdx mouse muscle following chronic AMPK activation. *Hum Mol Genet*. 2015;24(5):1243-1255.

229. Chan MC, Rowe GC, Raghuram S, Patten IS, Farrell C, Arany Z. Post-natal induction of PGC-1α protects against severe muscle dystrophy independently of utrophin. *Skelet Muscle*. 2014;4(1):2.

230. Matsakas A, Yadav V, Lorca S, Narkar V. Muscle ERRγ mitigates Duchenne muscular dystrophy via metabolic and angiogenic reprogramming. *FASEB J*. 2013;27(10):4004-4016.

231. Schiaffino S, Sandri M, Murgia M. Activity-dependent signaling pathways controlling muscle diversity and plasticity. *Physiology*. 2007;22(4):269-278.

232. Merrick D, Stadler LKJ, Larner D, Smith J. Muscular dystrophy begins early in

embryonic development deriving from stem cell loss and disrupted skeletal muscle formation. *Dis Model Mech*. 2009;2(7-8):374-388.

233. Deconinck AE, Rafael JA, Skinner JA, et al. Utrophin-dystrophin-deficient mice as a model for Duchenne muscular dystrophy. *Cell*. 1997;90(4):717-727.

234. Grady RM, Teng H, Nichol MC, Cunningham JC, Wilkinson RS, Sanes JR. Skeletal and cardiac myopathies in mice lacking utrophin and dystrophin: a model for Duchenne muscular dystrophy. *Cell*. 1997;90(4):729-738.

235. Sandri M, Coletto L, Grumati P, Bonaldo P. Misregulation of autophagy and protein degradation systems in myopathies and muscular dystrophies. *J Cell Sci*. 2013;126(23):5325-5333.

236. De Palma C, Perrotta C, Pellegrino P, Clementi E, Cervia D. Skeletal muscle homeostasis in duchenne muscular dystrophy: modulating autophagy as a promising therapeutic strategy. *Front Aging Neurosci*. 2014;6(JUL):188.

237. Pauly M, Daussin F, Burelle Y, et al. AMPK activation stimulates autophagy and ameliorates muscular dystrophy in the mdx mouse diaphragm. *Am J Pathol*. 2012;181(2):583-592.

238. Laplante M, Sabatini DM. mTOR signaling in growth control and disease. *Cell*. 2012;149(2):274-293.

239. Shimobayashi M, Hall MN. Making new contacts: the mTOR network in metabolism and signalling crosstalk. *Nat Rev Mol Cell Biol*. 2014;15(3):155-162.

240. Shimobayashi M, Hall MN. Multiple amino acid sensing inputs to mTORC1. *Cell Res*. 2016;26(1):7-20.

241. Heberle AM, Prentzell MT, van Eunen K, Bakker BM, Grellscheid SN, Thedieck K. Molecular mechanisms of mTOR regulation by stress. *Mol Cell Oncol*. 2015;2(2):e970489.

242. Mounier R, Théret M, Lantier L, Foretz M, Viollet B. Expanding roles for AMPK in skeletal muscle plasticity. *Trends Endocrinol Metab*. 2015;26(6):275-286.

243. Kjøbsted R, Hingst JR, Fentz J, et al. AMPK in skeletal muscle function and metabolism. *FASEB J*. 2018;32(4):1741-1777.

244. Steinberg GR, Kemp BE. AMPK in Health and Disease. *Physiol Rev*. 2009;89(3):1025-1078.

245. Hardie DG, Ross FA, Hawley SA. AMPK: a nutrient and energy sensor that maintains energy homeostasis. *Nat Rev Mol Cell Biol*. 2012;13(4):251-262.

246. Narita M, Young ARJ, Arakawa S, et al. Spatial coupling of mTOR and autophagy augments secretory phenotypes. *Science*. 2011;332(6032):966-970.

247. Pezze PD, Ruf S, Sonntag AG, et al. A systems study reveals concurrent activation of AMPK and mTOR by amino acids. *Nat Commun*. 2016;7:1-19.

248. Pereira O, Teixeira A, Sampaio-Marques B, Castro I, Girão H, Ludovico P. Signalling mechanisms that regulate metabolic profile and autophagy of acute myeloid leukaemia cells. *J Cell Mol Med*. 2018;22(10):4807-4817.

249. Conn CS, Qian S-B. mTOR signaling in protein homeostasis: less is more? *Cell Cycle*. 2011;10(12):1940-1947.

250. Ciechanover A, Kwon YT a. Degradation of misfolded proteins in neurodegenerative diseases: therapeutic targets and strategies. *Exp Mol Med*. 2015;47(3):e147.

USC UNIVERSIDADE DE SANTIAGO DE COMPOSTELA

USC
UNIVERSIDADE
DE SANTIAGO
DE COMPOSTELA